

TECHNICAL UNIVERSITY OF CIVIL ENGINEERING BUCHAREST

Faculty of Mechanical Engineering and Robotics in Construction Department of Construction Machinery and Mechatronics

DOCTORAL THESIS SUMMARY

DIPL. ENG. CHIRIȚĂ ALEXANDRU-POLIFRON

THEORETICAL AND EXPERIMENTAL CONTRIBUTIONS ON OPTIMIZING THE DYNAMIC PARAMETERS OF MULTIPURPOSE MOTOR TRUCKS BY USING HYDROSTATIC TRANSMISSIONS

DOCTORAL SUPERVISOR PROF. PHD ENG. PAVEL CRISTIAN

Annotation

to the doctoral thesis titled "Theoretical and experimental contributions on optimizing the dynamic parameters of multipurpose motor trucks by using hydrostatic transmissions" presented by Dipl. Eng. Alexandru-Polifron Chiriță for being awarded the degree of Doctor of Engineering Sciences

The thesis has 7 chapters (acc. to Annex 1), totaling 276 pages – of which 178 pages make up the main body of the thesis, 193 figures (acc. to Annex 2), 4 tables, 151 references entries (acc. to Annex 3 and Annex 4), and 44 annexes.

TABLE OF CONTENTS

Acknowledgment	3
Abstract	5
Chapter 1 – Introduction	7
Chapter 2 – State of the art in the field of mobile hydraulic transmissions and in the fi of motor trucks equipped with them	
Chapter 3 – Theoretical elements regarding the mathematical modeling of hydrostation drive components and systems	c 8
Chapter 4 – Physical experimentation, in the laboratory, of a closed-circuit primary control hydrostatic transmission	10
Chapter 5 – Optimization and virtual experimentation using numerical simulation	16
5.1 Virtual experience of the A10VG28EP4 servo-pump	16
5.2 Virtual experimentation and optimization of the subsystems of a closed-circuit primary control hydrostatic transmission	19
5.3 Virtual experimentation of a multipurpose motor truck and optimization of its dynamic parameters by equipping it with a closed-circuit primary control hydrostatic transmission	
Chapter 6 - Applicability of the research	36
Chapter 7 – Conclusions, personal contributions and perspectives	37
7.1 General conclusions of the thesis	37
7.2 A synthesis of the personal contributions	39
7.3 Perspectives for further research	40
Annex 1 - Thesis structure (table of contents)	42
Annex 2 - Thesis List of Figures	44
Annex 3 - Thesis References	47
Annex 4 - Thesis bibliometric statistics	50

Acknowledgment

This doctoral thesis has been developed within the Department of Construction Machinery and Mechatronics, part of the Faculty of Mechanical Engineering and Robotics in Construction (FIMRC) of Technical University of Civil Engineering Bucharest (UTCB).

To carry out the research, I benefited from a scholarship for doctoral studies from the Doctoral School within UTCB, during the first 3 years of studies.

At the end of the doctoral research activity, I would like to thank Mr. Cristian Pavel, University Professor at the Technical University of Civil Engineering Bucharest, Doctoral supervisor of the present thesis, for the proficient guidance during these years of doctoral studies. I also thank Professor Pavel for showing understanding, for generously supporting my motivation and effort, for the help and encouragement I have enjoyed from him throughout this period.

I would also like to thank the Guidance Committee for guiding my doctoral research in the field of multipurpose motor trucks.

On this occasion, I would also like to thank all the people from the Department of Construction Machinery and Mechatronics, as well as the other professors from the Faculty of Mechanical Engineering and Robotics in Construction of UTCB for the collaboration and the advice given.

I would like to thank the Hydraulics and Pneumatics Research Institute INOE 2000 - Subsidiary IHP in Bucharest, of which I am an employee, with a scientific title of CS (research scientist), and which, through its management and employees, has supported me in conducting this research, along all the stages, both by making available the existing research infrastructure in its laboratories and by providing me with theoretical and practical knowledge, arising from the vast experience in the field of hydraulics possessed by the specialists of this institution. I am grateful to my colleagues at the Institute for their collaboration - for the kind assistance provided during the laboratory testing presented in Chapter 4 of the thesis, for the professional discussions we had, for their suggestions and observations, which have been useful to me at all stages of the work - as well as for the moral support provided.

This doctoral research is a continuation of the scientific research conducted at INOE 2000-Subsidiary IHP, in the framework of the research project titled "Electrohydraulic equipment (EHE) with high energy efficiency (HEE) for multipurpose motor vehicles (MPV)", acronym ECHIPEFEN, Financial agreement no. 11PTE/2016, financed by UEFISCDI under PNCDI III - Programme 2 - Subprogramme 2.1 - Project of transfer to the economic operator (PTE-2016). Part of the theoretical research included in this thesis has been carried out by the author during 2019, within the 'OPTRONICA VI' research-development NUCLEU Programme of INOE 2000, phase titled "Theoretical and experimental research on the dynamic behavior of hydrostatic equipment and transmissions on mobile machinery". Experimental research has been partially carried out by the author in 2021, the author completing the rest in 2022, with financing provided by the 'OPTRONICA VI' research-development NUCLEU Programme of INOE 2000, phase titled "Developing advanced methods, stands, equipment and teaching materials in order to enlarge specific knowledge in the fields of hydrotronic, pneumotronic and digital hydraulic components and systems".

I also thank the management of the Institute for the chance to make use of the user licenses for the computer software needed – licences owned by INOE 2000 - Subsidiary IHP - with the help of which I have been able to carry out the research for this thesis under optimal conditions, both in the stage of physical experimentation, in the laboratory, and in that of virtual experimentation, with the help of numerical simulation, of a closed-circuit primary control hydrostatic transmission.

My thanks also go to the members of the Doctoral Committee – PhD. Eng. Virgil Florescu, Assoc. Prof., Dean of FIMRC (UTCB) and President of the Doctoral Committee, PhD. Eng. Cristian Pavel, Prof. at FIMRC (UTCB) and Doctoral supervisor of the present thesis, PhD. Eng. Radu-Iulian Rădoi, 2nd rank research scientist (CS II) at INOE 2000-IHP, PhD. Eng. Silviu Marian Năstac, Prof. at "Dunărea de Jos" University of Galați - Faculty of Engineering and Agronomy in Brăila, and PhD. Eng. Ion David, Prof. at FIMRC (UTCB) - for the honor they have done me in accepting this role, as well as to everyone who gave me feedback, assessments and appreciations on this thesis.

Last but not least, my warmest thanks go to my family and friends for their trust in me and for their continuous and unconditional support throughout the development of my doctoral thesis.

DOCTORAL COMMITTEE

PRESIDENT OF THE COMMITTEE	ASSOC. PROF. PHD. ENG. VIRGIL FLORESCU	TECHNICAL UNIVERSITY OF CIVIL ENGINEERING BUCHAREST	
DOCTORAL SUPERVISOR	PROF. PHD. ENG. CRISTIAN PAVEL	TECHNICAL UNIVERSITY OF CIVIL ENGINEERING BUCHAREST	
OFFICIAL REFEREE	CS II PHD. ENG. RADU-IULIAN RĂDOI	INOE 2000-IHP	
OFFICIAL REFEREE	PROF. PHD. ENG. SILVIU MARIAN NĂSTAC	"DUNĂREA DE JOS" UNIVERSITY OF GALAȚI	
OFFICIAL REFEREE	PROF. PHD. ENG. ION DAVID	TECHNICAL UNIVERSITY OF CIVIL ENGINEERING BUCHAREST	

Abstract

The selling price of a multipurpose motor truck is composed of: the cost of the truck, that of the components and technological equipment with which it is equipped, the trade margin set by the integrator, as well as the costs - not negligible at all - of the research necessary to optimize the parameters of the multipurpose motor truck.

Currently, there can be purchased: * from integrators - trucks equipped with various technological equipment; these trucks cannot fully meet the needs of the technological process, since the speed of movement provided by the mechanical transmission is not adequate; * from importers - vans equipped with various technological equipment and hydrostatic transmissions, which achieve adequate technological speeds, but which have the disadvantage of low productivity due to their low loading capacity; * from integrators / importers - UNIMOG model compact trucks, which are equipped with a hydrodynamic transmission that allows movement at low speeds but are energy inefficient in this mode of movement; another disadvantage they pose is the fact that they have a small loading capacity.

In the above-described context, the aim of this thesis, namely to optimize the dynamic parameters of multipurpose trucks, is attainable by equipping them with a closed circuit primary control hydrostatic transmission and a PID controller; this transmission will enable multipurpose trucks to achieve lower travel speeds than the mechanical transmission with which the trucks are already equipped. Moreover, the travel speed of multipurpose trucks will be uniform and can be continuously adjusted to meet the needs of any technological process. The multipurpose truck with the previously specified features combines the advantages of all the previously mentioned trucks. It will have an authorized mass of 18 tons, will be able to travel upwards and downwards a rough road with a 45% gradient at a maximum speed of 4.3 km/h, and upwards a paved road with a 15% gradient at a maximum speed of 7.35 km/h. Under these conditions, the truck will reach 99.85% of its maximum speed in 3 seconds. Regarding the minimum travel speed, the motor truck can travel at 0.045 km/h. The truck will achieve low travel speeds with better energy efficiency compared to trucks equipped with hydrodynamic transmissions; the two distinct transmissions which the truck will be equipped with can be used independently, according to the needs of the technological process, thus ensuring two modes of travel, both efficient from an energy point of view.

The objectives of the thesis leading to the fulfilment of its aim, and the distribution by chapters can be summarized as follows:

- In **Chapter 1**, the framework is established in which research will be carried out regarding the equipping of multipurpose trucks with hydrostatic transmissions;
- In **Chapter 2**, an analysis of the state of the art in the field of mobile hydraulic transmissions and in the field of motor trucks is carried out;
- In **Chapter 3**, the mathematical models of the parts of a hydrostatic transmission and those of the pump displacement servo-control system are presented;
- In **Chapter 4** the characteristics of a servo-pump are determined experimentally, as well as the control performance of a closed circuit primary control transmission;
- In **Chapter 5** the dynamic parameters of multipurpose motor trucks equipped with closed circuit primary control hydrostatic transmissions are optimized virtually, with the help of

numerical simulation. Also in **Chapter 5**, the influence that reducing the energy consumption of the subsystems has on the closed circuit hydrostatic transmission is studied, with the help of numerical simulation. Moreover, in **Chapter 5** the possibility of obtaining optimized parameters of multipurpose trucks is demonstrated; such parameters fully meet the requirements of technological processes: travel speed rates that are lower than those of the mechanical transmission and steadier, and also continuous adjustment of the travel speed rate.

• The present thesis makes available to integrators a data set with a benchmark value; this set can be found, in a concise form, in **Chapter 5**, and in detail – in Annex 39 of the thesis.

In order to fulfil the intended objectives, it has been necessary for the author of the thesis to build an experimental bench for the study of the control capabilities of a servo-pump and those of a closed circuit primary control hydrostatic transmission. Both bench control and experimental data acquisition have been performed using the LabVIEW software; a total of 8 laboratory experiments have been carried out. Physical testing, in the laboratory, has been continued virtually, with the help of numerical simulation by using the Simcenter AMESim software; the data obtained in the laboratory have been used to validate the numerical simulation models, also being the initial parameters of the 3 numerical simulation models developed by the author. They continue the study of the servo-pump control capabilities, analyse the influence that reducing the energy consumption of the subsystems has on the closed circuit hydrostatic transmission, leading, at the end of the research, to the optimization of the dynamic parameters of multipurpose motor trucks.

The thesis is based on extensive bibliography; from its analysis, a large number of bibliographic references (documentary sources directly related to the content of the thesis) has resulted; their structure may be summarized as follows:

	<u>New</u> references (≥ year 2013)	Old references (< year 2013)	TOTAL of references	*Since the publication date of the information on the websites could not be determined, the related references (marked as "n.d." – "no date") have been all considered older than 2013.	
Scientific Articles / Papers	59	23	82		
Books	5	26	31		
TOTAL of Articles / Papers and Books	64	49	113		
Datasheets	20	8	28		
Websites	0	10*	10		
GRAND TOTAL	84	67	151		

In its 7 chapters (and especially in Chapter 5 – Optimization and virtual experimentation using numerical simulation) the thesis comprises a large number of figures (graphs, diagrams), with the role of providing information in an eloquent, dense and, at the same time, visually appealing form; also, the information in the thesis is detailed by a significant number of accompanying materials, annexes of this thesis.

Chapter 1 - Introduction

In this chapter, the framework has been established in which the research has been carried out regarding the equipping of multipurpose motor trucks with hydrostatic transmissions; at the same time, this chapter also had the role of narrowing the field of research, as well as the role of presenting the terminology used in the thesis. In order to be able to study the issue of multipurpose motor trucks equipped with hydraulic transmissions, in this chapter, a brief presentation of some introductory notions about hydraulic transmissions has been made, including their classification and the particularities of each type of transmission. Also, the notion of "multifunctional motor truck" has been defined and an overview of their possible applications (Fig. 1 (Figure 1.8 in the full-length thesis)) has been outlined, with an insight into the advantages brought by equipping them with hydrostatic transmissions.



Fig. 1 (Figure 1.8): Example of technological equipment that a multipurpose motor truck used in the construction sector can be equipped with.

Chapter 2 – State of the art in the field of mobile hydraulic transmissions and in the field of motor trucks equipped with them

In this chapter, an analysis has been made on the state of the art of research in the field of mobile hydraulic transmissions and that in the field of motor trucks; also, some of the best performing models of servo-pumps and servo-motors / hydrostatic motors have been presented, as well as the subsystems of the transmissions. As a conclusion of the analysis in this chapter, the hydraulic schematic diagram in Fig. 2 (Figure 2.39) has been chosen as the optimal solution, with the arrangement of positive displacement machines on the motor truck as shown in Fig. 3 (Figure 2.41).

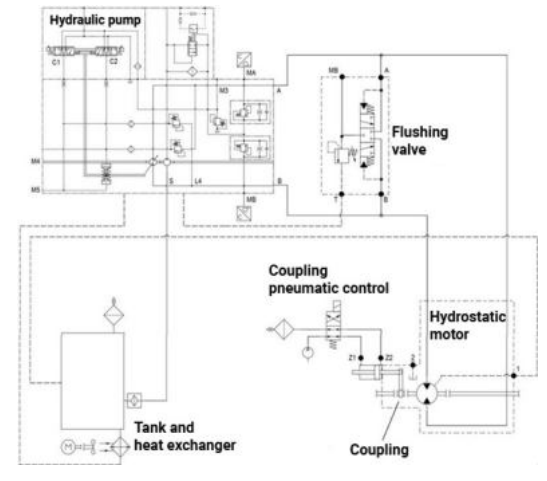






Fig. 3 (Figure 2.41): Application example for a split type primary control hydrostatic transmission.

In addition, in this chapter, the disambiguation of the 'multipurpose motor truck' concept has been made and the aim and objectives of the thesis have been stated.

The aim of this thesis is to optimize the dynamic parameters of multipurpose motor trucks, using a hydrostatic transmission to this end.

In order to achieve the aim of the thesis, the following **objectives** have been considered:

- Establishing the framework in which research will be carried out regarding the equipping of multipurpose motor trucks with hydrostatic transmissions;
- Making an analysis of the state of the art in the field of mobile hydraulic transmissions and in the field of motor trucks that can be equipped with such transmissions;
- Studying the parts of a hydrostatic transmission and the pump capacity displacement servo-control system, through mathematical modeling;
- Experimental determination, in the laboratory, of the characteristics of a servo-pump and the control performance of a closed-circuit primary control transmission;
- Virtual optimization of the dynamic parameters of multipurpose motor trucks equipped with closed-circuit primary control hydrostatic transmissions, with the help of numerical simulation;
- Studying the influence that reducing the energy consumption of the subsystems has on the closed-circuit hydrostatic transmission, with the help of numerical simulation;
- Demonstrating the possibility of obtaining optimized parameters of multipurpose motor trucks, which would fully meet the requirements of technological processes;
- Making available to integrators a data set with a benchmark value regarding the parameters of hydraulic components and those of closed-circuit transmission subsystems, so that the motor truck equipped by the integrator with the hydrostatic transmission could meet the requirements of the technological process efficiently and safely.

Chapter 3 – Theoretical elements regarding the mathematical modeling of hydrostatic drive components and systems

In order to fulfill the aim and objectives of the thesis, mathematical modeling and dynamic analysis in non-permanent regime of the main hydraulic components and hydrostatic drive systems have been necessary. In this chapter, the mathematical models of the components of a hydrostatic transmission (Fig. 4 (Figure 3.1), Fig. 5 (Figure 3.2), Fig. 6 (Figure 3.3)) and those of the pump capacity displacement servo-control system (Fig. 7 (Figure 3.4)) have been presented.

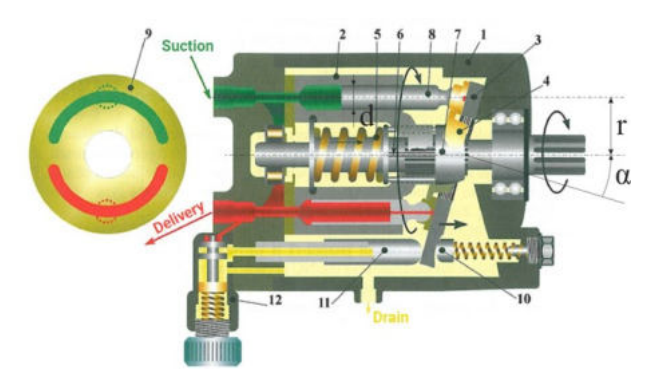
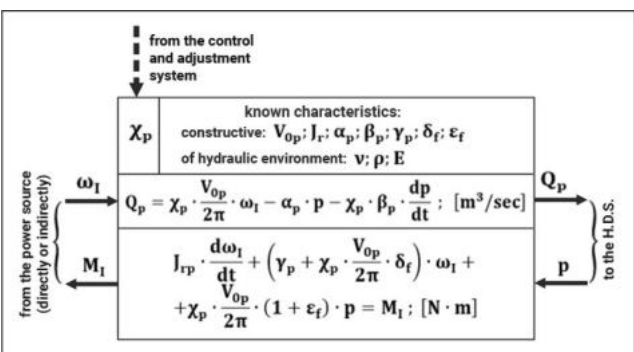
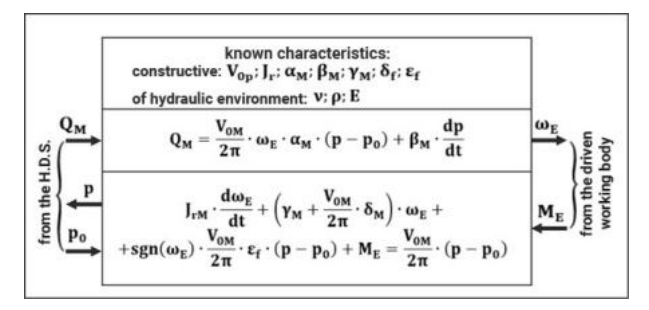


Fig. 4 (Figure 3.1): Swash plate hydraulic pump.



Dynamic mathematical model of a pump.



Dynamic mathematical model of a high-speed fixed-displacement motor.

$$\begin{aligned} Q_M &= \left(\frac{V_{0M}}{2\pi} - k^*\right) \cdot \omega_e + \alpha_M^* \cdot p^2 + \beta_M \cdot \frac{dp}{dt}; \\ J_{SM} \cdot \frac{d\omega_e}{dt} &+ \left(\frac{V_{0M}}{2\pi} - k^*\right) \cdot \delta_M^* (\omega_e - \omega_S)^2 + M_E = \\ &= \left(\frac{V_{0M}}{2\pi} - k^*\right) \cdot p; \end{aligned}$$

$$\alpha_M^* = (\pi \cdot d \cdot z \cdot k \cdot j^3 / 96 \cdot b \cdot \eta) \cdot 2\pi \cdot d \cdot z \cdot k / \rho \cdot g \cdot V_{0M}$$

Dynamic mathematical model of a low-speed radial piston motor.

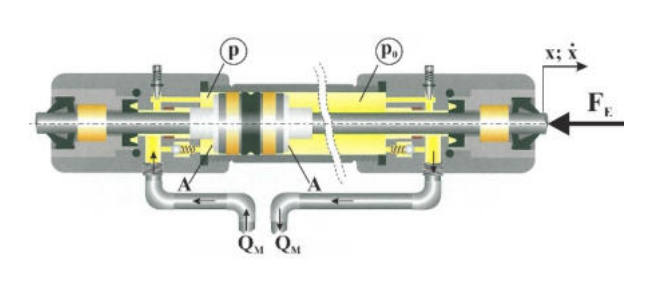
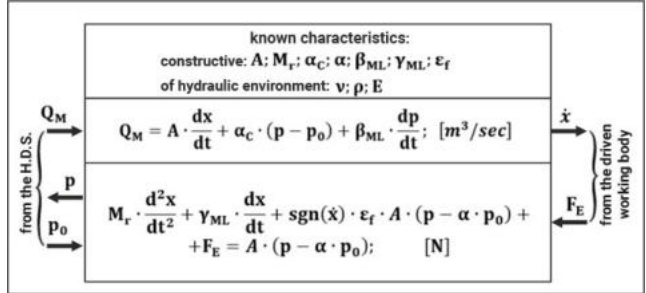


Fig. 5 (Figure 3.2): Hydraulic cylinder.



Dynamic mathematical model of a hydraulic cylinder.

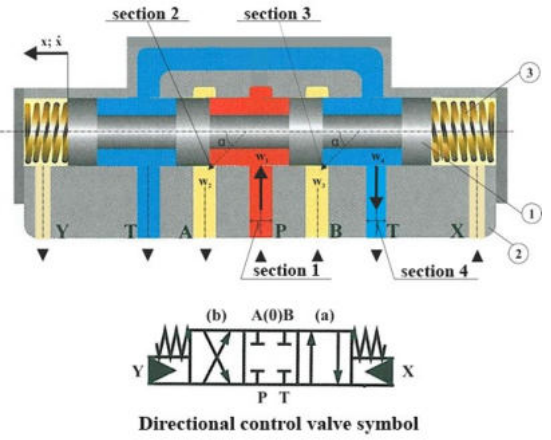
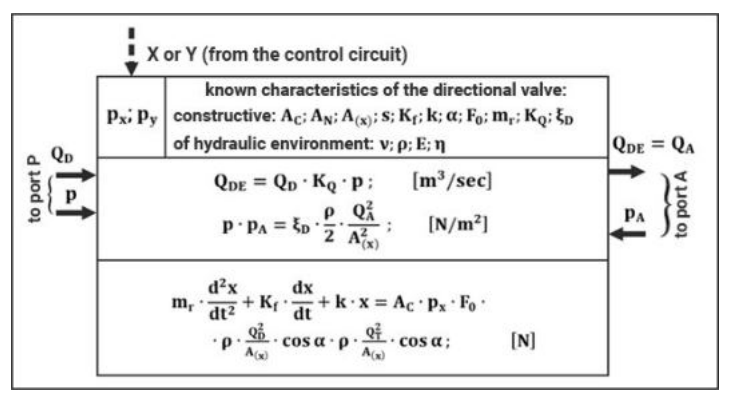
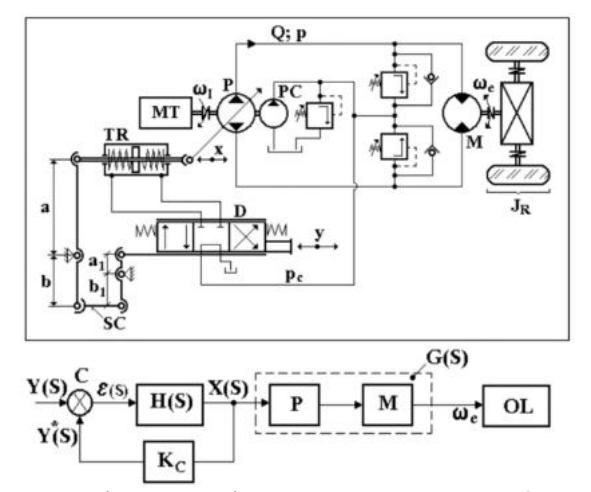


Fig. 6 (Figure 3.3): Hydraulically controlled spool directional valve.



Dynamic mathematical model of hydraulic directional control valves.



$$\omega_{HS} = \sqrt{\frac{E_r \cdot V_{0M}^2 + 4\pi^2 \cdot \alpha_{PM} \cdot \left(\gamma_M + \frac{V_{0M}}{2\pi} \cdot \delta_M\right) \cdot E_r}{4\pi^2 \cdot V \cdot J_R}}$$

$$\omega_C = \sqrt{\frac{k \cdot \Delta_2 + K_C \cdot A \cdot \Delta_1}{(m_{TR} + m_C) \cdot \Delta_2}};$$

$$\xi_C = \frac{1}{2} \cdot \frac{\gamma_R + \gamma_C + \frac{A}{\Delta_2}}{\sqrt{\left(k + K_C \cdot A \cdot \frac{\Delta_1}{\Delta_2}\right) \cdot (m_{TR} + m_C)}}$$

$$R(S) = \frac{\omega_e(S)}{Y(S)} = \frac{K_{SC} \cdot \omega_C^2}{S^2 + 2\xi_C \cdot \omega_C \cdot S + 1} \cdot \frac{K_{SE} \cdot \omega_{HS}^2}{S^2 + 2\xi_H \cdot \omega_{HS} \cdot S + 1}$$

Fig. 7 (Figure 3.4): Schematic diagram of the servo-system for hydrostatic proportional control of the capacity displacement of a pump connected to a closed-circuit primary control transmission, and its mathematical model.

Chapter 4 – Physical experimentation, in the laboratory, of a closed-circuit primary control hydrostatic transmission

This chapter had as its objective to experimentally determine, in the General Hydraulics Laboratory of INOE 2000-IHP, the control characteristic of the A10VG28 servo-pump connected to the A6VM28 servo-motor and the response of the hydrostatic transmission to a step signal.

The matrix of experiments has been designed in such a way that at the end of the testing the following questions could be answered:

- How long does it take for the servo-pump to reach maximum flow rate? Does this time depend on the load? What about from maximum flow rate to 0 (the neutral position of the servo-pump swash plate)?
- What is the maximum flow rate of the servo-pump? Does it depend on the load?
- What is the minimum flow rate of the servo-pump? Does it depend on the load?
- From what values of the control current is the pump flow rate proportional to it? Does it depend on the load?

Methodology of transmission and servo-pump experimentation

To achieve the previously mentioned objective, an existing bench of IHP intended for testing hydrostatic motors has been modified and transformed into a bench equipped with a closed-circuit primary control transmission. The physical embodiment of this test bench is shown in Fig. 8 (Figure 4.1) and Fig. 9 (Figure 4.2).



Fig. 8 (Figure 4.1): The experimental test bench front view.



Fig. 9 (Figure 4.2): The experimental test bench - side view.





Fig. 10 (Figure 4.3): The electric cabinet for the bench and electric motor control.

As one can see in Fig. 8 (Figure 4.1), Fig. 9 (Figure 4.2) and Fig. 10 (Figure 4.3), the test bench consists of four distinct components:

- The first of these components is the electric pump, which has an asynchronous electric motor with the power of 30 kW and the synchronism speed of 1500 rev/min as one of its parts and the A10VG28 servo-pump;
- Load simulation unit, comprising: the hydraulic oil tank, the panel with digital displays for speed, temperature and torque, the A6VM servo-motor and the F112A fixed displacement pump;
- Experimental data acquisition system, consisting of a laptop equipped with LabVIEW experimental data acquisition software, NI 6211 experimental data acquisition board, various transducers and a programmable voltage source;
- Electric cabinet for the bench and electric motor control, shown in Fig. 10 (Figure 4.3), with the following parts: 30-kW circuit breaker, star delta starter, 24 V power supply, 12 V power supply, 1P 10 A automatic fuse, 3P 1 A automatic fuse, IEM3255 three-phase meter with Modbus RTU communication and ±10 V proportional controller.

The hydraulic schematic diagram of the experimental test bench on which the research on the closed-circuit primary control hydrostatic transmission has been carried out is shown below in Fig. 11 (Figure 4.21).

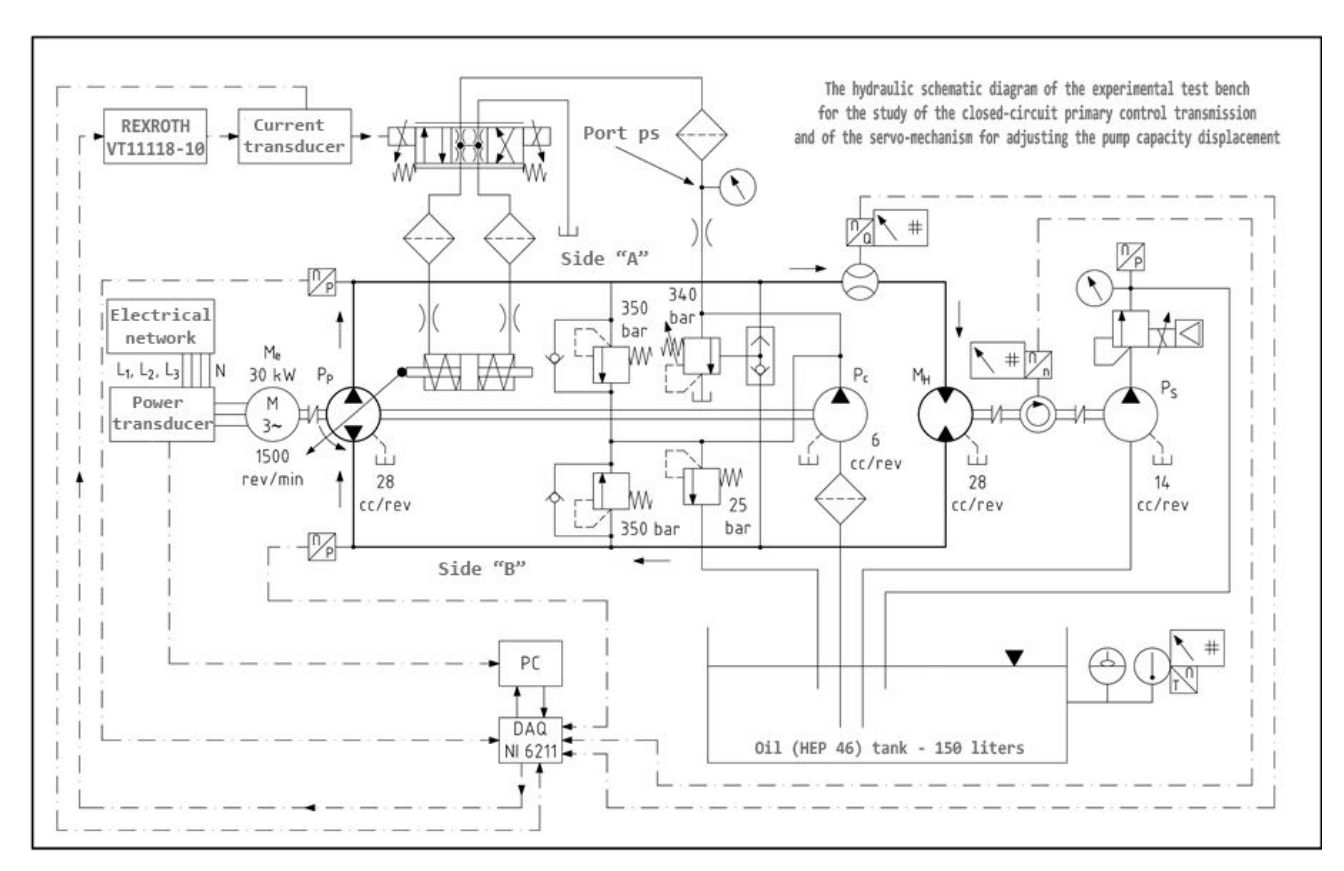


Fig. 11 (Figure 4.21): Hydraulic schematic diagram of the experimental test bench for the study of the closed-circuit primary control transmission and the pump displacement control servo-mechanism – The hydraulic diagram at a larger size can be found in Annex 25 (of the thesis).

Notations in the hydraulic diagram: M_e -electric motor, P_P - main pump, P_c - compensation pump, M_H - hydrostatic motor, P_S - load pump, DAQ - experimental data acquisition board, PC - laptop and REXROTH VT11118-10 - signal conditioner for driving the pump servo-mechanism.

Operation of the experimental test bench: one supplies the test bench with electricity and opens the LabVIEW application related to the experiment to be performed; from the electrical cabinet, the electric motor is turned on; one waits for it to switch from star to delta, and then presses the "start" button of the LabVIEW application. The control signal is transmitted from the PC to the experimental data acquisition board, which converts it to voltage (0 - 10 V); this voltage reaches the VT11118-10 proportional controller which conditions the signal and transforms it into the control current (0 - 600 mA) of the electromagnets of the proportional directional valve which is part of the pump displacement control servo-mechanism. The proportional directional valve controls the displacement of the hydraulic cylinder with bilateral rods; this displacement is directly proportional to the control signal, the swash plate angle, the main pump displacement, and its flow rate. After the swash plate angle exceeds the value of $+3^{\circ}$, the main pump discharges, on branch "A", a flow of hydraulic fluid that passes through the flow transducer and reaches the hydrostatic motor; the flow rate determines the speed rate of the hydrostatic motor, which is measured by the speed transducer; this speed rate drives the load pump, whose flow is forced through the proportional pressure control valve, which creates a resisting torque on the motor shaft; this torque is proportional to the pressure reached at the pressure control valve. Given the ratio of the displacement of the hydrostatic motor to that of the load pump, when on the high-pressure branch of the closed circuit the pressure is 70 bar, a pressure of 140 bar is installed at the proportional pressure control valve. The flow rate of the compensation pump, with a value of approximately 9 L/min at a pressure of 25 bar, provides the required flow rate to the servo-mechanism at a pressure of 20 bar, measured at port ps, compensates the volumetric losses of the pump with the help of check valves, and the rest of the flow drains to the tank through the pressure control valve set at 25 bar. The throttle between the compensation pump and the proportional directional control valve is meant to limit the pressure pulsations of the compensation pump that would reach the directional control valve. The throttles on the ports of the hydraulic cylinder have the role of equalizing its displacement speed and delaying the response of the servo-mechanism to the control signal. The pressure control valves set at 350 bar act as safety valves, and the pressure control valve (set at 340 bar) which is controlled by the pressure in the closed circuit branches via the selector valve has the role of reducing the pump capacity if the pressure in the closed circuit exceeds the set value. The power transducer directly communicates to the PC the time-variation of the power absorbed by the electric motor, and the rest of the transducers transmit to the PC, by means of the experimental data acquisition board, signals proportional to the parameter values measured by them. After the data acquisition completion condition has been reached, the acquisition stops automatically; then the electric motor and the power supply to the stand are switched on; after performing these operations, the results of the experiment can be saved.

Results of physical experimentation in the laboratory

In order to answer the questions posed at the beginning of this chapter, the experiments have been divided into two main categories:

- Response to step signal (A)
- Control characteristic (B)

A. The experiments related to **the response to step signal** have been, in turn, divided as follows:

- With load created by the hydrostatic motor:
 - response to step signal
 - lag detail

- With no load, short-circuiting the closed circuit with a 90° bend
 - o response to step signal
 - lag detail

B. The experiments related to **the control characteristics** have been, in turn, divided as follows:

- With load created by the hydrostatic motor:
 - o and the maximum control signal
 - o and the minimum control signal
- With no load, short-circuiting the closed circuit with a 90° bend
 - o and the maximum control signal (experiment not presented in this summary)
 - o and the minimum control signal (experiment not presented in this summary)

A10VG28EP4 servo-pump response to step signal

The LabVIEW application for step signal response uses 4 (four) analog 0 – 10 V inputs from the data acquisition board: electromagnet current, servo-pump flow rate, pressure on branches "A" and "B". An analog output of the acquisition board is used for control. The parameter values shown on the graphs are scaled from the voltage signal (1...5 V) to the measurement ranges of the transducers. The control signal is connected to the input of the controller that controls the pump flow rate. The application panel - Fig. 12 (Figure 4.22) - The application panel includes graphical blocks for: current, flow rate, control signal, and PA and PB values. The step signal is controlled, at a value that can be set in the range 0...10 V, with the help of a button on the application panel.

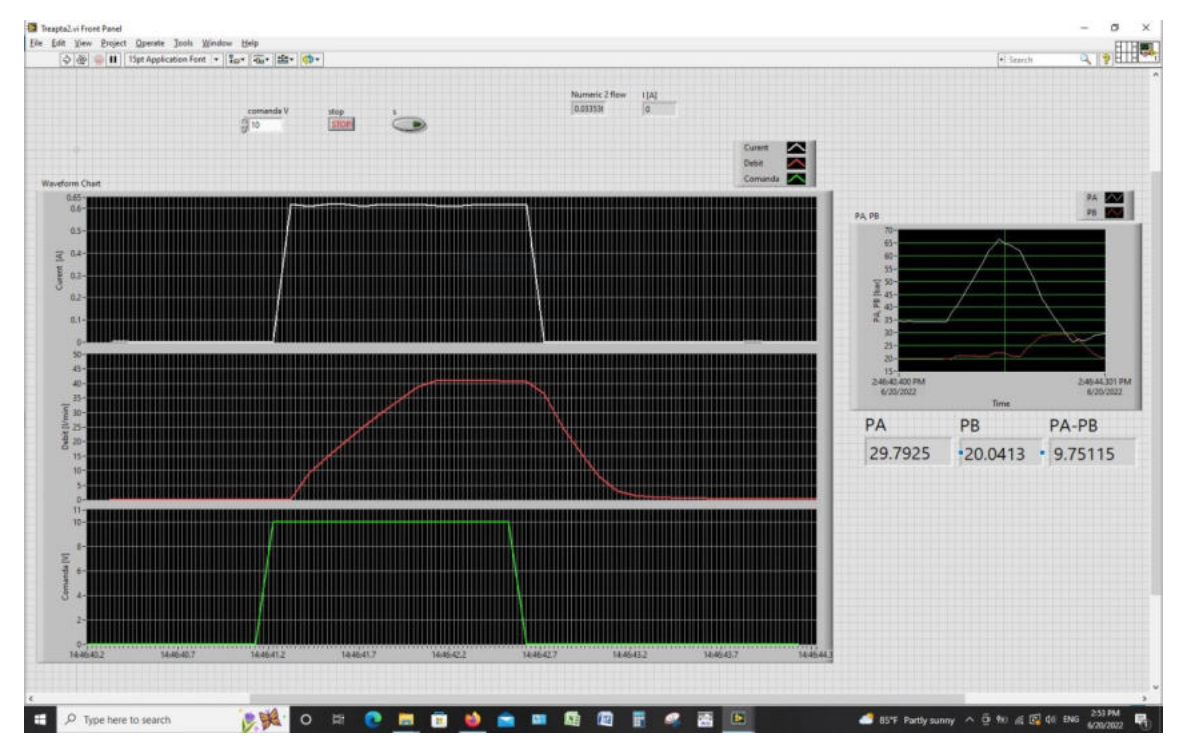


Fig. 12 (Figure 4.22): Application panel – A10VG28EP4 servo-pump response to step signal.

To be able to have an overview of the experiments in this section of the chapter and for an easier interpretation of the results of the experiments carried out, the experimental data related to the servo-pump flow rate, measured with the flowmeter placed in the closed circuit, have been imported into MS. Excel. There, the four curves have been superimposed so that the lag shown in Fig. 13 (Figure 4.28) can be read on the "X" axis of the graph.

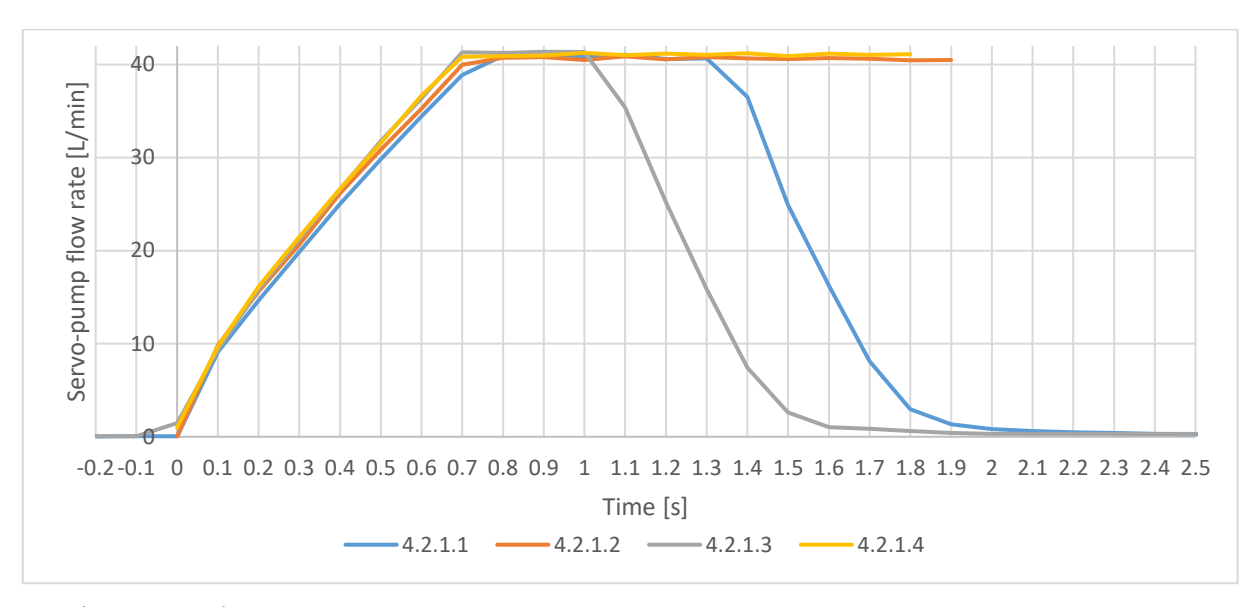


Fig. 13 (Figure 4.28): Response to step signal – centralized results.

A10VG28EP4 servo-pump flow rate/control characteristic and transmission characteristic

The application panel related to the experimentation with load created by the hydrostatic motor and the maximum control signal is shown in Fig. 14 (Figure 4.38), while for the minimum control signal the application panel is shown in Fig. 15 (Figure 4.40). These panels contain pump and transmission characteristics on the first row, and on the second row, as a function of time, there are shown variation of power absorbed by the electric motor, variation of the control current of the proportional directional valve in the servo-pump structure, and pressure variation on the branches of the closed circuit.

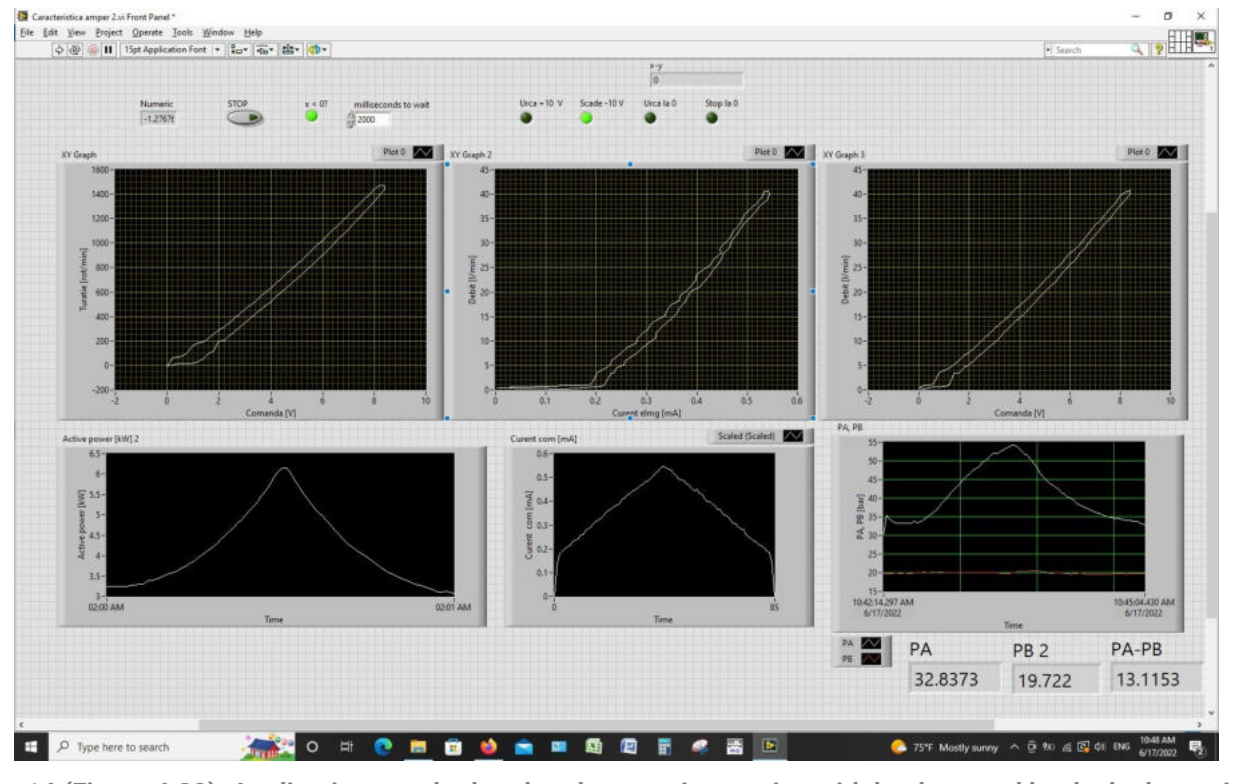


Fig. 14 (Figure 4.38): Application panel related to the experimentation with load created by the hydrostatic motor and the maximum control signal.

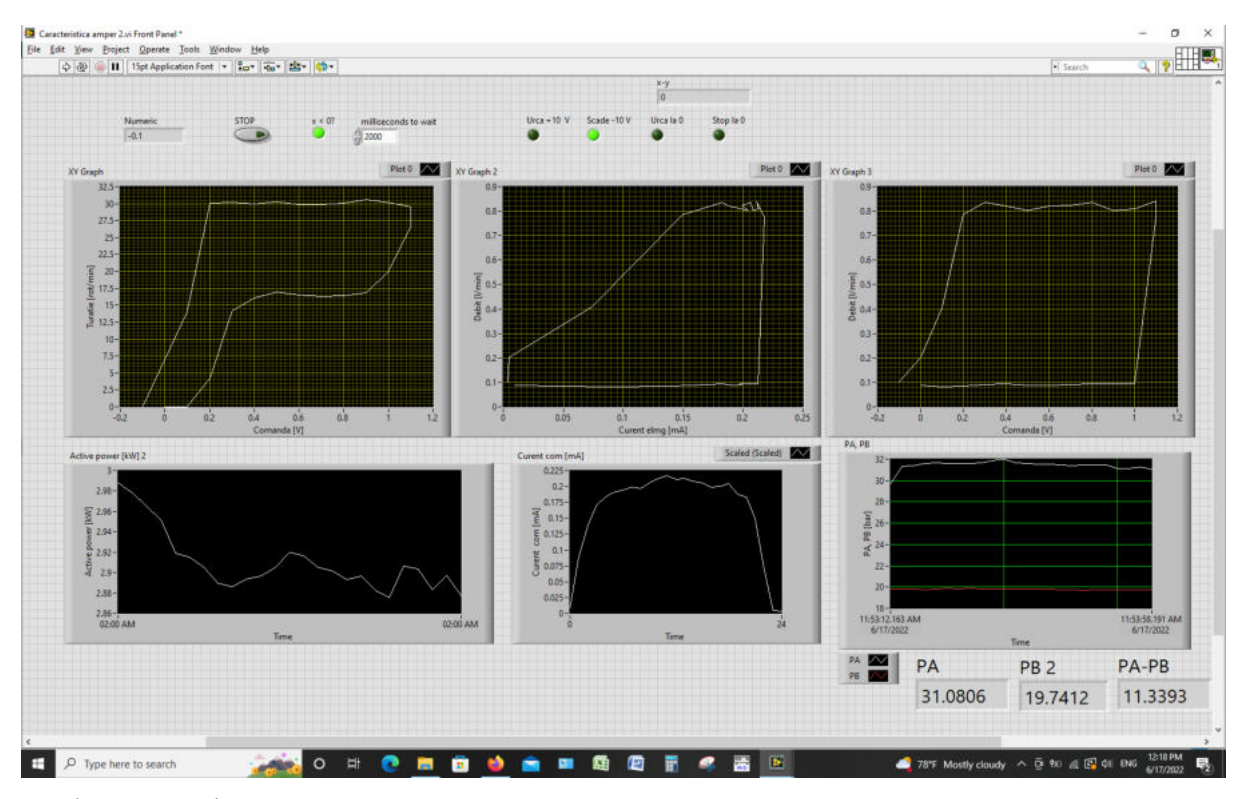


Fig. 15 (Figure 4.40): Application panel related to the experimentation with load created by the hydrostatic motor and the minimum control signal.

Conclusions of the laboratory experimentation

The answers to the questions posed at the beginning of this chapter, answers resulting from the experiments, are presented in the following paragraph.

- The time needed for the servo-pump to reach maximum flow rate varies between 0.83 seconds and one second; it is measured between the time when the voltage control signal has been given and the time when the pump has reached maximum flow rate. If we exclude the time for processing the electrical signals from the calculation, one can see that the servo-pump reaches the maximum flow rate in 0.7 0.8 seconds. Regardless of the angle of the pump swash plate (0° or 33°) from which the voltage control is given, or of the load in the closed circuit, the servo-pump reaches maximum flow rate or 0 flow rate in no more than one second.
- The maximum theoretical flow rate of the servo-pump if it were to be driven at the synchronism speed of the asynchronous electric motor, is 42 L/min; two values have been determined experimentally, 40.77 L/min (with load) and 41.17 L/min (no load). The maximum flow rate of the servo-pump is load dependent: in proportion to the increase in pressure, volumetric losses also increase. The flow rate of the servo-pump is also influenced by the variation of the speed rate of the asynchronous motor; this variation occurs as a result of the slippage between the stator and the rotor of the electric motor, which slippage is influenced by the resistive torque on its shaft, which torque is directly proportional to the pressure in the closed circuit.
- The minimum flow rate of the servo-pump is 0.116 L/min; it depends on the load since volumetric losses are proportional to pressure. The minimum flow rate is 0.2762% of the maximum theoretical flow rate of the servo-pump at a speed of 1500 rev/min, (0.116/42 * 100 = 0.2762 %).
- The pump flow rate becomes proportional to the control signals from the value of about 0.8 L/min, proportional adjustment starting from the voltage value of 1.1 volts

and the control current value of **215 mA**. The proportional relationship between the servo-pump flow rate and the control current is not significantly influenced by the load (pressure) in the closed circuit as long as the pump is operated at the nominal conditions specified by the manufacturer; the increase in pressure causes the increase in volumetric losses, and the latter reduce the flow rate for the same control current.

The results of the experiments presented in this chapter have been used in Chapter 5 for parameterization and validation of numerical simulations.

Chapter 5 – Optimization and virtual experimentation using numerical simulation

5.1 Virtual experience of the A10VG28EP4 servo-pump

This subchapter continues the research presented in Chapter 4, using it to parameterize and validate the numerical simulation model of the servo-pump and the electronics that controls its displacement volume. The numerical simulation model of the servo-pump, created in this subchapter and validated by previous experiments, will be integrated into the numerical simulation of the motor truck equipped with a hydrostatic transmission.

Methodology of virtual experimentation of the servo-pump

The initial data of the experimentation and those of the numerical simulation of the servopump are identical, including the control signal. In this subsection, the initial parameters of the components will be presented briefly; they, together with the simulation settings, can be found in detail in Annex 34 (of the thesis), in order to fully meet the research reproducibility requirements.

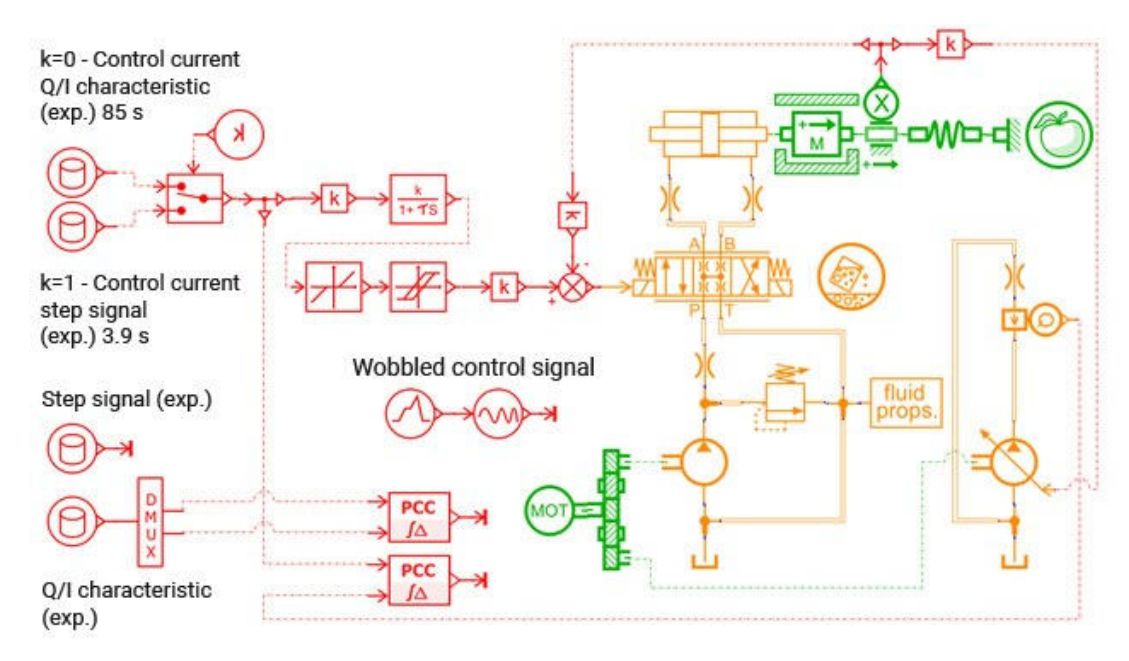


Fig. 16 (Figure 5.2): Servo-pump simulation network.

The servo-pump simulation network is presented in Fig. 16 (Figure 5.2); on it, one can identify: in green color - mechanical components, in red - electronic components or those

carrying various signals, and in orange - hydraulic components, which also take thermal phenomena into account; without them, the results of the numerical simulation could not have been compared with the results of the laboratory experiments. The current control signal is the one determined experimentally; it passes through the electronic blocks, which condition it and send it to the servo-mechanism that controls the pump displacement volume (flow rate) proportional to the value of the control current. The main pump has a displacement of 28 cm³/rev, and the compensation pump - a displacement of 6 cm³/rev, the hydraulic fluid is ISO VG 46, and the pressure control valve is set at 20 bar.

Servo-pump response to step signal

In Fig. 17 (Figure 5.9) one can see that the time-variation of the simulated servo-pump flow rate is almost identical to the experimental one; the control current is common.

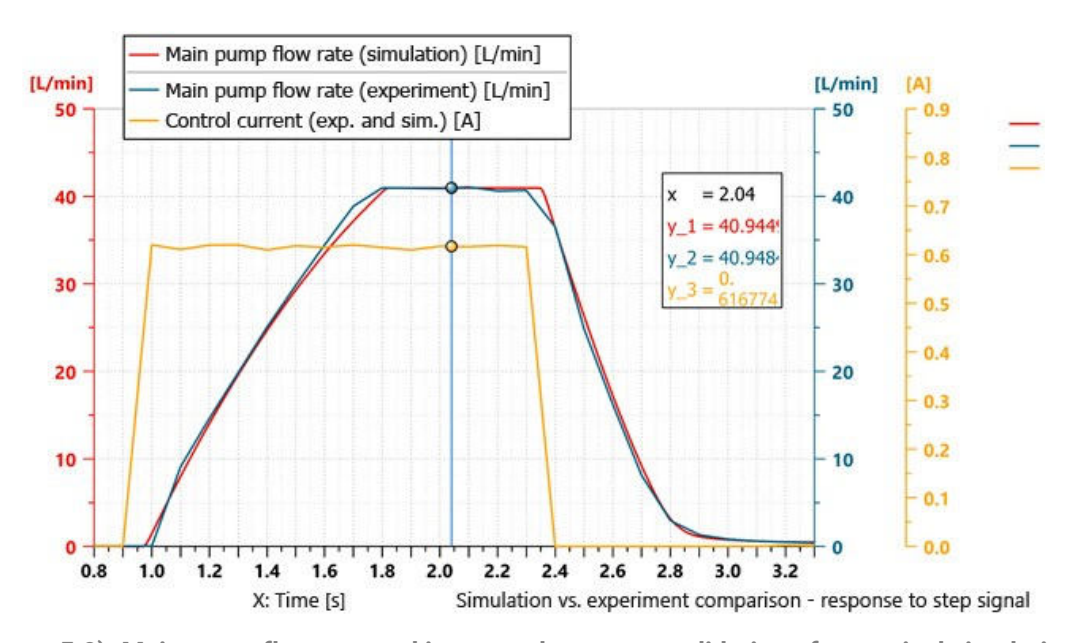


Fig. 17 (Figure 5.9): Main pump flow rate and its control current – validation of numerical simulation.

Flow rate/control characteristic of the servo-pump

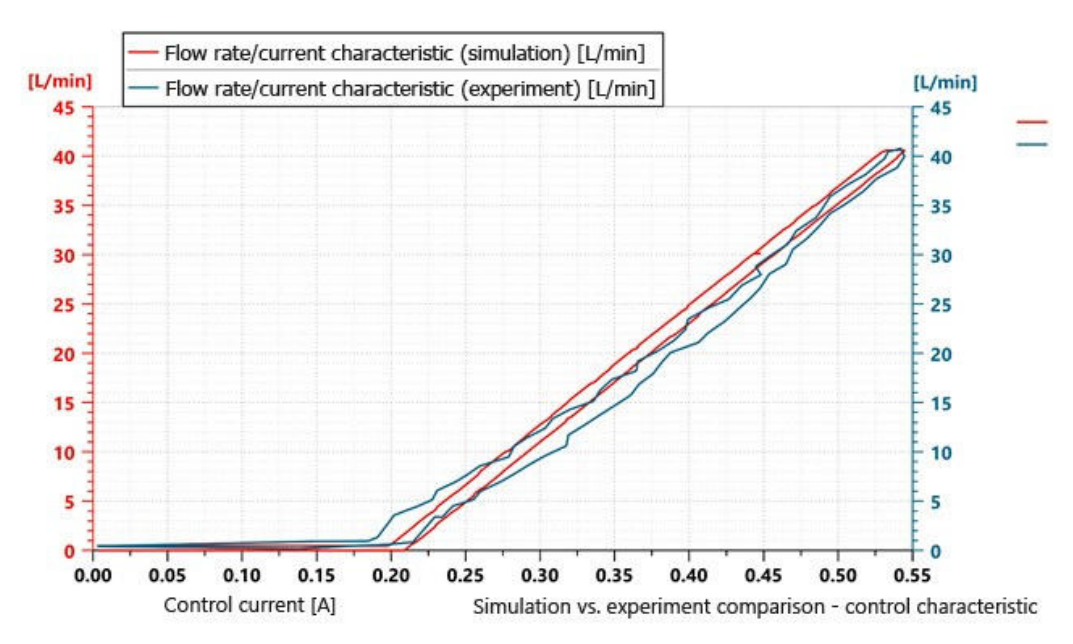


Fig. 18 (Figure 5.16): Flow rate/control current characteristic - validation of numerical simulation results.

In Fig. 18 (Figure 5.16) one can see that the simulation results coincide with those of physical experimentation; the maximum flow rate is identical, and the current value from which the control of the pump displacement starts is similar; in this case, too, the control current is common.

The linear correlation coefficient, Fig. 19 (Figure 5.17), estimates - as the name suggests - the linear correlation of two signals (physical parameters), in the present case, the linear correlation of the pump displacement control current, measured in amperes, and the servo-pump flow rate. A value of 0 or close to 0 of this coefficient indicates no linear correlation of the two signals, while a value close to 1, whether positive or negative, indicates a good linear correlation of the two signals.

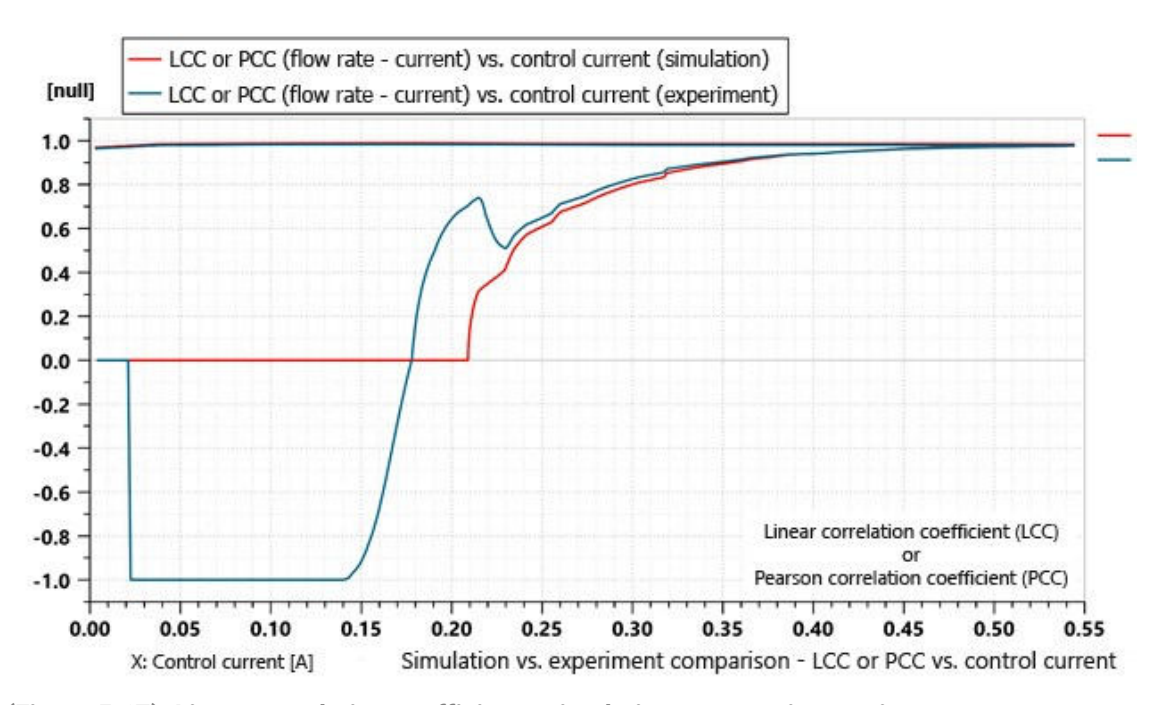


Fig. 19 (Figure 5.17): Linear correlation coefficient - simulation vs. experimentation.

The control current with which the displacement of servo-pumps for mobile applications is controlled has an insensitive "dead zone", in which the pump rate flow does not respond to the control signal, to avoid the alternate rectilinear movement of the motor truck when the swash plate of the servo-pump is in the neutral position and oscillates around it. In this case, the numerical simulation shows a superior linear correlation of the control current and the pump flow rate, because in simulation the conditions can be better controlled.

Frequency response of the servo-pump to the wobble control signal

Frequency response of the servo-pump flow rate to the wobble control signal - constant amplitude and variable frequency control signal - is necessary for the correct tuning of the PID controller in the structure of the hydrostatic transmission of the motor truck.

Frequency response of the servo-pump flow rate is shown in Fig. 20 (Figure 5.20); on this graph, one can see what percentage of the flow rate amplitude is still available for a certain frequency, and also the phase shift. Comparing the results in this figure with the characteristics of the pump P7, one can see that the pump P7 achieves small amplitude flow rates at a maximum frequency of 17 Hz and a pressure of 70 bar, and the simulation reveals that the simulated servo-pump achieves small amplitude flow rates at 12 Hz, at a pressure of 20 bar.

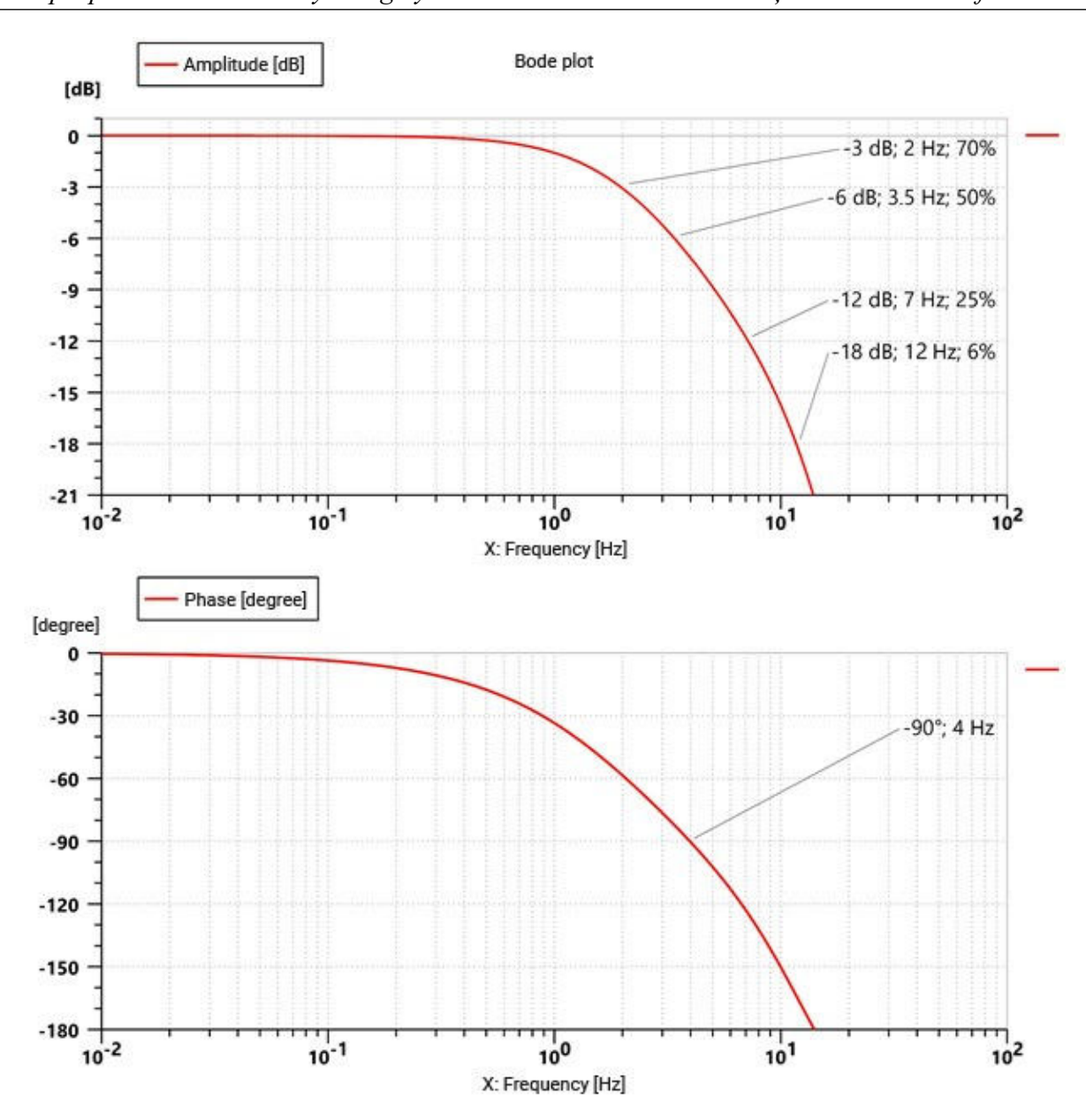


Fig. 20 (Figure 5.20): Bode plot for frequency response of the servo-pump flow rate.

5.2 Virtual experimentation and optimization of the subsystems of a closed-circuit primary control hydrostatic transmission

This subchapter aims to study the influence that reducing the energy consumption of the subsystems has on the hydrostatic transmission.

Methodology of virtual experimentation of hydrostatic transmission subsystems

For the study of closed-circuit primary control hydrostatic transmission subsystems, the simulation network shown in Fig. 21 (Figure 5.21) has been developed. This shows the three transmissions, each with a different subsystem. All the main pumps, the ones with variable flow rate, have a displacement of 210 cm³/rev; all of them are driven at 1000 rev/min and receive the same control signal for the time-variation of the displacement. The pressure control valves in the closed circuit are all set at the maximum pressure prescribed by the manufacturer, that is 500 bar. All hydrostatic motors have the same displacement, 1400 cm³/rev, and all load simulation mechanisms are identical.

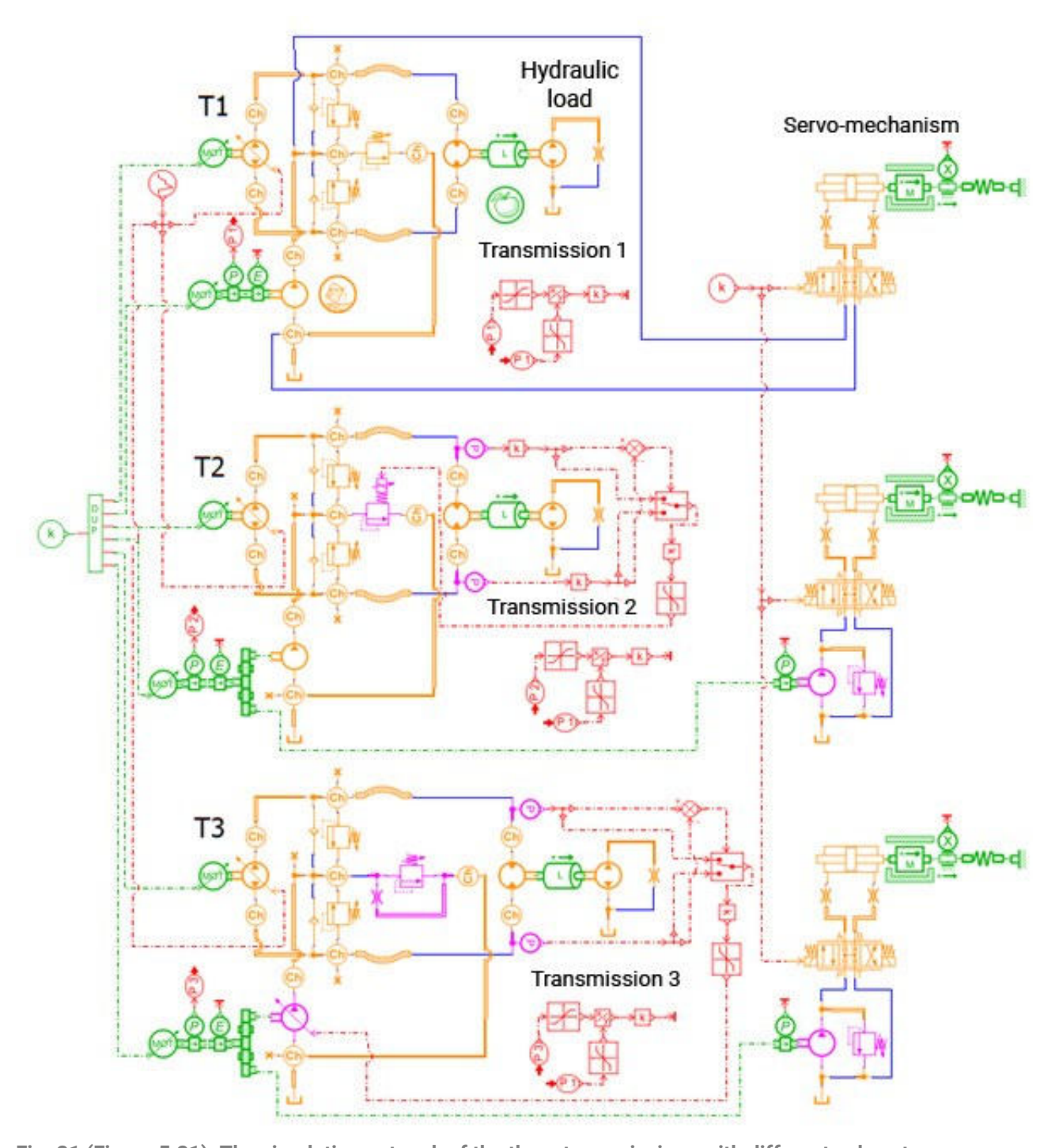


Fig. 21 (Figure 5.21): The simulation network of the three transmissions with different subsystems.

The servo-control mechanisms in this simulation do not have a functional role; they only act as energy consumers. In order to fully meet the research reproducibility requirement, the initial parameters of the simulation, in their entirety, as well as the numerical simulation settings, can be found in Annex 35 (of the thesis). As one can see from the simulation network, certain hydraulic components are highlighted in purple; these are the different components of the 3 subsystems, and in the following, the differences between the 3 transmissions will be presented in detail.

Transmission no. 1 is the classic one; its role is control and benchmarking with the other transmissions. It is equipped with a compensation pump with a displacement of 46 cm³/rev, and the valve of this pump is set at the value of 25 bar, which is standard for closed-circuit hydrostatic transmissions.

Transmission no. 2 has a proportional pressure control valve in its structure, which replaces the compensation pump pressure control valve. Two pressure transducers can also be noted on the same figure, located on the branches of the closed circuit; they are connected to a series of electronic blocks, which have the role of comparing the two pressures and selecting the greater one. The two amplifiers in close proximity to the pressure transducers have the role of setting a minimum pressure rate for the maximum pressure selection system to work properly. The amplifier between the signal selection block has the role of scaling the pressure from the values in the closed circuit (500 bar) to the maximum value of 25 bar, at which the proportional pressure control valve is set; the last electronic block, the one before the proportional pressure control valve, has the role of setting the minimum and maximum limit of the valve pressure. The role of this system is to adjust the pressure in the compensating circuit in proportion to the pressure in the closed circuit. A very small displacement pump (control pump) and its associated pressure control valve have been added to the transmission, because the compensation pump pressure was no longer high enough for the servo-mechanism to work properly.

Transmission no. 3 is similar to transmission no. 2, with the exception of the fact that depending on the pressure in the closed circuit, the flow rate of the compensation pump is adjusted proportionally. The minimum pressure of the hydraulic compensating circuit (5 bar) is controlled by the throttle, and when the pressure drop on the throttle exceeds 10 bar, the flow rate of the compensating pump passes through the pressure control valve acting as a safety valve. In this case, too, a control pump is required, because the pressure in the compensation circuit is no longer high enough to meet the demands of the servo-mechanism.

Presentation of the results of the virtual experimentation of the hydrostatic transmission subsystems

The time-variation of the power consumed by the subsystems of the 3 transmissions can be found in Fig. 22 (Figure 5.34). On this graph, one can see that, in the worst-case scenario, the subsystem of transmission no. 3 consumes only one third of the power consumed by the subsystem of transmission no. 1.

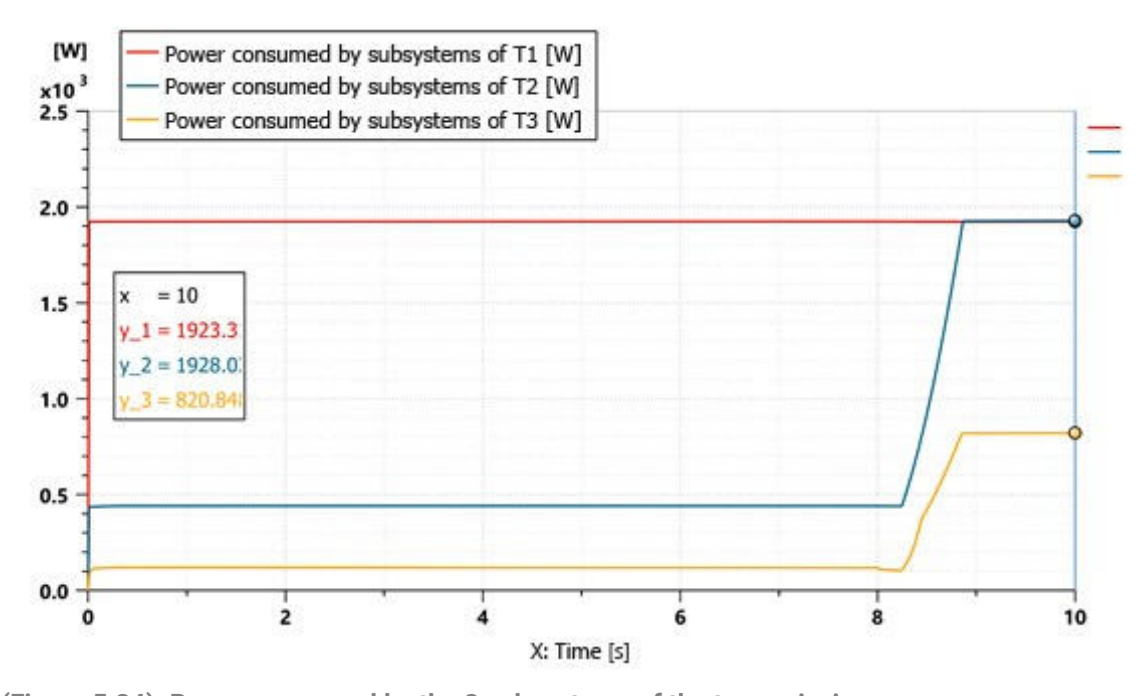


Fig. 22 (Figure 5.34): Power consumed by the 3 subsystems of the transmissions.

In Fig. 23 (Figure 5.36), one can see that subsystem no. 2 consumes, on average, 59.2%, and subsystem no. 3 consumes, on average, 25.8% of the power consumed by transmission subsystem no. 1.

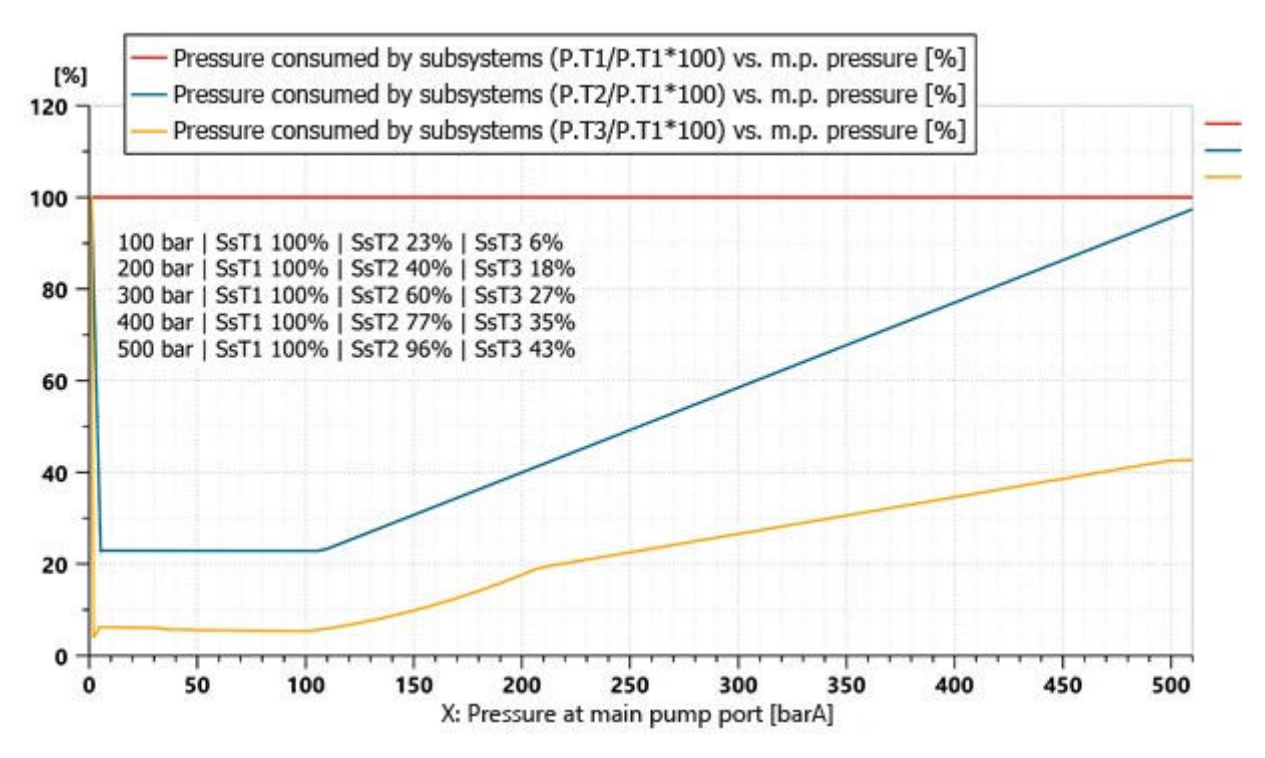


Fig. 23 (Figure 5.36): Power consumed by the 3 subsystems, expressed as a percentage, depending on the pressure in the closed circuit, relative to the consumption of subsystem no. 1.

Fig. 24 (Figure 5.37) shows the time-variation of the energy consumed by the 3 subsystems of the transmissions for the torque produced by the 3 hydrostatic motors and their speed rate.

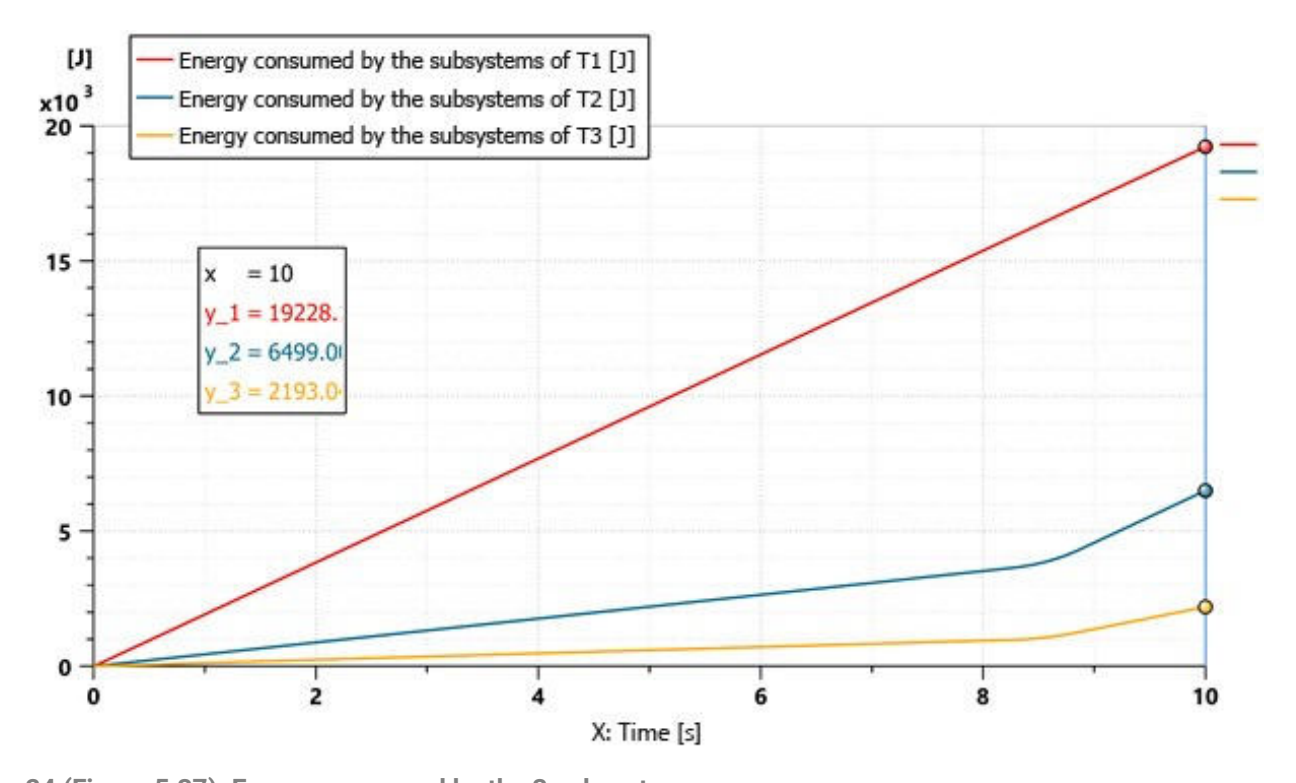


Fig. 24 (Figure 5.37): Energy consumed by the 3 subsystems.

Conclusions of virtual experimentation of hydrostatic transmission subsystems

The energy consumption of hydrostatic transmission subsystems can be considerably reduced by adopting the constructive solutions presented in this subchapter, with no negative impact on the components of the transmissions or on their control performance.

On average, subsystem no. 3 consumes only 25.8% of the power consumed by subsystem no. 1; comparing the same subsystems from the point of view of energy consumption, subsystem no. 3 consumes only 11.4% of the energy consumed by subsystem no. 1, for the duty cycle presented.

The variable flow rate of the compensation pump in subsystem no. 3 does not necessarily have to be supplied by a servo-pump; this flow rate varies between 10 and 44 L/min and can be achieved using a gear pump with a displacement of 11 cm³/rev, driven by an electric motor with variable speed ranging from 1000 to 4000 rev/min; this would consume 770 W at most, and the only condition that must be met for optimal operation of the gear pump is to ensure, as in the case of all pumps, a suction pressure equal to the atmospheric pressure, regardless of the speed rate at which the pump is driven. The solution presented in subsystem no. 2 is less complex, but achieves lower energy savings.

5.3 Virtual experimentation of a multipurpose motor truck and optimization of its dynamic parameters by equipping it with a closed-circuit primary control hydrostatic transmission

The numerical simulation in this subchapter combines and uses all the results and conclusions of the previous subchapters; all previously presented research coalesces in this subchapter to fulfill the aim of the thesis.

At the end of the experimentation with the help of numerical simulation, done in this subchapter, it will be possible to answer the following questions:

- Which are the dynamic parameters of the multipurpose motor truck, equipped with a hydrostatic transmission that have been improved, compared to a motor truck equipped with a mechanical transmission, in the first gear?
 - o Which is the maximum travel speed?
 - o Which is the minimum travel speed?
- Which is the maximum slope that the multipurpose motor truck can travel upwards on?
- How long does the multipurpose motor truck take to reach its maximum travel speed?
- How accurate is the speed control of the multipurpose motor truck?
 - In the case of steady-state control of the travel speed;
 - And in the case of continuous control of the travel speed.

To achieve the parameters mentioned in Chapter 2, it is necessary to choose a truck platform that has enough variants available and allows the various interventions necessary to be equipped with the hydrostatic transmission. To this end, the platform made available by MAN, TGM 18.320 model, with all-wheel drive and two axles - Fig. 25 (Figure 5.38), has been chosen; this model has the maximum authorised mass in Europe of 18 tonnes and the net mass on delivery, with full tank and with driver, of 6 tonnes; it has been estimated that a

maximum of 2 tonnes will be added to this mass by the integrator, resulting in the possibility of loading the motor truck with another 10 tonnes. The tires on both axles of the truck are sized 295/80R22.5. The motor truck is equipped with a heat engine of 320 horsepower; the D0836 LFL52 model delivers 240 kW at maximum speed rate of 1900 rev/min, maximum speed which is specified in the intervention manual of this series of trucks; the torque developed by the heat engine at the minimum speed of 1000 rev/min is 1020 Nm, Fig. 26 (Figure 5.39), and minimum travel speed, at the same rpm, is 2.16 km/h.



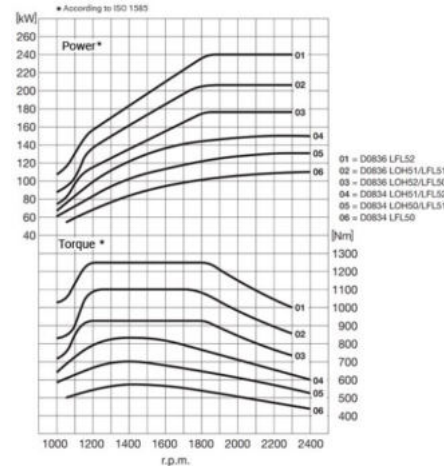


Fig. 25 (Figure 5.38): MAN TGM 18.320 motor truck with 4x4 drive.

Fig. 26 (Figure 5.39): Torque and power characteristic of the D0836 LFL52 heat engine depending on its rpm - Annex 36 (of the thesis).

The motor truck simulation network is shown in Fig. 27 (Figure 5.43); this integrates the volumetric efficiency of the main pump from the previous simulation. The servo-pump is connected to the power take-off (NMV 221) of the heat engine, which can transmit a maximum torque of 2000 Nm.

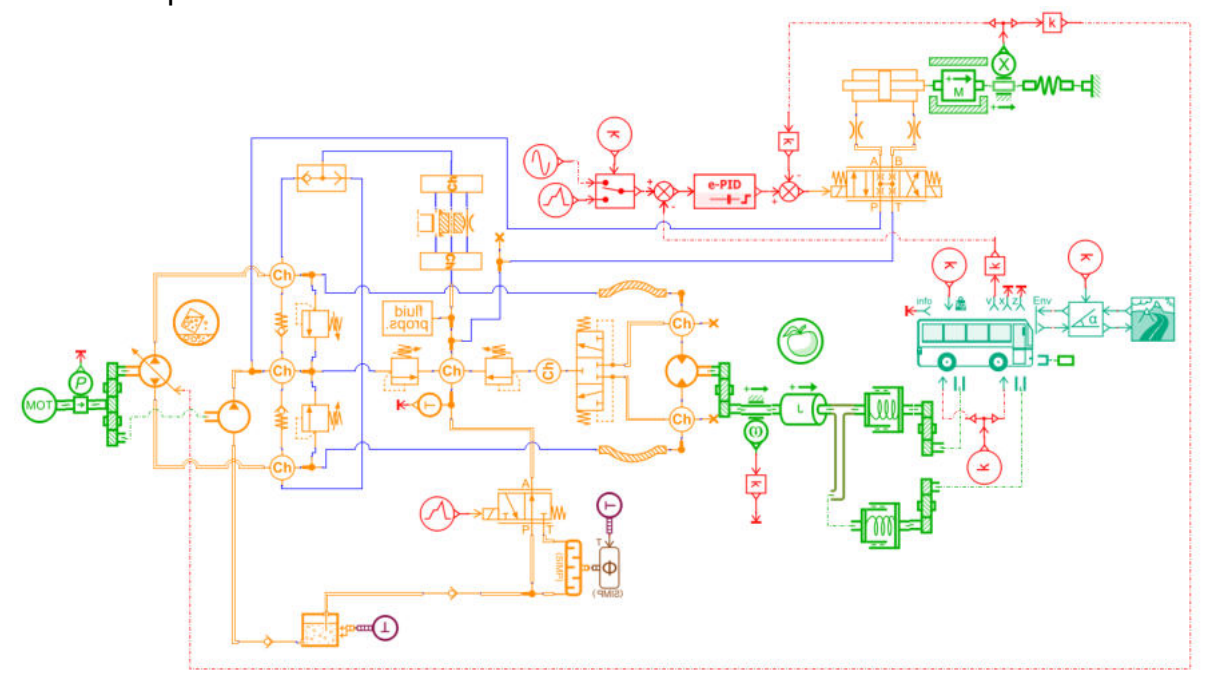


Fig. 27 (Figure 5.43): The simulation network of the motor truck equipped with closed-circuit primary control hydrostatic transmission.

The initial parameters of the simulation are: the speed of the heat engine is constant and has a value of 1000 rev/min; the main pump displacement is 210 cm³/rev and is variable,

and that of the compensation pump is 32 cm³/rev; the pressure control valves in the closed circuit are set at the value of 450 bar, the pressure control valve of the compensating circuit is set at 25 bar, and the pressure control valve of the flushing valve is set at 20 bar; the hydrostatic motor, model CDM10, has a displacement of 1352 cm³/rev; the pump displacement control servomechanism is identical to the one in the previous chapters, being experimentally validated. The transmission ratio of the transfer case has the value of 1.625 and the value of 1.007, and that of the differentials has a value of 4, according to Annex 37 (of the thesis). The total mass of the motor truck is 18 tonnes; tire size is 295/80R22.5; the motor truck model is detailed; coefficients of friction, longitudinal slip (skidding of the tires on the asphalt), distribution of the load on the axles of the motor truck (60% on the rear axle and 40% on the front axle), moment of inertia of the wheels, air friction and road slope are all taken into account.

The numerical simulation also has a PID controller with "feedforward", "feedback" and advanced capabilities for compensation of non-linear phenomena. Automatic tuning of the PID controller is shown in Fig. 28 (Figure 5.44); on it, one can see that the maximum frequency of the signal transmitted to the pump displacement control servo system does not exceed 22 Hz; also in this figure one can see that the application assesses the system as stable, and the response time to step signal, 0.8 – 0.9 seconds, is identical to that from laboratory experiments or from previous simulations.

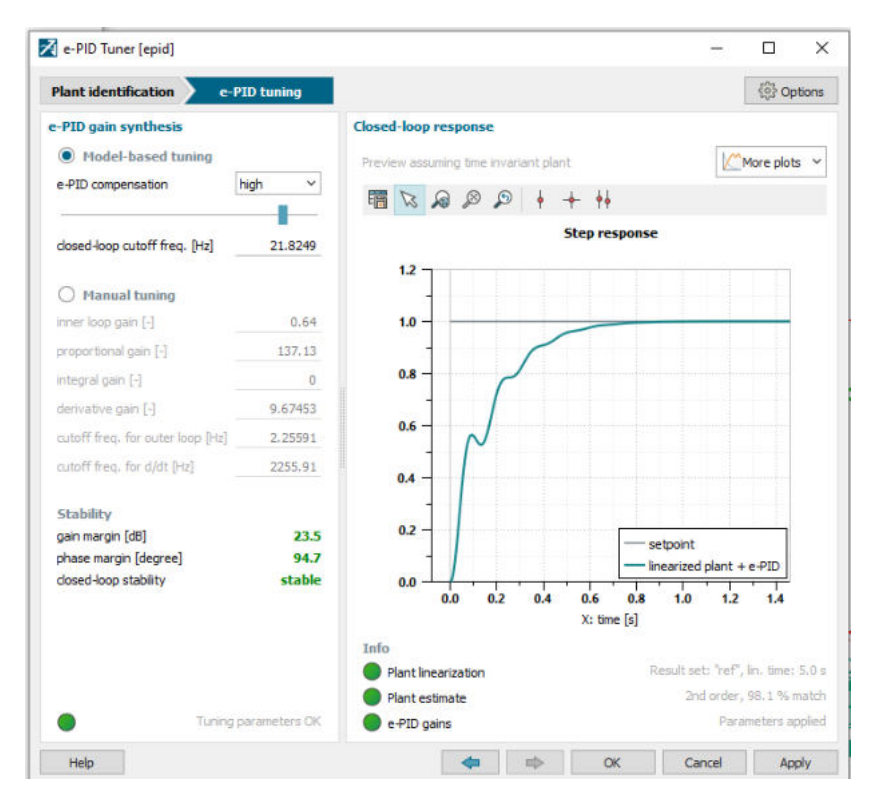


Fig. 28 (Figure 5.44): PID controller automatic tuning and the response to step signal.

In the numerical simulation, the library of hydraulic components has been used, which also simulates the thermal phenomena that occur during operation; the hydraulic fluid model, ISO VG46, takes into account the content of dissolved and undissolved gases in the hydraulic oil; density and viscosity are temperature dependent; the compressibility and inertia of the hydraulic fluid are taken into account, as well as the elasticity and capacitance of the hydraulic lines. The simulation model also includes a hydraulic fluid cooling system; the 3/2 proportional directional control valve next to the heat exchanger could act as a thermostat, along with the temperature transducer located on the discharge of the pressure

control valves; the 3/2 directional control valve has been used to bypass the cooling circuit and study the behaviour of the transmission without cooling. Since cavitation on the suction port of pumps is a problem in closed-circuit hydrostatic transmissions, advanced cavitation modeling laws have been used.

Results of the virtual experimentation of the motor truck

Continuous control of the technological travel speed of the motor truck simultaneously with going up and down a slope with a 45% gradient and maximum authorised mass

In Fig. 29 (Figure 5.45) one can notice the time-variation of the torque consumed by the transmission - it does not exceed the maximum value that the heat engine can provide, while Fig. 30 (Figure 5.46) shows the time-variation of the main pump parameters; these parameters do not exceed the maximum values.

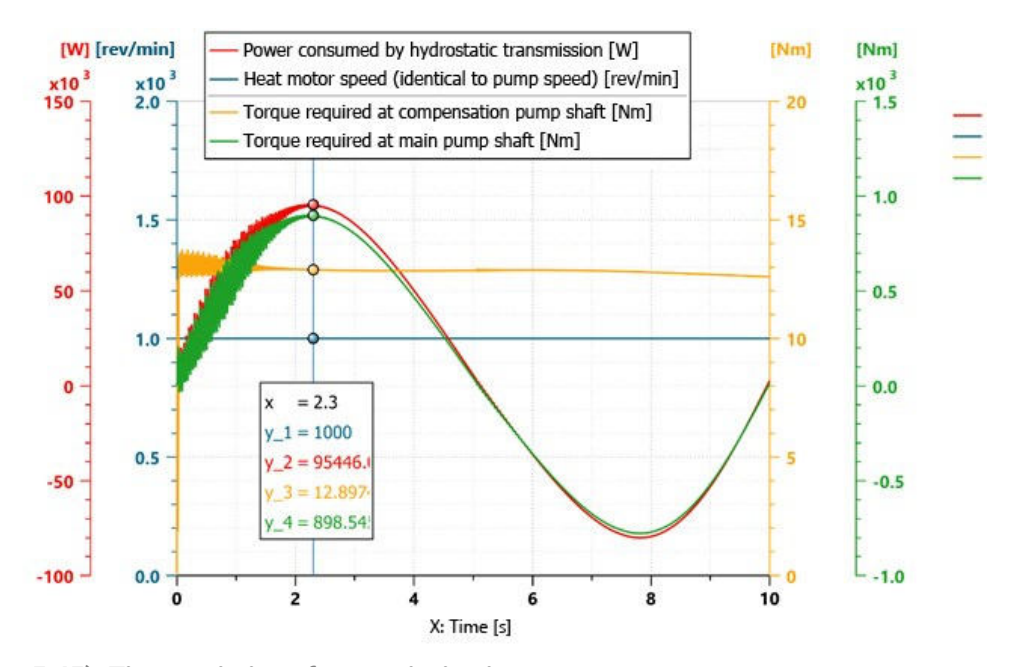


Fig. 29 (Figure 5.45): Time-variation of transmission input parameters.

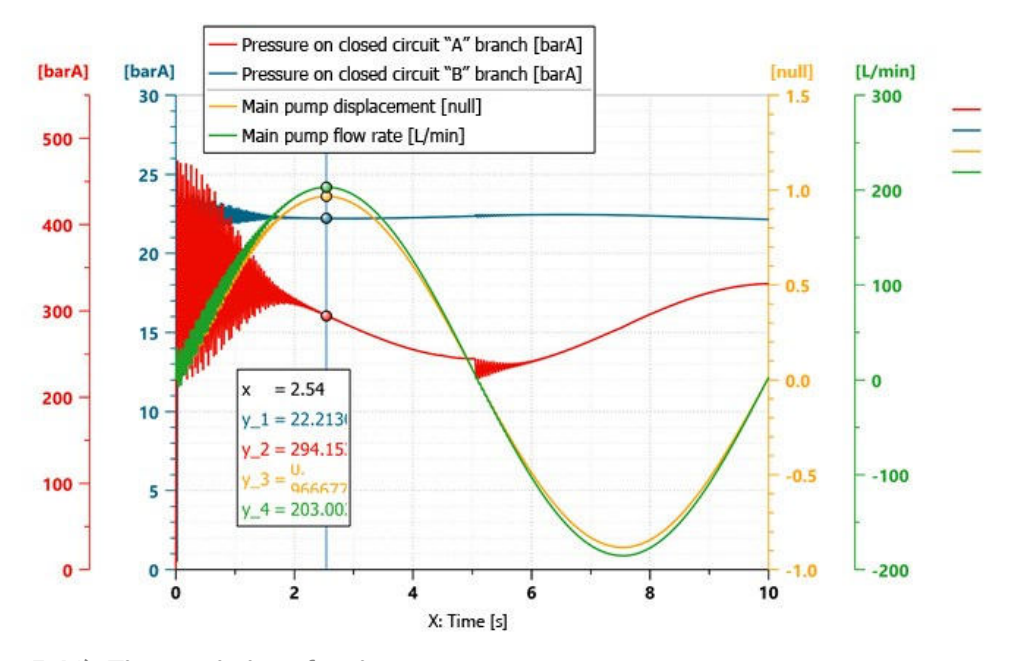


Fig. 30 (Figure 5.46): Time-variation of main pump parameters.

In Fig. 31 (Figure 5.57) one can notice the behavior of the motor truck upon startup, on a slope. As the mass distribution on the two axles is different (60% on rear axle and 40% on front axle), the percentage of longitudinal wheel slip is different. In Fig. 32 (Figure 5.58) the traction parameters of the motor truck can be seen.

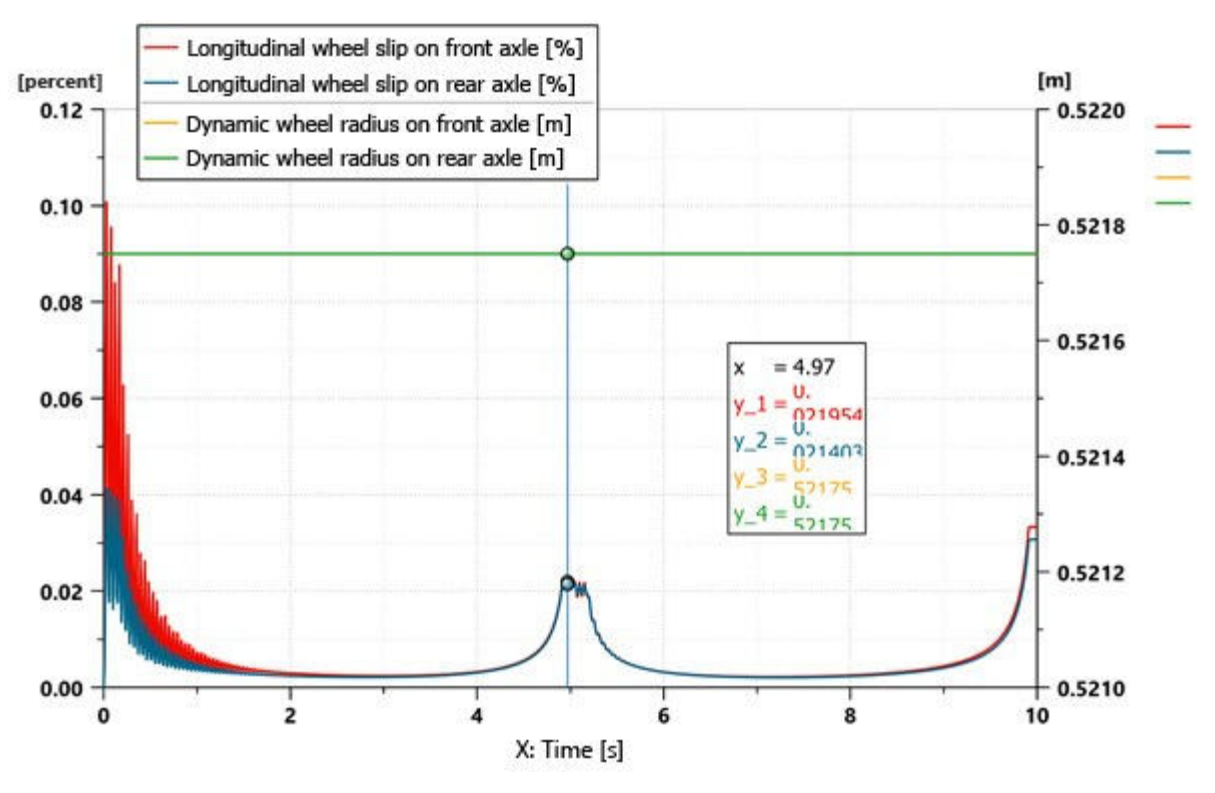


Fig. 31 (Figure 5.57): Time-variation of motor truck wheel parameters.

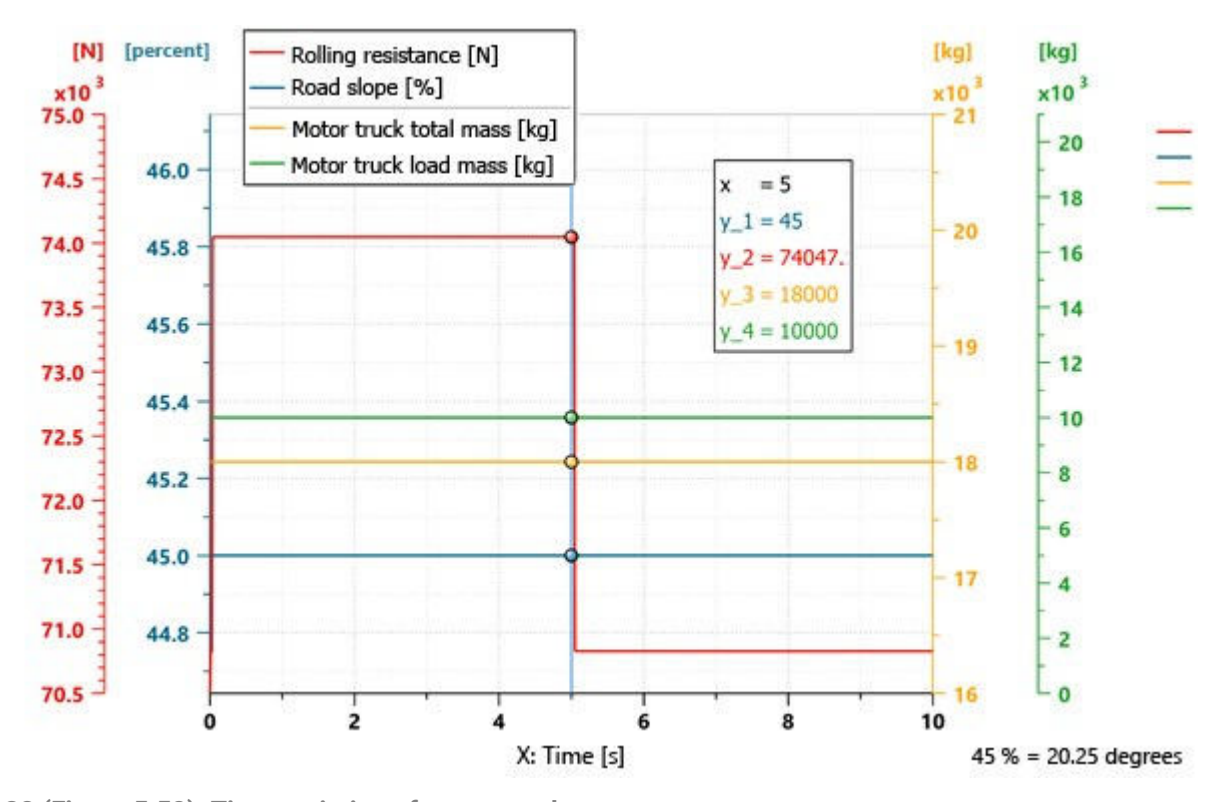


Fig. 32 (Figure 5.58): Time-variation of motor truck parameters.

In Fig. 33 (Figure 5.59) one can see that acceleration reaches the maximum value of 3 m/s².

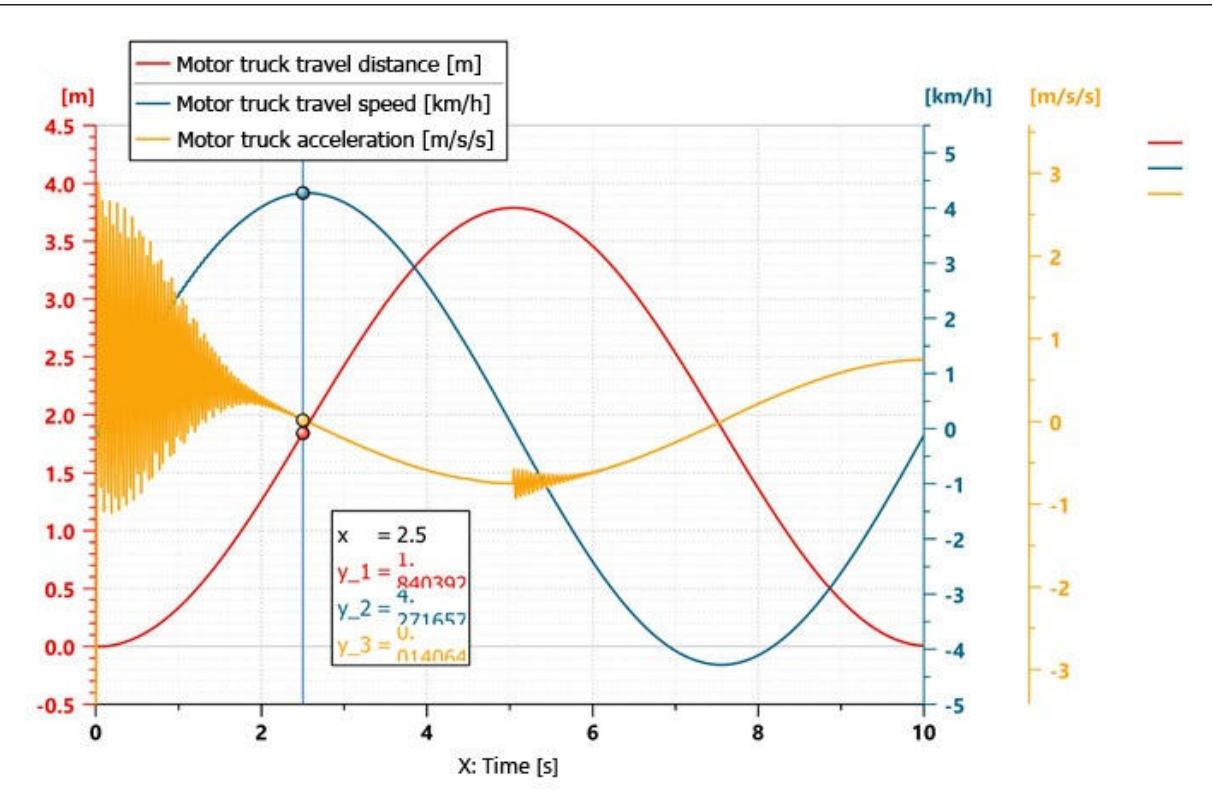


Fig. 33 (Figure 5.59): Time-variation of motor truck dynamic parameters.

In Fig. 34 (Figure 5.60) one can see that the instantaneous error during the continuous control of the motor truck speed varies in the range \pm 0.12 km/h; it occurs as a result of the lag between the control signal and the speed achieved by the motor truck.

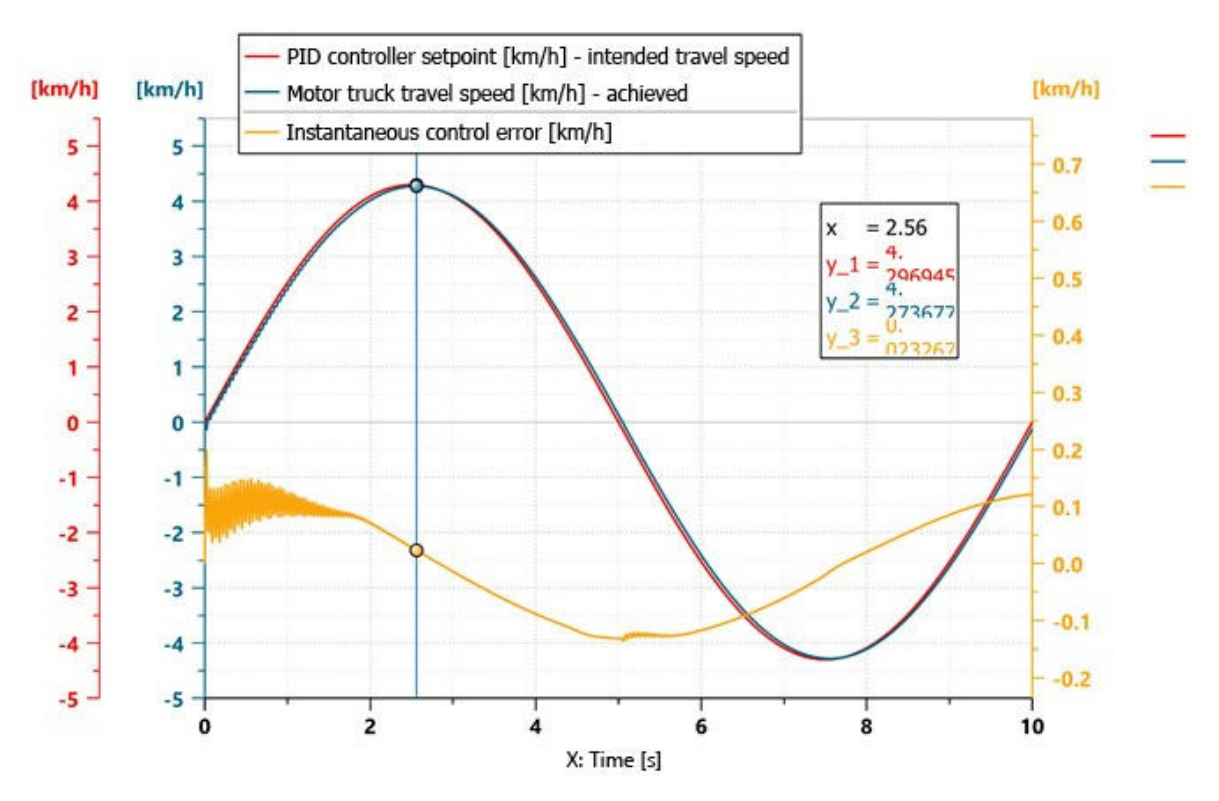


Fig. 34 (Figure 5.60): Performance of continuous control of motor truck travel speed.

In the present case, the minimum speed of the motor truck is not limited by the minimum flow rate of the pump; the limitation is caused by the minimum uniform rotation speed of

the hydrostatic motor, Fig. 35 (Figure 5.61); this speed is 1.5 rev/min, and at this rotation speed the motor truck reaches a travel speed of 0.0449 km/h.

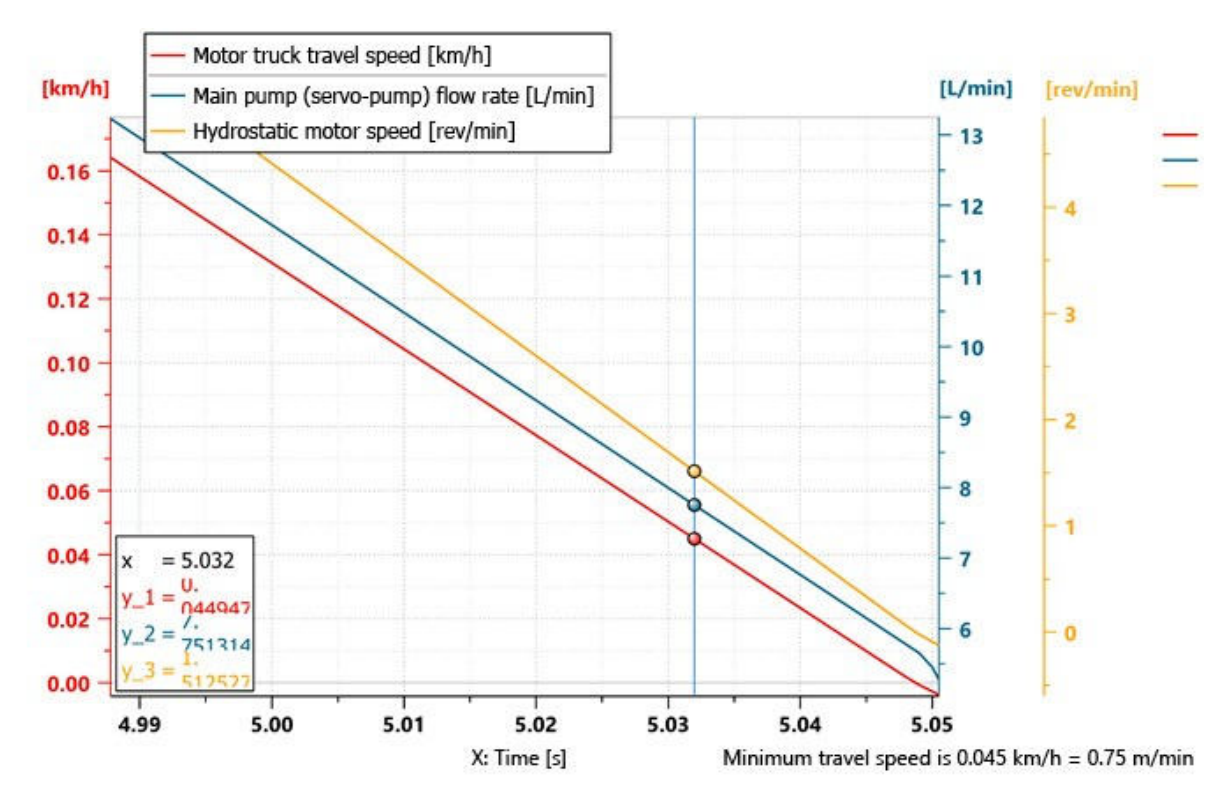


Fig. 35 (Figure 5.61): Motor truck minimum travel speed.

Because transient behaviours occur on the previous graphs, near the frequency of 19 Hz, the stability of the system has been analyzed using the root locus, for the case where the PID controller has been tuned automatically and for another particular case, where the PID controller has been tuned manually.

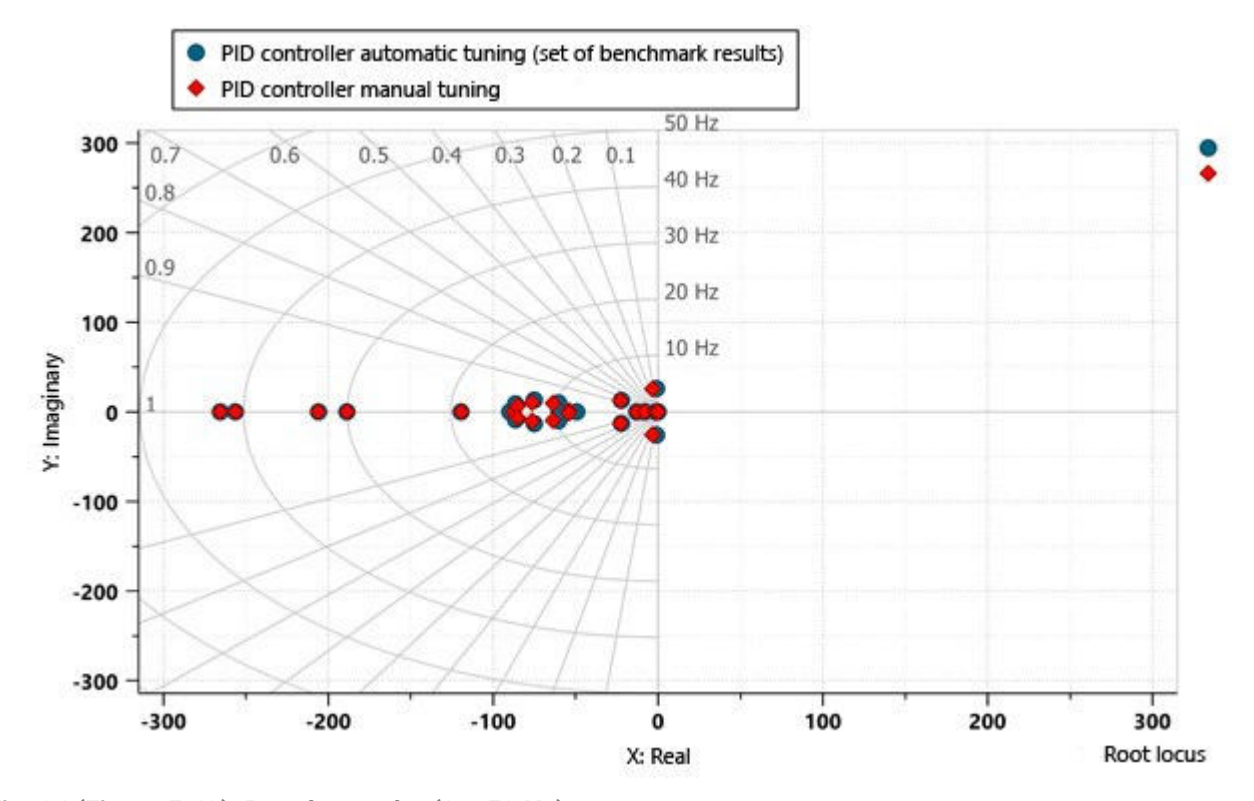


Fig. 36 (Figure 5.63): Root locus plot (0 - 50 Hz).

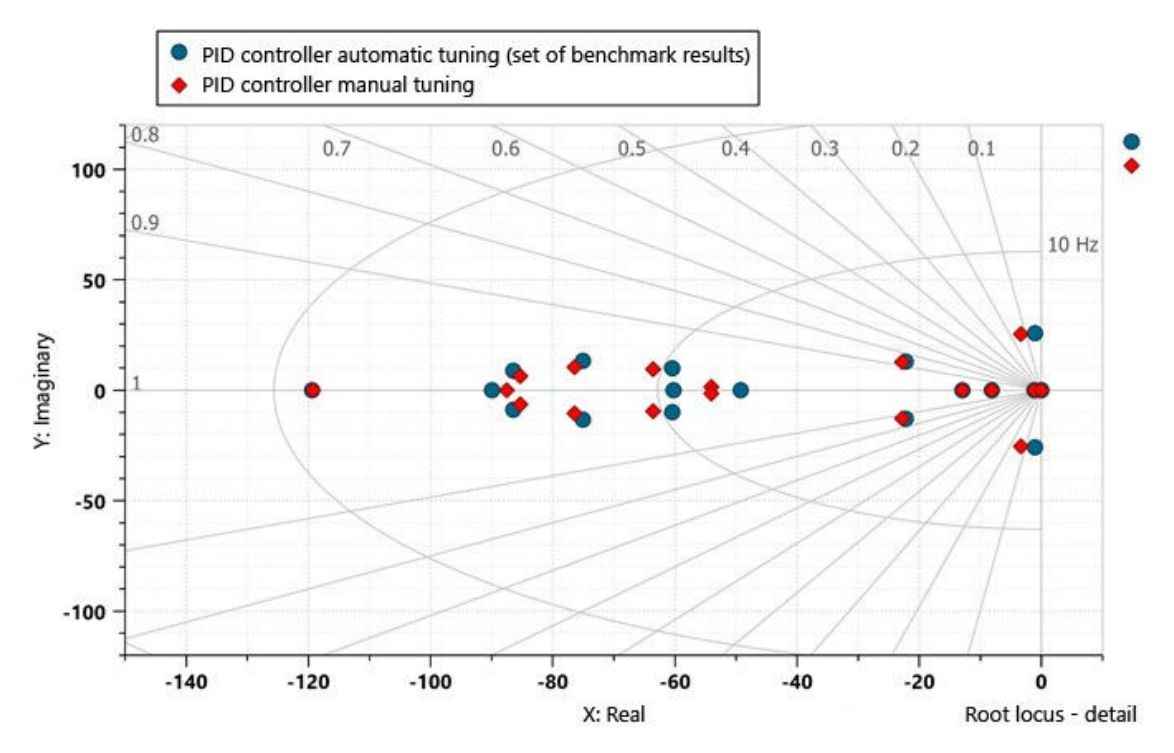


Fig. 37 (Figure 5.64): Root locus plot (0 - 25 Hz) - detail.

There are marginal differences between automatic tuning and manual tuning of the PID controller; it can be stated that in the case of manual tuning the system is better damped for frequency rates lower than 15 Hz.

In Fig. 36 (Figure 5.63) and Fig. 37 (Figure 5.64) the graphs related to the system stability analysis are presented; since all the points on these graphs lie to the left of the imaginary axis and in close proximity to the real number axis, according to Fig. 38 (Figure 5.65), it can be confidently and reasonably stated that the system is well damped and stable. In the green border drawn in Fig. 38 (Figure 5.65) the particular cases related to the stability of this control system are presented.

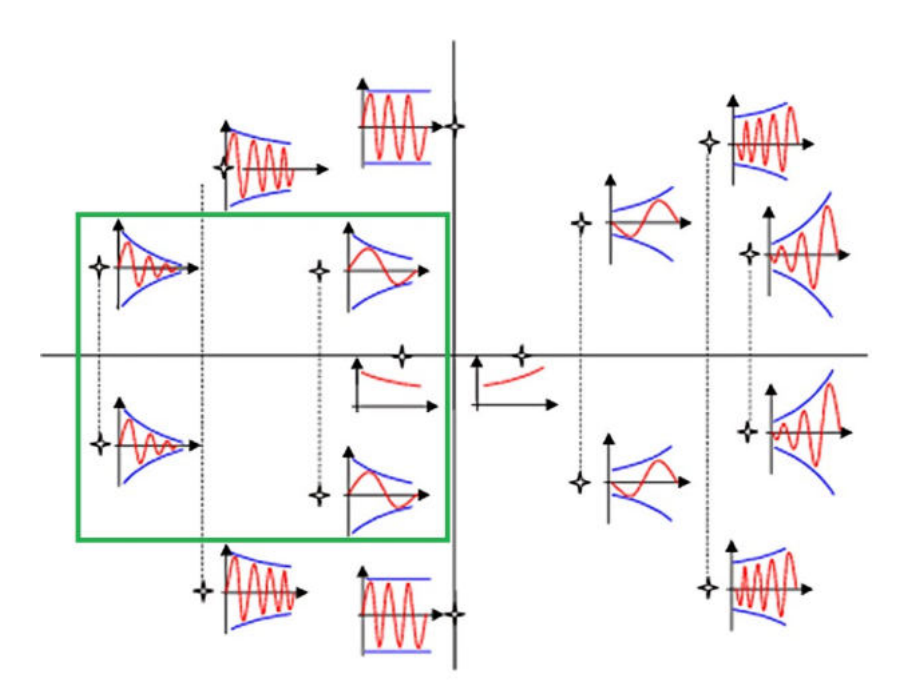


Fig. 38 (Figure 5.65): Particular cases of stability and damping of the automatic speed control system.

Maximum speed of technological travel of the motor truck on a slope with a 45% gradient and maximum authorised mass

In Fig. 39 (Figure 5.72) one can see the time-variation of the motor truck dynamic parameters.

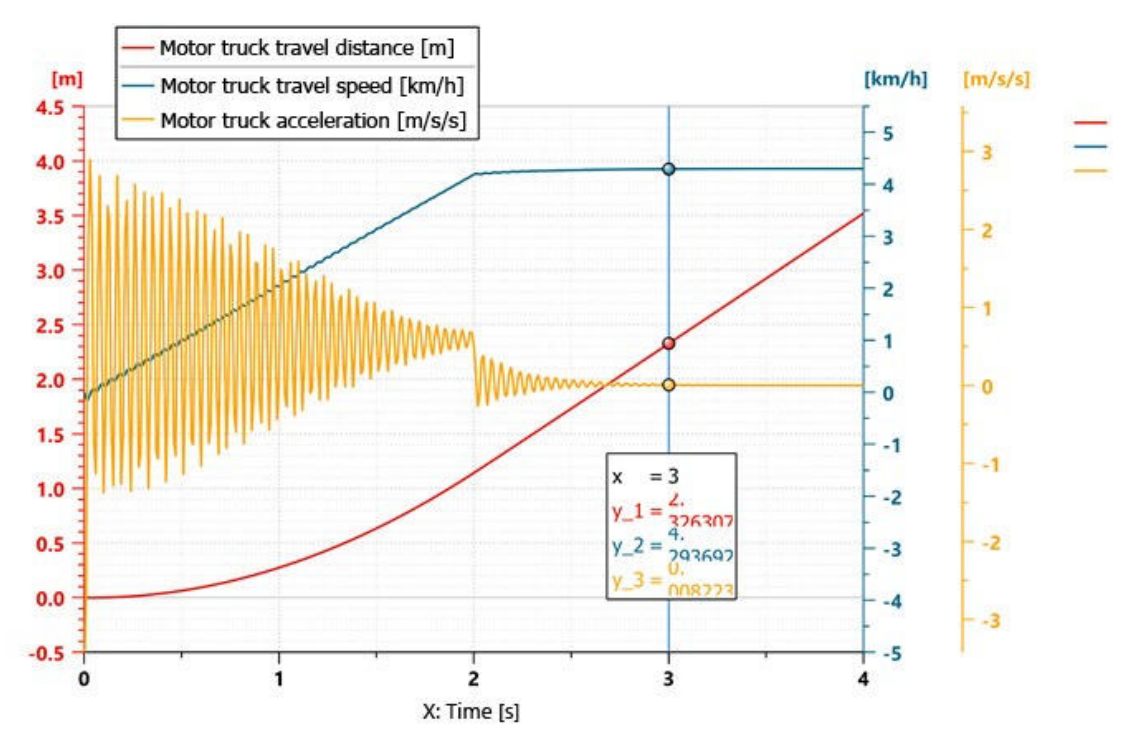


Fig. 39 (Figure 5.72): Time-variation of motor truck dynamic parameters.

In Fig. 40 (Figure 5.73) one can see that the motor truck reaches 97.5% of its maximum speed in 2 seconds, 99.85% of maximum speed in 3 seconds, and in 4 seconds the speed control error is 0.

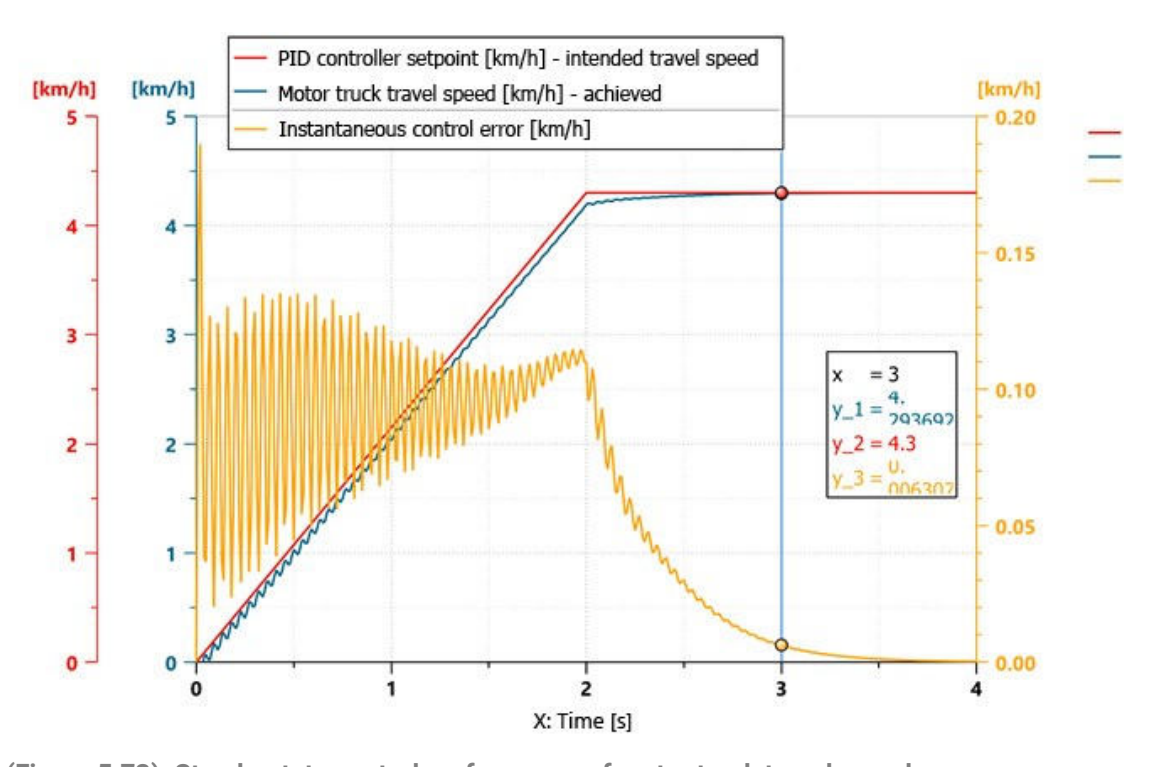


Fig. 40 (Figure 5.73): Steady-state control performance of motor truck travel speed.

Fig. 41 (Figure 5.75) and Fig. 42 (Figure 5.76) show the time-evolution of the temperature of the servo-pump and the temperature of the hydrostatic motor.

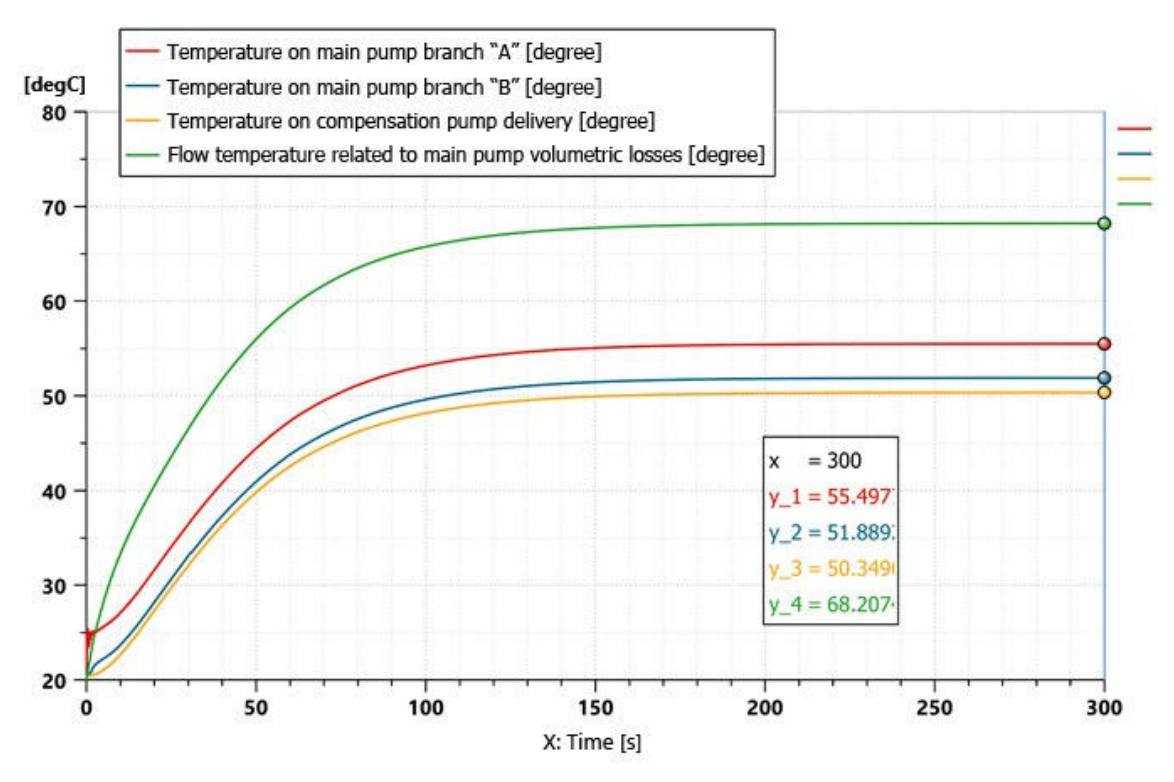


Fig. 41 (Figure 5.75): Time- variation of temperatures in various areas of the main pump.

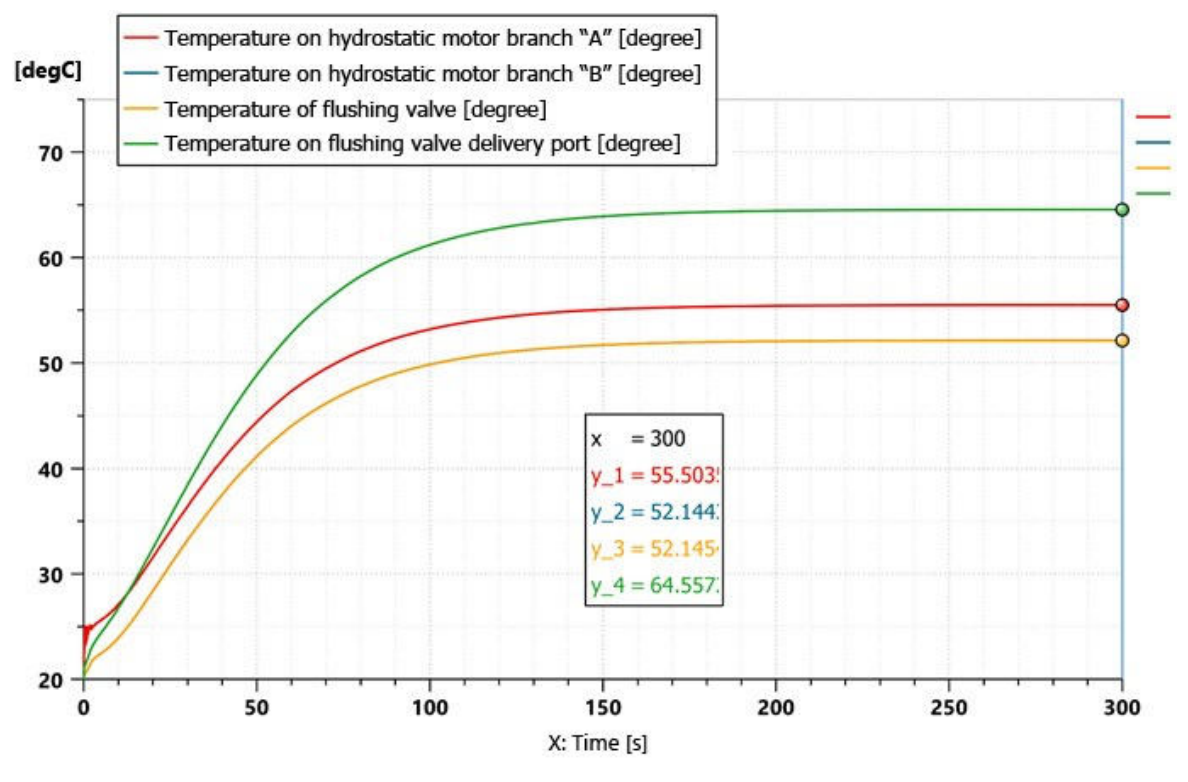


Fig. 42 (Figure 5.76): Time-variation of temperatures in various areas of the hydrostatic motor.

In Fig. 43 (Figure 5.77) one can see that the kinematic viscosity of the hydraulic fluid is kept within the limits of the optimal values; these values are recommended by the manufacturers of the hydrostatic pump and the motor.

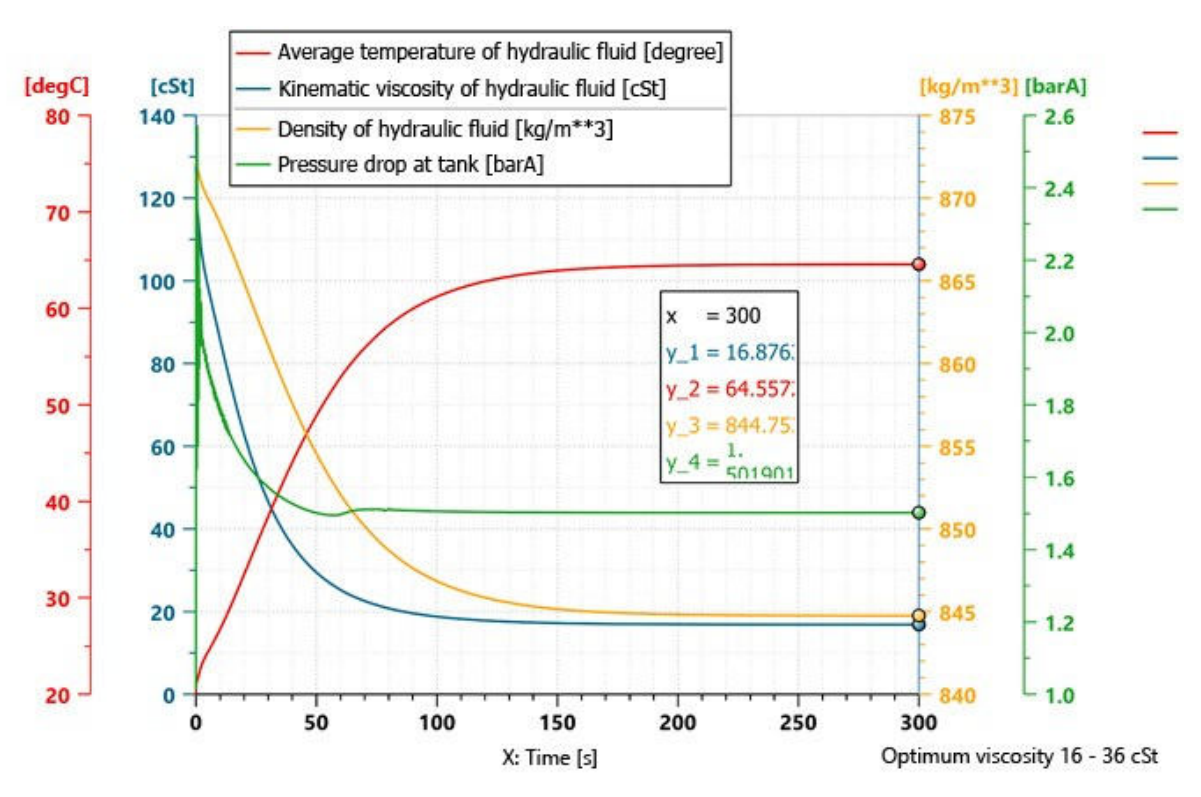


Fig. 43 (Figure 5.77): Time-variation of hydraulic fluid parameters.

The time-variation of the tank and cooler hydraulic parameters is plotted in Fig. 44 (Figure 5.78) and Fig. 45 (Figure 5.79).

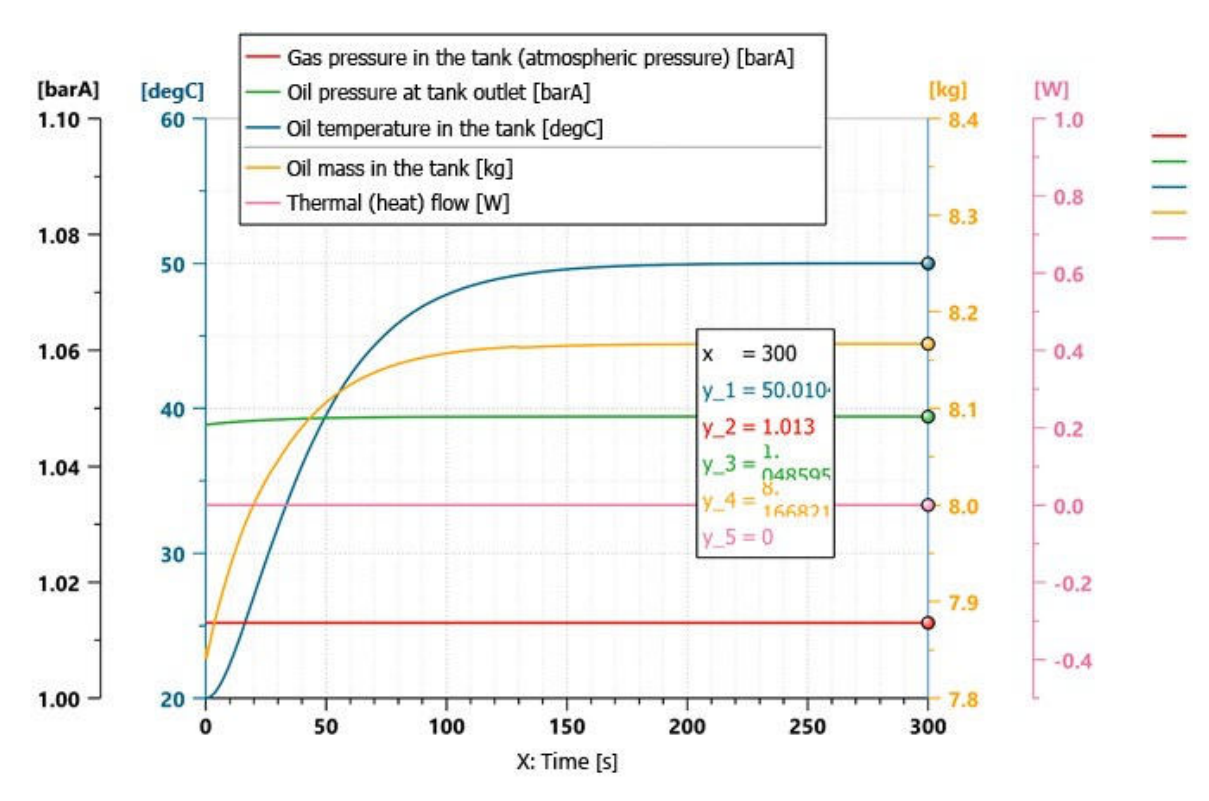


Fig. 44 (Figure 5.78): Time-variation of hydraulic fluid tank parameters.

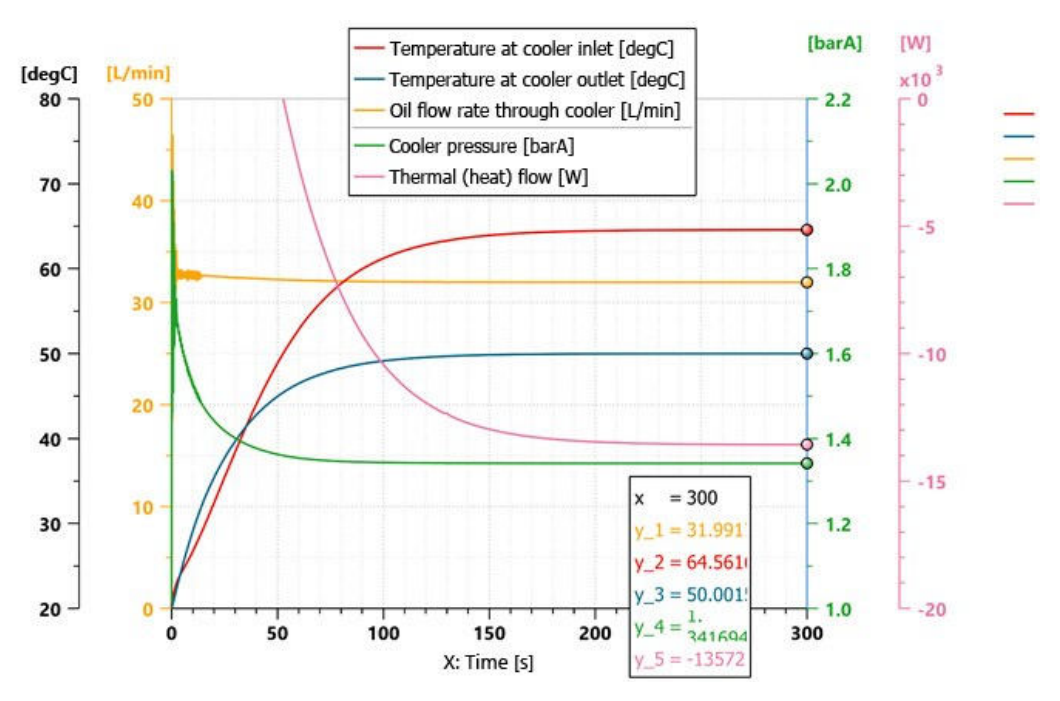


Fig. 45 (Figure 5.79): Time-variation of cooler (heat exchanger) parameters.

Maximum speed of technological travel of the motor truck on a slope with a 15% gradient and maximum authorised mass

The time-variation of the motor truck travel distance, along with its speed and acceleration, are shown in Fig. 46 (Figure 5.84). In this figure, one can see that the average acceleration has the value of about 1 m/s 2 in the first two seconds; in the same figure, one can also note that the motor truck movement is uniform and without shocks, even upon startup.

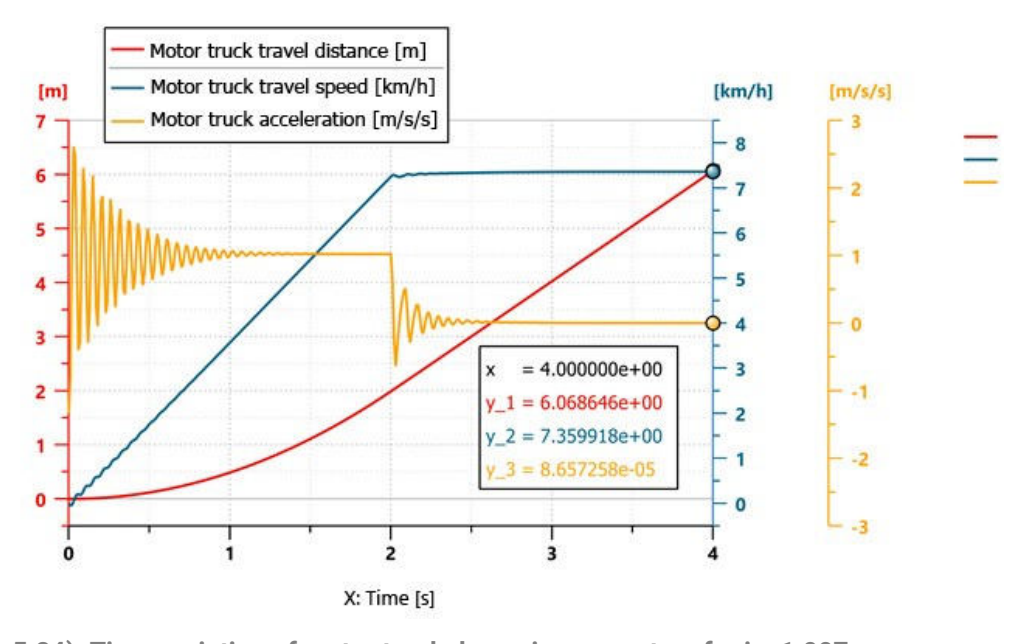


Fig. 46 (Figure 5.84): Time-variation of motor truck dynamic parameters for i = 1.007.

In Fig. 47 (Figure 5.85) one can see that the motor truck reaches 97.6% of its maximum speed (7.35 km/h) in 2 seconds, 99.84% of maximum speed in 3 seconds, and in 4 seconds the speed control error is 0.000082 km/h.

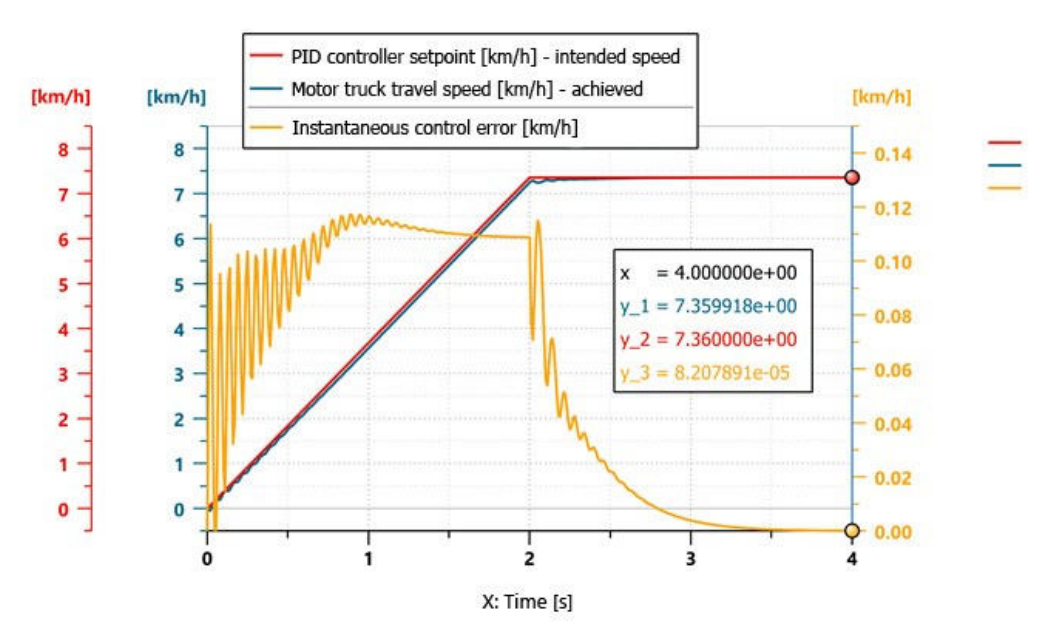


Fig. 47 (Figure 5.85): Steady-state control performance of motor truck travel speed for i = 1.007.

Conclusions of the virtual experimentation of the motor truck and hydrostatic transmission

Dynamic parameters of the multipurpose motor truck, equipped with a hydrostatic transmission that have been improved compared to a motor truck equipped with a mechanical transmission, in the first gear, are pictured in Fig. 48 (Figure 5.86).

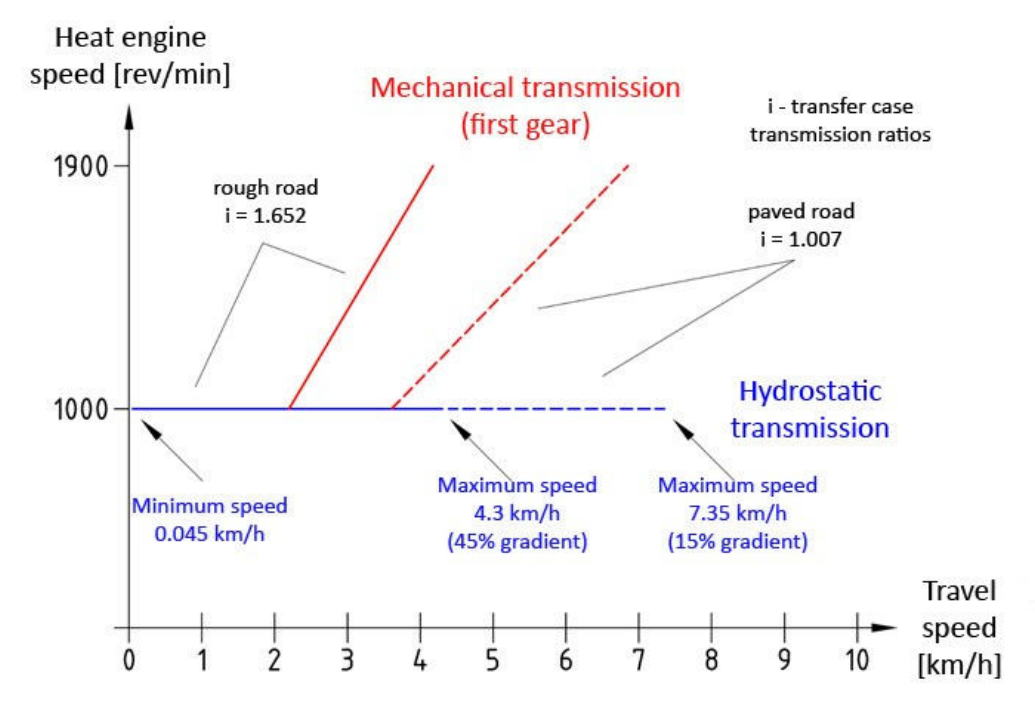


Fig. 48 (Figure 5.86): Comparison between the optimized dynamic parameters of the motor truck equipped with closed-circuit primary control hydrostatic transmission and the TGM 18 motor truck.

- Maximum travel speed of the motor truck equipped with closed-circuit primary control hydrostatic transmission is 4.3 km/h, on a rough road with a 45% gradient, while on a paved road with a 15% gradient its maximum speed is 7.35 km/h.
- Minimum travel speed of the motor truck is 0.045 km/h.

- The motor truck can go upwards and downwards a road with a 45% maximum gradient at a speed of 4.3 km/h.
- The motor truck reaches 97.5% of maximum speed in 2 seconds, 99.85% of maximum speed in 3 seconds, and in 4 seconds the speed control error is 0.
- Instantaneous control error during the continuous control of the motor truck travel speed varies in the range ± 0.12 km/h

Chapter 6 - Applicability of the research

The research in the present thesis is useful both for the private economic environment and for the academic environment:

- It is useful for integrators or for workshops / service stations that equip motor trucks with closed-circuit hydrostatic transmissions or make changes to them, so that they can be used in various fields Fig. 49 (Figure 6.1) shows such a multipurpose motor truck used in the construction sector. The thesis provides integrators with a set of useful benchmark data regarding the parameters of hydraulic components and those of closed-circuit transmission subsystems, so that the motor truck with a maximum mass of 18 tonnes, equipped by an integrator with hydrostatic transmission, meets the requirements of the technological process efficiently and safely.
- Theoretical research in the field of hydrotronics can be used by the academic professional staff as a university course support, while experimental (physical or virtual) research can be used within the laboratory classes of Hydraulic Drives, Automatic Control Systems and Mechatronics; the simulation and the results of virtual experimentation with the help of numerical simulation of the dynamic parameters of the motor truck can be used as a case study for the subject "Traction vehicles" and the specific subjects of the specialization "Road vehicles".



Fig. 49 (Figure 6.1): Multipurpose motor truck used in the construction sector, equipped with an example of technological equipment.

Among the accessories that can equip the motor vehicles (trucks or vans, depending on the gauge), giving them a multifunctional character, one can list equipment pieces such as: blade, blower or plow for snow removal; salt / sand spreader for spreading anti-skid material;

tank with deicing liquid; mowing arm; hedge / branch / twig trimmer; trench unclogging cutter; road spraying and washing cistern; carriage body or gripping device for utility transport services; folding platform; height access platform; street sweeping rotary brush; angled brush for cleaning tunnels, walls, dry canal beds or other inclined or vertical surfaces; street vacuum cleaner; insecticide tank for spraying green areas or disinfectant solution tank for sanitizing / decontaminating public areas; grab bucket; log transporting bucket; log splitter; plant chopper; fertilizer spreader; bale handling tongs; fork for loading and transporting garbage; emulsion spreader with lance; sump pump. All these pieces of equipment fit out utility vehicles used mainly by municipalities, in the field of urbanistic works. In Fig. 50 (Figure 6.2) some examples of such vehicles that perform public utility works on the roadway and in the immediate proximity are pictured.



Fig. 50 (Figure 6.2): Utility vehicles performing works on the roadway or in the immediate proximity.

Chapter 7 - Conclusions, personal contributions and perspectives

7.1 General conclusions of the thesis

The aim of this thesis, that is to optimize the dynamic parameters of multipurpose motor trucks, has been achieved by equipping them with a hydrostatic transmission in a closed circuit, with primary adjustment and a PID controller, this transmission enabling multipurpose motor trucks to achieve lower travel speeds than the mechanical transmission with which the motor trucks are already equipped. Moreover, the travel speed of multipurpose motor trucks is uniform and can be continuously adjusted to meet the requirements of any technological process.

The multipurpose motor truck with an authorized mass of 18 tonnes can go up and down a rough road with a 45% gradient at a maximum speed of 4.3 km/h, and can go up a paved road with a 15% gradient at a maximum speed of 7.35 km/h. Under these conditions, the motor truck will reach 97.5% of its maximum speed in 2 seconds and 99.85% of its maximum speed in 3 seconds, and in 4 seconds the speed adjustment error is 0. Regarding the minimum travel speed, the motor truck can travel at 0.045 km/h. The motor truck with the previously mentioned features adds up the advantages of all the motor trucks mentioned in the state of the art section of the thesis: achieves low travel speeds with superior energy efficiency compared to motor trucks equipped with hydrodynamic transmissions; being equipped with two distinct transmissions, they can be used independently, depending on the requirements of the technological process, ensuring two modes of travel, both efficient from an energy point of view; compared to "vans" / "municipal vehicles", the motor truck has 2 or 3 times more transport capacity, which improves the productivity of the technological process.

All the objectives of the thesis, stated in Chapter 2, subchapter 2.4, have been achieved, as follows:

- In Chapter 1, the framework has been established in which research will be carried out regarding the equipping of multipurpose motor trucks with hydrostatic transmissions;
- In Chapter 2, an analysis of the state of the art in the field of mobile hydraulic transmissions and in the field of motor trucks that can be equipped with such type of transmissions has been carried out;
- In Chapter 3, the mathematical models of the parts of a hydrostatic transmission and those of the pump capacity displacement servo-control system have been presented;
- In Chapter 4 the characteristics of a servo-pump have been determined experimentally, in the laboratory, as well as the control performance of a closedcircuit primary control transmission;
- In Chapter 5 the dynamic parameters of multipurpose motor trucks equipped with closed-circuit primary control hydrostatic transmissions have been optimized virtually, with the help of numerical simulation;
- Also in Chapter 5, the influence that reducing the energy consumption of the subsystems has on the closed-circuit hydrostatic transmission has been studied, with the help of numerical simulation.
- Moreover, in Chapter 5 the possibility of obtaining optimized parameters of multipurpose motor trucks has been demonstrated; such parameters fully meet the needs of technological processes: travel speed rates that are lower than those of the mechanical transmission and steadier, and also continuous adjustment of the travel speed rate.
- The present thesis makes available to integrators a data set with a benchmark value; this set can be found, in a concise form, in Chapter 5, subchapter 5.4.2, and in detail in Annex 39 (of the full-length thesis); these data regarding the parameters of closed-circuit transmission hydraulic components and subsystems can be useful to the integrator, so that the motor truck equipped by the integrator with the hydrostatic transmission meets the requirements of the technological process efficiently and safely.

7.2 A synthesis of the personal contributions

A) In the following, the original contributions will be presented, with a mention of the chapter and subchapter in the thesis where one can discover them.

- Analysis of the state of the art for research in the field of mobile hydraulic transmissions and research in the field of motor trucks that can be equipped with such type of transmissions - carried out in Chapter 2.
- Disambiguation of the multipurpose motor truck concept made in Chapter 1, subchapter
 1.2 and Chapter 2, subchapter 2.3.
- Presentation of the mathematical models of a hydrostatic transmission and those of the system for pump displacement servo-control - made in Chapter 3.
- Experimental determination, in the laboratory, of the characteristics of a servo-pump and the control performance of a closed-circuit primary control transmission - carried out in Chapter 4. The author has carried out 8 sets of physical experiments in the General Hydraulics laboratory of INOE 2000-IHP; the LabVIEW software has been used to control the hydraulic and electronic components and to acquire the experimental data.
- Continuation of the physical tests, conducted in the laboratory, with the help of virtual experimentation, through numerical simulation, of the servo-pump in the structure of the hydrostatic transmission - carried out in Chapter 5, subchapter 5.2.
- Study and virtual optimization, with the help of numerical simulation, of the subsystems of a closed-circuit primary control hydrostatic transmission carried out in Chapter 5.
- Virtual experimentation of a multipurpose motor truck and optimization of its dynamic parameters by equipping it with a closed-circuit primary control hydrostatic transmission - carried out in Chapter 5, subchapter 5.4;
- In total, in Chapter 5, the author carried out 3 distinct numerical simulations: simulation of a servo-pump, simulation of the closed-circuit transmission subsystems and simulation of the motor truck equipped with a closed-circuit primary control hydrostatic transmission; all three simulations have been performed using the AMESim software.
- B) Physical embodiment For conducting research in the laboratory, an experimental test bench has been built by the author of the thesis, which aimed to physically test the control characteristics of a servo-pump and those of a closed-circuit primary control hydrostatic transmission. The test bench, which as regards the "Technology Readiness Level" (TRL) is TRL 5, by enabling "laboratory testing of integrated systems in a relevant environment" (acc. to Annex 40 of the thesis), is presented in the thesis in Chapter 4, subchapter 4.1, Figure 4.1 and Figure 4.2, and its hydraulic schematic diagram can be found in the same chapter and subchapter of the thesis, in Figure 4.21.
- C) In addition to the personal contributions listed above, which are an integral part of the thesis, 4 (four) patent applications on the topic of the thesis, filed out to OSIM and published in the Official Industrial Property Bulletin (BOPI) during the doctoral research stage, can also be mentioned; the author of this thesis is among the co-authors, as follows:
 - "Mixed transmission, mechanical and hydraulic, for all-wheel drive multipurpose vehicles", patent application registered at OSIM with no. A/00638 of 05.09.2018 (Annex 41 of the thesis), published in BOPI no. 3, March 2020, page 40, having as authors: Lepădatu Ioan, Dumitrescu Liliana, Chiriţă Alexandru-Polifron.
 - "Mixed transmission, mechanical and hydraulic, for rear-wheel drive multipurpose vehicles", patent application registered at OSIM with no. A/00637 of 05.09.2018 (Annex 42 of the thesis), published in BOPI no. 3, March 2020, page 54, having as authors: Lepădatu Ioan, Dumitrescu Liliana, Chiriță Alexandru-Polifron.

- "Test bench for hydraulic pumps and motors", patent application registered at OSIM with no. A/01046 of 04.12.2018 (Annex 43 of the thesis), published in BOPI no. 5, May 2020, page 57, having as authors: Dumitrescu Liliana, Lepădatu Ioan, Şefu Ştefan-Mihai, Chiriţă Alexandru-Polifron.
- "Spraying equipment with hydrostatic drive and pneumatic spraying", patent application registered at OSIM with no. A/01056 of 05.12.2018 (Annex 44 of the thesis), published in BOPI no. 6, June 2020, page 17, having as authors: Cristescu Corneliu, Chiriţă Alexandru-Polifron, Rădoi Radu-Iulian.

The first two patent applications are technical solutions that integrate closed-circuit primary control hydrostatic transmissions, whereas the other two patent applications contain an open-circuit hydrostatic transmission.

- D) During the doctoral research stage, the author of this thesis has developed 6 (six) scientific articles / papers on the theme of the thesis; 3 (three) of them have already been published in the proceedings of international conferences and in a specialized journal in the field of Fluid Power; all of them are indexed in international databases; the other 3 (three) articles have been accepted for publication and are about to be published in the proceedings of an international conference, and in two specialized journals, respectively, one of which is indexed in WoS. The authors of the mentioned scientific articles in order of appearance, the titles of the articles / papers, as well as the related periodicals are presented below:
 - Alexandru-Polifron Chiriță, Cristian Pavel. "Agricultural platform equipped with a hydrostatic transmission capable of continuously adjustable travel velocity and non-linear disturbance compensation capabilities". INMATEH - Agricultural Engineering, vol. 69, no. 1 (April 2023): [article accepted for publication];
 - Alexandru-Polifron Chiriță, Cristian Pavel. "Mathematical modeling, laboratory testing and numerical simulation of a servo-pump as part of a closed circuit primary control hydrostatic transmission for multi-purpose trucks". "Hidraulica" Magazine, no. 4 (December 2022): [article accepted for publication];
 - Alexandru-Polifron Chiriță. "The influence of hydraulic fluid temperature on the adjustment capabilities of servo-mechanisms and closed-circuit hydrostatic transmissions". Proceedings of 2022 International Conference on Hydraulics and Pneumatics HERVEX (November 2022): [paper accepted for publication];
 - Alexandru-Polifron Chiriță, Radu Iulian Rădoi, Bogdan Alexandru Tudor, Ștefan-Mihai Șefu, Ana-Maria Popescu. "Control performance of an energy efficient hydrotronic transmission". "Hidraulica" Magazine, no. 2 (June 2022): pp. 7-14;
 - Ioan Lepădatu, Corneliu Cristescu, Alexandru-Polifron Chiriță, Cristian Mărculescu. "Four-wheel drive high efficiency hybrid transmission for multipurpose motor vehicles". Proc. of 2017 International Conference on Hydraulics and Pneumatics – HERVEX (November 2017): pp. 140-146;
 - **Alexandru-Polifron Chiriță**, Liliana Dumitrescu, Radu Sauciuc. "Numerical simulation of the dynamic behavior of a multifunctional motor vehicle equipped with a primary adjustment hydrostatic transmission". *Proceedings of ISB-INMA TEH'* 2017 International Symposium (October 2017): pp. 375-380.

7.3 Perspectives for further research

As for the continuation of research on the topic of the thesis, the path remains open, and new scientific challenges can be identified and addressed; specifically, starting from the results obtained in this thesis, at least the following scientific approaches are considered:

- Elaboration of a scientific article and submission for publication (with financing provided under the project SUPERCONEX belonging to INOE 2000-IHP, Financial agreement no. 18PFE/30.12.2022, in the framework of PNCDI III Programme 1- Development of the national research-development system Subprogramme 1.2 Institutional Performance Projects Funding Excellence in R&D&I (PFE-CDI)) in the journal "IEEE Transactions on Vehicular Technology", e-ISSN: 1939-9359, p-ISSN: 0018-9545, WoS-quoted (indexed in Web of Science, with impact factor) journal; the article will integrate the theoretical and experimental research on multipurpose motor trucks carried out by the author.
- Filing out a new patent application to OSIM, this time regarding the technical solution to improve the energy consumption of the closed-circuit hydrostatic transmission subsystems.
- After filing out the patent application, the aim is to continue the research on the efficiency of the energy consumption of the closed-circuit hydrostatic transmission subsystems and to publish the results of this research in the international scientific stream, in journals / conference proceedings indexed in international databases.
- Publishing a book on the topic of the influence of temperature and cooling on the adjustment capabilities of hydrostatic transmissions and on their efficiency;
- The virtual experimentation in this thesis takes into account the volumetric efficiency of the servo-pump, because it influences in a negative way the capabilities of adjusting the dynamic parameters; however, the mechanical efficiency of the components has not been taken into account. It is considered that, later on, the numerical simulation model will be completed by taking into account the mechanical efficiency of the components, too.
- A new related direction of research is, in perspective, the virtual experimentation, with the help of numerical simulation, of a closed-circuit primary control hydrostatic transmission which has a hydrostatic motor with two displacement volumes as part of its structure; such a motor is presented in this thesis in Chapter 2, subchapter 2.1.2.3; it would enable the motor truck to travel at twice the speed of the single-displacement volume hydrostatic motor version, maintaining the dynamic parameters of the single-displacement volume motor for the first half of the speed range achieved.
- The numerical simulation model of the motor truck equipped with closed-circuit hydrostatic transmission has been thought and made to be scalable for vehicles with transport capacity starting from 0.5 tonnes up to 100 tonnes and hydrostatic transmission power rates between 1 kW and 1 MW. Moreover, the mathematical model of the motor truck can also take into account the variation of the mass of the motor truck during the travel, as well as the attachment of a piece of technological equipment, for example a snow blower, to the front plate of the motor truck.
- Since various metal structures with various roles are added to the original mass of the motor truck, and they reduce the useful transport capacity of the motor truck, reducing their mass should be considered, if possible even by means of structural topological optimization; for example, hydrostatic motor and servo-pump mounts would be some of the targeted components for such an endeavour.
- Although at the present moment the efficiency of the hydrostatic pumps and that of the hydrostatic motors have reached very good values (95% - for low rotating speed rates and optimal pressure rates), there is still room for improvement. In order to optimize the volumetric losses of hydrostatic machines, the use of CFD-type simulation can be considered later on.

Annex 1 - Thesis structure (table of contents)

List of Figures	15
List of Tables	21
Chapter 1 - Introduction	23
1.1 Hydraulic transmissions	23
1.1.1 Classification of hydraulic transmissions	23
1.1.2 Classification of hydrostatic transmissions	24
1.1.3 Classification of closed-circuit hydrostatic transmissions	25
1.1.3.1 Closed-circuit primary control hydrostatic transmission	26
1.1.3.2 Closed-circuit secondary control hydrostatic transmission	26
1.1.3.3 Closed-circuit mixed control hydrostatic transmission	27
1.2 – Multipurpose motor trucks	27
1.2.1 Particularities and issues of multipurpose motor trucks	29
1.2.2 Multipurpose motor trucks equipped with hydrostatic transmissions - advantages and disadvantages	30
Chapter 2 – State of the art in the field of mobile hydraulic transmissions and in the field of motor trucks equipped with them	31
2.1 State of the art regarding the components and subsystems that make up hydrostatic transmissions	31
2.1.1 Hydrostatic pumps for mobile transmissions	32
2.1.1.1 A4VG series 35 servo-pump	32
2.1.1.2 A4VG series 40 servo-pump	34
2.1.1.3 A10VG series 10 servo-pump	35
2.1.1.4 P7 GOLD CUP® series servo-pump	37
2.1.1.5 P90 - 250 servo-pump	39
2.1.2 Hydrostatic motors	41
2.1.2.1 A6VM series 63 servo-motor	42
2.1.2.2 CDM 10 (CDM 222-050) hydrostatic motor	43
2.1.2.3 CDM 20 hydrostatic motor	44
2.1.3 Subsystems of closed-circuit hydrostatic transmissions	45
2.2 State of the art regarding hydrostatic drive systems	47
2.2.1 Open-circuit hydrostatic transmissions	48
2.2.2 Closed-circuit hydrostatic transmissions	49
2.3 State of the art regarding multipurpose motor vehicles equipped with various transmissions	56
2.4 Aim and objectives of the thesis	59
Chapter 3 – Theoretical elements regarding the mathematical modeling of hydrostatic drive components and systems	61
3.1 Dynamic mathematical models of the main components of a hydrostatic transmission	61
3.1.1 Dynamic mathematical model of a variable displacement, swash plate and rotating block pump	61
3.1.2 Dynamic mathematical models of hydraulic (rotary and linear) motors	63
3.1.2.1 Dynamic mathematical model of the high-speed fixed-displacement motor	63
3.1.2.2 Dynamic mathematical model of the low-speed radial piston motor	64
3.1.2.3 Dynamic mathematical model of linear hydraulic motors (hydraulic cylinders)	65
3.1.3 Dynamic mathematical model of hydraulic directional control valves	66
3.2 Dynamic mathematical modeling of hydrostatic drive systems	70
3.2.1 Overview	70
3.2.2 Dynamic analysis of a servo-system for hydrostatic proportional control of the capacity displacement of a pump connect a closed-circuit primary control transmission	
3.2.2.1 Problem formulation	71
3.2.2.2 Dynamic mathematical model of the automatic control system	72
3.2.2.3 Global transfer function of the hydrostatic automatic control system (H.A.C.S.)	79
Chapter 4 - Physical experimentation, in the laboratory, of a closed-circuit primary control hydrostatic transmission	
4.1 Methodology of transmission and servo-pump experimentation	81

4.1.1 A10VG28EP4 servo-pump response to step signal	93
4.1.2 A10VG28EP4 servo-pump flow rate/control characteristic and transmission characteristic	94
4.2 Results of physical experimentation, in the laboratory	96
4.2.1 A10VG28EP4 servo-pump response to step signal	96
4.2.1.1 Response to step signal with the load created by the hydrostatic motor	97
4.2.1.2 Lag detail with the load created by the hydrostatic motor	98
4.2.1.3 Response to step signal with no load	99
4.2.1.4 Lag detail with no load	100
4.2.2 A10VG28EP4 servo-pump flow rate/control characteristic and transmission characteristic	101
4.2.2.1 Test with the load created by the hydrostatic motor and maximum control signal	101
4.2.2.2 Test with the load created by the hydrostatic motor and minimum control signal	102
4.2.2.3 No-load test, short-circuiting the closed circuit with a 90° bend and maximum control signal	103
4.2.2.4 No-load test, short-circuiting the closed circuit with a 90° bend and minimum control signal	104
4.3 Conclusions of the laboratory experimentation	
Chapter 5 – Optimization and virtual experimentation using numerical simulation	107
4.1.2 A10VG28EP4 servo-pump flow rate/control characteristic and transmission characteristic. 4.2.1 Response to step signal with the load created by the hydrostatic motor. 4.2.1.2 Response to step signal with the load created by the hydrostatic motor. 4.2.1.3 Response to step signal with no load. 4.2.1.4 Lag detail with the load created by the hydrostatic motor. 4.2.1.4 Lag detail with no load. 4.2.1.4 Lag detail with no load. 4.2.2 A10VG28EP4 servo-pump flow rate/control characteristic and transmission characteristic 4.2.2.1 Test with the load created by the hydrostatic motor and maximum control signal. 4.2.2.2 Test with the load created by the hydrostatic motor and minimum control signal. 4.2.2.3 No-load test, short-circuiting the closed circuit with a 90° bend and maximum control signal. 4.2.2.4 No-load test, short-circuiting the closed circuit with a 90° bend and minimum control signal. 4.2.2 No-load test, short-circuiting the closed circuit with a 90° bend and minimum control signal. 4.3 Conclusions of the laboratory experimentation apter 5 - Optimization and virtual experimentation using numerical simulation 5.1 Introduction - Presentation of the numerical simulation software. 5.2 Virtual experimentation of the A10VG28EP4 servo-pump 5.2.1 Methodology of the servo-pump virtual experimentation. 5.2.2 Presentation of the results of the servo-pump virtual experimentation. 5.2.2 Servo-pump frequency response to wobble control signal. 5.2.3 Conclusions of the servo the virtual experimentation of hydrostatic transmission subsystems. 5.3.3 Methodology of the virtual experimentation of hydrostatic transmission subsystems. 5.3.3 Conclusions of the virtual experimentation of hydrostatic transmission subsystems. 5.3.3 Conclusions of the virtual experimentation of hydrostatic transmission subsystems. 5.3.4 Nethodology of the virtual experimentation of the motor truck and the hydrostatic transmission. 5.4.1 Introduction. 5.4.2 Methodology of the virtual experimentation of the motor truck and the hydrostatic transmiss	
5.2 Virtual experimentation of the A10VG28EP4 servo-pump	110
5.2.1 Methodology of the servo-pump virtual experimentation	110
5.2.2 Presentation of the results of the servo-pump virtual experimentation	111
5.2.2.1 Servo-pump response to step signal	111
5.2.2.2 Servo-pump flow rate / control characteristic	114
5.2.2.3 Servo-pump frequency response to wobble control signal	118
5.2.3 Conclusions of the servo-pump virtual experimentation	
5.3 Experimentation and virtual optimization of the subsystems of a closed-circuit primary control hydrostatic transmission	n121
5.3.1 Methodology of the virtual experimentation of hydrostatic transmission subsystems	121
5.3.2 Presentation of the results of the virtual experimentation of hydrostatic transmission subsystems	124
5.3.3 Conclusions of the virtual experimentation of hydrostatic transmission subsystems	130
5.4 Virtual experimentation of a multipurpose motor truck and optimization of its dynamic parameters by equipping it with circuit primary control hydrostatic transmission	a closed- 131
5.4.1 Introduction	131
5.4.2. Methodology of the virtual experimentation of the motor truck and the hydrostatic transmission	133
5.4.3. Presentation of the results of the virtual experimentation of the motor truck equipped with a hydrostatic transmissi	on 137
5.4.3.1 Continuous adjustment of the technological travel speed of the motor track simultaneously with going up and slope with a 45% gradient and maximum authorised mass	
5.4.3.2 Maximum technological travel speed of the motor track on a slope with a 45% gradient and maximum authoris mass	
5.4.3.3 Maximum technological travel speed of the motor track on a slope with a 15% gradient maximum authorised r	nass 155
5.4.4. Conclusions of the virtual experimentation of the motor truck and the hydrostatic transmission	158
Chapter 6 - Applicability of the research	159
Chapter 7 - Conclusions, personal contributions and perspectives	161
7.1 General conclusions of the thesis	161
7.2 A synthesis of the personal contributions	162
7.3 Perspectives for further research	164
References	167
Bibliometric statistics	178
Annovos	170

Annex 2 - Thesis List of Figures

- Figure 1.1: Torque converter with integrated clutch (Kaps Automatic, n.d.).
- Figure 1.2: Hydrostatic transmission (Magnom, n.d.).
- Figure 1.3: Open-circuit transmission (Costa and Sepehri, 2015).
- Figure 1.4: Closed-circuit transmission (Costa and Sepehri, 2015).
- Figure 1.5: Closed-circuit primary control hydrostatic transmission (simplified hydraulic diagram) (Costa and Sepehri, 2015).
- Figure 1.6: Closed-circuit secondary control hydrostatic transmission (simplified hydraulic diagram) (Costa and Sepehri, 2015).
- Figure 1.7: Closed-circuit mixed control hydrostatic transmission (simplified hydraulic diagram) (Costa and Sepehri, 2015).
- Figure 1.8: Example of technological equipment that a multipurpose motor truck used in the construction sector can be equipped with (Poclain Hydraulics, n.d. b).
- Figure 1.9: Examples of pieces of technological equipment that multipurpose motor trucks can be equipped with (Grădinariu, n.d.; Poclain Hydraulics, n.d. b).
- Figure 2.1: A4VG series 35 (Bosch Rexroth AG, 2020 b) Annex 1.
- Figure 2.2: A4VG series 35 (with compensation pump) (Bosch Rexroth AG, 2020 b) Annex 1.
- Figure 2.3: A4VG series 35 (without compensation pump) (Bosch Rexroth AG, 2020 b) Annex 1.
- Figure 2.4: A4VG series 40 (Bosch Rexroth AG, 2020 c) Annex 2.
- Figure 2.5: A4VG series 40, EP electric proportional control (Bosch Rexroth AG, 2020 c) Annex 2.
- Figure 2.6: A4VG series 40, HW proportional hydraulic control with servo-mechanism (Bosch Rexroth AG, 2020 c) Annex 2.
- Figure 2.7: A10VG series 10 (Bosch Rexroth AG, 2020 a) Annex 3.
- Figure 2.8: A10VG series 10, EP electric proportional control (Bosch Rexroth AG, 2020 a) Annex 3.
- Figure 2.9: Vertical section through A10VG series 10 pump, EP model (Bosch Rexroth AG, n.d. b) Annex 4.
- Figure 2.10: Section through A10VG series 10 pump, EP model, displacement control servo-mechanism (Bosch Rexroth AG, n.d. b) Annex 4.
- Figure 2.11: P7 series GOLD CUP® (Parker Hannifin Corporation, 2022) Annex 5 and (Parker Hannifin Corporation, 2014) Annex 6.
- Figure 2.12: Performance curves of P7 pump at maximum displacement (Parker Hannifin Corporation, 2022) Annex 5.
- Figure 2.13: P7 pump control parameters and performance (Parker Hannifin Corporation, 2022) Annex 5.
- Figure 2.14: Minimum pressure on P7 pump suction (Parker Hannifin Corporation, 2022) Annex 5.
- Figure 2.15: Section through P90 250 pump (Poclain Hydraulics, 2017 b) Annex 7.
- Figure 2.16: Hydraulic diagram of P90 250 pump (Poclain Hydraulics, 2017 b) Annex 7.
- Figure 2.17: Efficiency of P90 250 pump (Poclain Hydraulics, 2017 b) Annex 7.
- Figure 2.18: Section through A6VM series 63 servo-motor (Bosch Rexroth AG, 2012 b) Annex 8.
- Figure 2.19: Control characteristic and hydraulic diagram of A6VM series 63 servo-motor processed after (Bosch Rexroth AG, 2016) Annex 9.
- Figure 2.20: Vertical section through CDM 10 Creep Drive Motor™ hydrostatic motor.
- Figure 2.21: Efficiency and torque produced by the hydrostatic motor (Poclain Hydraulics, 2021 a) Annex 10.
- Figure 2.22: CDM 20 Creep Drive Motor™ hydrostatic motor (Poclain Hydraulics, 2020) Annex 12.
- Figure 2.23: Hydraulic diagram of CDM 20 hydrostatic motor (Poclain Hydraulics, 2021 b) Annex 13.
- Figure 2.24: Hydraulic diagram of a closed-circuit mixed control hydrostatic transmission processed after (Bosch Rexroth AG, 2020 c) Annex 2 and (Bosch Rexroth AG, 2016) Annex 9.
- Figure 2.25: Closed-circuit transmission equipped with flushing valve (Costa and Sepehri, 2015).
- Figure 2.26: Hydraulic diagram and characteristic of the adjustable flushing valve (Poclain Hydraulics, 2021 c) Annex 14.
- Figure 2.27: Hydraulic diagram of an open-circuit transmission for one hydraulic motor or two hydraulic motors (ASSOFLUID, 2007).
- Figure 2.28: Hydraulic diagram of an open-circuit transmission (alternative variant) (Sunny et al., 2014).
- Figure 2.29: Arrangement of the pump in relation to the motor compact transmissions, also called power-split (Costa and Sepehri, 2015).
- Figure 2.30: Hydraulic diagram of a closed-circuit primary control transmission (Costa and Sepehri, 2015).
- Figure 2.31: Hydraulic diagram of a closed-circuit primary control transmission with flushing valve (Costa and Sepehri, 2015).
- Figure 2.32: Hydraulic diagram of a closed-circuit mixed control transmission processed after (Bosch Rexroth AG, 2020 c) Annex 2 and (Bosch Rexroth AG, 2016) Annex 9.
- Figure 2.33: Efficiency of a closed-circuit mixed control transmission for 100% (left) and 70% (right) of the pump displacement (Rahmfeld ans Skirde, 2010).
- Figure 2.34: Hydro-mechanical diagrams of some closed-circuit mixed control transmissions (6 out of 36 possible diagrams) (Rossetti and Macor, 2019).
- Figure 2.35: Efficiency of the transmissions shown in Figure 2.34 depending on the instantaneous capacity of hydraulic machines (Rossetti and Macor, 2019).
- Figure 2.36: Application of the compact transmission also called power-split (Bosch Rexroth AG, n.d. a).
- Figure 2.37: Detailed mechano-hydraulic diagram of a compact, in-line, power-split, closed-circuit mixed control hydraulic transmission (Wu et al., 2020).
- Figure 2.38: Split type hydrostatic transmission (Costa and Sepehri, 2015).
- Figure 2.39: Complete hydraulic diagram of a split type primary control hydrostatic transmission (Poclain Hydraulics, 2021 b) Annex 13.
- Figure 2.40: Efficiency of a split type primary control hydrostatic transmission (Zarotti et al., 1979).
- Figure 2.41: Example of split type transmission application (Poclain Hydraulics, n.d. a).
- Figure 2.42: "Multipurpose motor vehicles" available at the integrator (maximum 18 tonnes, equipped with mechanical transmission) (Grădinariu, n.d.).
- Figure 2.43: "Multipurpose municipal motor vehicles vans" available at the importer (maximum 6.5 tonnes, equipped with hydrostatic transmission) (Costa Utilaje, n.d.).
- Figure 2.44: Unimog basic machine produced by Mercedes-Benz-Trucks (9 tonnes, equipped with hydrodynamic transmission and automatic gearbox) (Mercedes-Benz, n.d.).
- Figure 2.45: Multipurpose motor truck used in the construction sector (Poclain Hydraulics, n.d. b).
- Figure 3.1: Swash plate rotating block hydraulic pump processed after (ASSOFLUID, 2007).
- Figure 3.2: Hydraulic cylinder processed after (ASSOFLUID, 2007).
- Figure 3.3: Hydraulically controlled spool directional valve processed after (ASSOFLUID, 2007).
- Figure 3.4: Schematic diagram of the servo-system for proportional hydrostatic control of displacement of a pump connected to a closed-circuit primary control transmission.
- Figure 3.5: Block diagram of the automatic control system.
- Figure 3.6: Pump displacement control branch.

Thesis Summary - Theoretical and experimental contributions on optimizing the dynamic parameters of multipurpose motor trucks by using hydrostatic transmissions - Chirită Alexandru-Polifron

- Figure 4.1: Experimental test bench front view.
- Figure 4.2: Experimental test bench side view.
- Figure 4.3: Electric cabinet for the bench and electric motor control.
- Figure 4.4: A10VG servo-pump mounted on the bench with pressure transducers fitted and electrical connections made.
- Figure 4.5: A10VG28 servo-pump during commissioning.
- Figure 4.6: KOBOLD KZA-1865R20S3 gear flow transducer, mounted on the "A" branch of the A10VG servo-pump.
- Figure 4.7: A6VM28EP2/63W servo-motor mounted on the load simulation device.
- Figure 4.8: DBEME 10-51/315YG24K31M proportional pressure control valve with integrated electronics.
- Figure 4.9: F112A fixed-displacement pump.
- Figure 4.10: Pressure gauge with flexible hydraulic pipe.
- Figure 4.11: Hydraulic load simulation module.
- Figure 4.12: Pressure transducers on the closed circuit.
- Figure 4.13: IEM3255 three-phase meter used to measure the power absorbed by the asynchronous motor.
- Figure 4.14: VT11118-10 proportional controller and its voltage / current characteristic.
- Figure 4.15: ACS711EX current transducer.
- Figure 4.16: Kubler type 8.A020.3132.0360 speed transducer (encoder).
- Figure 4.17: Kubler type 0.571.012.E90 frequency voltage converter and digital display (top row, right side).
- Figure 4.18: Pepperl + Fuchs tip KFU8-FSSP-1.D frequency voltage converter.
- Figure 4.19: National Intruments USB 6211 data acquisition board.
- Figure 4.20: Hameg HM7044 programmable laboratory source.
- Figure 4.21: Hydraulic schematic diagram of the experimental test bench for the study of the closed-circuit primary control transmission and the pump displacement control servo-mechanism The hydraulic diagram at a larger size can be found in Annex 25.
- Figure 4.22: Application panel A10VG28EP4 servo-pump response to step signal.
- Figure 4.23: Application block diagram -A10VG28EP4 servo-pump response to step signal.
- Figure 4.24: Application panel –A10VG28EP4 servo-pump flow rate / control characteristic.
- Figure 4.25: Application block diagram first section.
- Figure 4.26: Application block diagram second section.
- Figure 4.27: Application block diagram third section.
- Figure 4.28: Step signal response centralized results.
- Figure 4.29: Time-variation of control voltage, control current and servo-pump flow rate The control panel related to this experiment can be found in Annex 26.
- Figure 4.30: Time-variation of pressure on the branches of the closed circuit, within the response to step signal with load created by the hydrostatic motor.
- Figure 4.31: Time-variation of control voltage, control current and servo-pump flow rate The control panel related to this experiment can be found in Annex 27.
- Figure 4.32: Time-variation of pressure on the branches of the closed circuit, as part of the experiment "Lag detail with load created by the hydrostatic motor".
- Figure 4.33: Time-variation of control voltage, control current and servo-pump flow rate The control panel related to this experiment can be found in Annex 28.
- Figure 4.34: Time-variation of pressure on the branches of the closed circuit, as part of the no-load step signal response.
- Figure 4.35: Time-variation of control voltage, control current and servo-pump flow rate The control panel related to this experiment can be found in Annex 29.
- Figure 4.36: Time-variation of pressure on the branches of the closed circuit, as part of the experiment "No-load lag detail".
- Figure 4.37: Servo-pump flow rate as a function of hydrostatic motor speed.
- Figure 4.38: Application panel related to experimenting with load created by the hydrostatic motor and the maximum control signal.
- Figure 4.39: Transmission control characteristic (left) and servo-pump control characteristic (right) The application panel at a larger size and all graphics related to this experiment can be found in Annex 30.
- Figure 4.40: Application panel related to experimenting with load created by the hydrostatic motor and the minimum control signal.
- Figure 4.41: Transmission control characteristic (left) and servo-pump control characteristic (right) The application panel at a larger size and all graphics related to this experiment can be found in Annex 31.
- Figure 4.42: Application panel related to experimenting with no load, short-circuiting the closed circuit and maximum control signal.
- Figure 4.43: Servo-pump control characteristics The application panel at a larger size and all graphics related to this experiment can be found in Annex 32.
- Figure 4.44: Application panel related to experimenting with no load, short-circuiting the closed circuit and minimum control signal.
- Figure 4.45: Servo-pump control characteristics The application panel at a larger size and all graphics related to this experiment can be found in Annex 33.
- Figure 5.1: Simcenter Amesim architecture (simplified view) processed after (Siemens, 2020).
- Figure 5.2: Servo-pump simulation network.
- Figure 5.3: Compensation pump parameters.
- Figure 5.4: Proportional directional control valve parameters.
- Figure 5.5: Hydraulic parameters of the servo-mechanism cylinder.
- Figure 5.6: Mechanical parameters of the servo-mechanism cylinder.
- Figure 5.7: Hydraulic fluid parameters.
- Figure 5.8: Main pump parameters.
- Figure 5.9: Main pump flow rate and its control current validation of numerical simulation.
- Figure 5.10: Compensation pump parameters.
- Figure 5.11: Proportional directional control valve parameters.
- Figure 5.12: Hydraulic parameters of the servo-mechanism cylinder.
- Figure 5.13: Mechanical parameters of the servo-mechanism cylinder.
- Figure 5.14: Hydraulic fluid parameters.
- Figure 5.15: Main pump parameters.
- Figure 5.16: Flow rate/control current characteristic validation of numerical simulation results.
- Figure 5.17: Linear correlation index simulation vs. experimentation.
- Figure 5.18: Wobble control signal and its frequency.
- Figure 5.19. Servo-pump flow rate in response to wobble control signal.
- Figure 5.20: Bode plot for frequency response of servo-pump flow rate.

Thesis Summary - Theoretical and experimental contributions on optimizing the dynamic parameters of multipurpose motor trucks by using hydrostatic transmissions - Chiriță Alexandru-Polifron

- Figure 5.21: Simulation network of the three transmissions with different subsystems.
- Figure 5.22: Transmission 1 simulation network.
- Figure 5.23: Transmission 2 simulation network.
- Figure 5.24: Transmission 3 simulation network.
- Figure 5.25: Flow rate of main pumps.
- Figure 5.26: Pressure at discharge port of main pumps.
- Figure 5.27: Speed of hydrostatic motors.
- Figure 5.28: Torque developed by the three hydrostatic motors.
- Figure 5.29: Suction pressure of main pumps.
- Figure 5.30: Flow rate sent to the tank by the three transmissions.
- Figure 5.31: Temperature of the flow rate sent to the tank by the three transmissions.
- Figure 5.32: Displacement of the 3 servo-mechanisms.
- Figure 5.33: Power consumed by a servo-mechanism.
- Figure 5.34: Power consumed by the 3 subsystems of the transmissions.
- Figure 5.35: Power consumed by the 3 subsystems as a function of the pressure in the closed circuit of the 3 transmissions.
- Figure 5.36: Power consumed by the 3 subsystems, expressed as a percentage, as a function of the pressure in the closed circuit, in relation to the consumption of subsystem no. 1.
- Figure 5.37: Energy consumed by the 3 subsystems.
- Figure 5.38: MAN TGM 18.320 motor truck with 4x4 drive (Man, n.d. b).
- Figure 5.39: Torque and power characteristic of D0836 LFL52 thermal motor depending on its speed (Man, n.d. a) Annex 36.
- Figure 5.40: Simulation network of efficiency of main pump in the servo-pump structure.
- Figure 5.41: Volumetric losses of main pump in the servo-pump structure (modeled in detail).
- Figure 5.42: Efficiency of main pump in the servo-pump structure.
- Figure 5.43: Simulation network of the motor truck equipped with closed-circuit primary control hydrostatic transmission.
- Figure 5.44: PID controller automatic tuning and step signal response.
- Figure 5.45: Time-variation of transmission input parameters.
- Figure 5.46: Time-variation of main pump parameters.
- Figure 5.47: Time-variation of compensation pump parameters.
- Figure 5.48: Time-variation of flow rate through the closed circuit valves.
- Figure 5.49: Time-variation of compensation circuit parameters.
- Figure 5.50: Time-variation of temperatures in the closed circuit.
- Figure 5.51: Time-variation of hydrostatic motor parameters.
- Figure 5.52: Time-variation of temperatures in the immediate proximity of the hydrostatic motor.
- Figure 5.53: Time-variation of parameters of the proportional directional control valve of the pump displacement control servomechanism.
- Figure 5.54. Time-variation of hydraulic fluid parameters.
- Figure 5.55: Time-variation of transfer case parameters.
- Figure 5.56: Time-variation of motor truck axle parameters.
- Figure 5.57: Time-variation of motor truck wheel parameters.
- Figure 5.58: Time-variation of motor truck parameters.
- Figure 5.59: Time-variation of motor truck dynamic parameters.
- Figure 5.60: Performances of continuous adjustment of motor truck travel speed.
- Figure 5.61: Minimum travel speed of motor truck.
- Figure 5.62: Frequency spectrum of main pump flow rate.
- Figure 5.63. Root locus plot (0 50 Hz). Figure 5.64: Root locus plot (0 25 Hz) detail.
- Figure 5.65: Particular cases of stability and damping of the automatic speed control system.
- Figure 5.66: Time-variation of hydrostatic transmission input parameters.
- Figure 5.67: Time-variation of main pump parameters.
- Figure 5.68: Time-variation of parameters of check and pressure control valves in the closed circuit.
- Figure 5.69. Time-variation of motor truck axle parameters.
- Figure 5.70: Time-variation of motor truck wheel parameters.
- Figure 5.71: Time-variation of motor truck parameters.
- Figure 5.72: Time-variation of motor truck dynamic parameters.
- Figure 5.73: Performances of steady-state control of motor truck travel speed.
- Figure 5.74: Time-variation of speed rate for extended simulation time.
- Figure 5.75: Time-variation of temperatures in various areas of the main pump.
- Figure 5.76: Time-variation of temperatures in various areas of the hydrostatic motor.
- Figure 5.77: Time-variation of hydraulic fluid parameters.
- Figure 5.78: Time-variation of hydraulic fluid tank parameters.
- Figure 5.79: Time-variation of cooler (heat exchanger) parameters.
- Figure 5.80: Time-variation of hydrostatic transmission input parameters for i = 1.007.
- Figure 5.81: Time-variation of main pump parameters for i = 1.007.
- Figure 5.82: Time-variation of motor truck wheel parameters for i = 1.007.
- Figure 5.83: Time-variation of motor truck traction parameters for i = 1.007.
- Figure 5.84: Time-variation of motor truck dynamic parameters for i = 1.007.
- Figure 5.85: Performances of steady-state control of motor truck travel speed for i = 1.007.
- Figure 5.86: Comparison between the optimized dynamic parameters of the motor truck equipped with a closed-circuit primary control hydrostatic transmission and the TGM 18 motor truck.
- Figure 6.1: Multipurpose motor truck used in the construction sector, equipped with an example of technological equipment (Poclain Hydraulics, n.d. b).
- Figure 6.2: Utility vehicles performing works on the roadway or in the immediate proximity (Grădinariu, n.d.).

Annex 3 - Thesis References

- * Ahn, S., Choi, J., Son, H., Kim, S., Lee, J., and Kim, H., 2016, "Development of a new sub-shift schedule and control algorithm for a hydromechanical transmission", **Advances in Mechanical Engineering** 8(12), pp. 1–14.
- * Akers, A., Gassman, M., and Smith, R., 2006, Hydraulic power system analysis, USA: CRC Press.
- * Allain, L., Neyrat, S., and Viel, A., 2009, "Linear Analysis Approach for Modelica Models", **Proceedings of the 7th International ModelicaConference**, pp. 646-656.
- * Allegro, 2013, Hall Effect Linear Current Sensor with Overcurrent Fault Output for <100 V Isolation Applications, electronic data sheet, accessed on October 21, 2020, <www.allegromicro.com>.
- * Amorțilă, V., Mereuță, E., Bălășoiu, G., Humelnicu, C., and Gingărașu, M., 2021, "Modeling and Simulation of a Simple Linear Suspension with Simcenter Amesim Software", **EuroEconomica** 40(2), pp. 180 186.
- * Antonelli, M., Baccioli, A., Francesconi, M., Psaroudakis, P., and Martorano L., 2015, "Small scale ORC plant modeling with the AMESim simulation tool: analysis of working fluid and thermodynamic cycle parameters influence", **Energy Procedia** 81, pp. 440 449.
- * ASSOFLUID, 2007, Hydraulics in Industrial and Mobile Applications, Brugherio (Milano): Grafiche Parole Nuove s.r.l.
- * Axinti, G. and Axinti, A. S., 2008 a, Acţionări hidraulice și pneumatice. Vol. 1. Componente și sisteme, funcții și caracteristici / Hydraulic and pneumatic drives. Vol. 1. Components and systems, functions and features, Chișinău: "Tehnica-Info" Publishing House.
- * Axinti, G. and Axinti, A. S., 2008 b, Actionări hidraulice și pneumatice. Vol. 2. Dinamica echipamentelor și sistemelor / Hydraulic and pneumatic drives. Vol. 2. Dynamics of equipment and systems, Chișinău: "Tehnica-Info" Publishing House.
- * Axinti, G. and Axinti, A. S., 2009, Acţionări hidraulice și pneumatice. Vol. 3. Baze de calcul, proiectare, exploatare, fiabilitate și scheme de acţionare / Hydraulic and pneumatic drives. Vol. 3. Bases of calculation, design, exploitation, reliability and drive diagrams, Chişinău: "Tehnica-Info" Publishing House.
- * Backas, J., Ghabcheloo, R., and Huhtala, K., 2017, "Gain scheduled state feedback velocity control of hydrostatic drive transmissions", Control Engineering Practice 58, pp. 214–224.
- * Barnwal, M. K., Gangwar, G. K., Kumar, N., Kumar, A., and Das, J., 2013, "Steady state performance analysis of hydrostatic transmission system (HST)", International Journal of Mechanical and Production Engineering 1(6), pp. 48–51.
- * Baumer, 2021, Pressure measurement PBM4, electronic data sheet, accessed on March 10, 2022, <www.baumer.com>.
- * Bauer, J. J., 1973, "Application of hydrostatic transmissions to small and medium horsepower vehicles", SAE Technical Paper, 730786.
- * Bălășoiu, V., Cristian, I., and Bordeașu, I., 2008, **Echipamente și siteme hidraulice de acționare și automatizare. Vol. 2. Aparatură hidraulică / Hydraulic drive and automation equipment and systems. Vol. 2. Hydraulic equipment**, Timișoara: Orizonturi Universitare Publishing House.
- * Bell, P. C., 1971, Mechanical Power Transmission, 1st edition, New York: Macmillan Publishers.
- * Berthoux, V., Furic, S., and Wagner, L., 2014, "Statecharts as a Means to Control Plant Models in LMS Imagine.Lab AMESim", **Proceedings of the 10th International ModelicaConference**, pp. 1237-1246.
- * Blackburn, J.F., Reethof, G., and Shearer, J.L., 1960, Fluid power control, Vol. 1, 2, 3, USA: Technology press of M.I.T. and John Wiley & Sons.
- * Bosch Rexroth AG, n.d. a, [EN] Bosch Rexroth: A41CT Compact Unit for Hydromechanical Power-Split Gearboxes, online video, YouTube, accessed on October 14, 2020, https://www.youtube.com/watch?v=T5vpql7Smlc.
- * Bosch Rexroth AG, n.d. b, Variable Pump A10VG 28-63 Series 10, Repair Manual RDE 92750-21-R/02.08, accessed on May 3, 2021, <www.boschrexroth.de>.
- * Bosch Rexroth AG, 2012 a, Analog amplifier module Type VT 11118 Component Series 1X, electronic data sheet, accessed on April 29, 2021, <www.boschrexroth.de>.
- * Bosch Rexroth AG, 2012 b, Axial Piston Variable Motor A6VM Series 63, Instruction manual RE 91604-01-B/01.2012, accessed on May 3, 2021, <www.boschrexroth.de>.
- * Bosch Rexroth AG, 2013, Proportional pressure relief valve, pilot operated Type DBEM and DBEME, electronic data sheet, accessed on April 29, 2021, <www.boschrexroth.de>.
- * Bosch Rexroth AG, 2016, Axial piston variable motor A6VM Series 63, electronic data sheet, accessed on April 29, 2021, <www.boschrexroth.de>.
- * Bosch Rexroth AG, 2020 a, Axial piston variable pump A10VG Series 10, electronic data sheet, accessed on April 29, 2021, <www.boschrexroth.de>.
- * Bosch Rexroth AG, 2020 b, Axial piston variable pump A4VG Series 35, electronic data sheet, accessed on April 29, 2021, <www.boschrexroth.de>.
- * Bosch Rexroth AG, 2020 c, Axial piston variable pump A4VG Series 40, electronic data sheet, accessed on April 29, 2021, <www.boschrexroth.de>.
- * Bury, P., Stosiak, M., Urbanowicz, K., Kodura, A., Kubrak, M., and Malesińska, A., 2022, "A case study of open- and closed-loop control of hydrostatic transmission with proportional valve start-up process", **Energies** 15, ID 1860.

 * Cao, W., Li, D., Chen, Z., Tang, W., Lv, Q., and Huang, M., 2015, "Research on Model and Simulation of Hydraulic Lifting System of the
- * Cao, W., Li, D., Chen, Z., Tang, W., Lv, Q., and Huang, M., 2015, "Research on Model and Simulation of Hydraulic Lifting System of the Wave Power Generating Platform based on AMESim", **Proceedings of the 2015 International Industrial Informatics and Computer Engineering Conference (IIICEC 2015)**, pp. 340-344.
- * Chapple, P. J., 2003, Principles of Hydraulic System Design, Oxford: Coxworth Publishing Company.
- * Chiriță, Al. P., 2022, [accepted for publication], "The influence of hydraulic fluid temperature on the adjustment capabilities of servo-mechanisms and closed-circuit hydrostatic transmissions", **Proceedings of 2022 International Conference on Hydraulics and Pneumatics HERVEX**.
- * Chiriță, Al. P., Dumitrescu L., and Sauciuc, R., 2017, "Numerical simulation of the dynamic behavior of a multifunctional motor vehicle equipped with a primary adjustment hydrostatic transmission", **Proceedings of ISB-INMA TEH' 2017 International Symposium,** pp. 375-380
- * Chiriță, Al. P. and Pavel, C., 2022, [accepted for publication], "Mathematical modeling, laboratory testing and numerical simulation of a servo-pump as part of a closed circuit primary control hydrostatic transmission for multi-purpose trucks", **Hidraulica Magazine** (4).
- * Chiriță, Al. P. and Pavel, C., 2023, [accepted for publication], "Agricultural platform equipped with a hydrostatic transmission capable of continuously adjustable travel velocity and non-linear disturbance compensation capabilities", INMATEH Agricultural Engineering 69(1).
- * Chiriță, Al. P., Rădoi R. I., Tudor, B. Ál., Şefu, Şt. M., and Popescu, A.-M., 2022, "Control performance of an energy efficient hydrotronic transmission", **Hidraulica Magazine** (2), pp. 07–14.
- * Comellas, M., Pijuan, J., Potau, X., Nogués, M., and Roca, J., 2013, "Efficiency sensitivity analysis of a hydrostatic transmission for an off-road multiple axle vehicle", International Journal of Automotive Technology 14(1), pp. 151–161.
- * Costa, G. K. and Sepehri, N., 2015, **Hydrostatic transmissions and actuators: operation, modelling and applications**, West Sussex: John Wiley & Sons, Inc., ISBN 9781118818909.

- * Costa, G. K. and Sepehri, N., 2018, "Understanding overall efficiency of hydrostatic pumps and motors", **International Journal of Fluid Power** 19(2), pp. 106–116.
- * Costa Utilaje, n.d., *Multifunctionale / Multipurpose motor vehicles*, *digital image*, accessed on May 11, 2022, https://costautilaje.ro/multifunctionale/>.
- * Czyński, M., 2008, "Energy efficiency of hydrostatic transmission. Comparing results of laboratory and simulation tests", **Scientific Problems of Machines Operation and Maintenance** 43 (2 / 154), pp. 59-70.
- * Dasgupta, K., Mandal, S.K., and Pan, S., 2012, "Dynamic analysis of a low speed high torque hydrostatic drive using steady-state characteristics", **Mechanism and Machine Theory** 52, pp. 1-17.
- * Deng, X., Sun, K., Zhang, H., Zhang, Y. and Li, T., 2020, "Modeling and Simulation of the Water Hydraulic Cylinder System Based on AMESim", **Journal of Physics: Conference Series** 1637, 8th Annual International Conference on Material Science and Engineering (ICMSE2020), ID 012146.
- * Ding, H. and Zhao, J., 2017, "Dynamic characteristic analysis of replenishing/leaking parallel valve control systems", **Automatika** 58(2), pp. 182-194.
- * Do, H. T. and Ahn, K. K., 2013, "Velocity control of a secondary controlled closed-loop hydrostatic transmission system using an adaptive fuzzy sliding mode controller", **Journal of Mechanical Science and Technology** 27(3), pp. 875-884.
- * Dobre, Al., Vasiliu, N., Hadăr, A., and Andreescu, C. N., 2015, "Modeling and simulation of the car suspensions with AMESim", Lucrările celei de-a X-a ediții a Conferinței anuale a ASTR / Proceedings of the 10th edition of the annual conference of ASTR, pp. 254–260.
- * Fu, Y. L. and Qi, H. T, 2011, *Tutorial Examples of LMS Imagine*. In **Lab AMESim System Modeling and Simulation**, Beijing: Beihang University Press.
- * Fuchshumer, F., 2009, Modellierung, Analyse und nichtlineare modellbasierte Regelung von verstellbaren Axialkolbenpumpen/Modelling, analysis and non-linear model-based control of variable axial piston pumps, Aachen: Shaker Verlag.
- * Galal Rabie, M., 2009, Fluid Power Engineering, New York: The McGraw-Hill Companies, Inc.
- * Gangwar, G. K., Barnwal, M. K., and Das, J., 2013, "Modeling and simulation of hydrostatic transmission system: A literature survey", International Journal of Mechanical and Production Engineering 1(6), pp. 43–47.
- * Gies, H. M. S., 2008, Fluidtechnik für mobile anwendungen / Fluid technology for mobile applications, Aachen: Shaker Verlag.
- * Grădinariu, n.d., Multifunctional de capacitate mare / Large-capacity multipurpose motor vehicle, accessed on October 20, 2020, https://www.gradinariu.ro/utilaj-multifunctional-de-capacitate-mare.
- * Guillon, M. and Thoraval, B., 1992, Commande et asservissement hydrauliques et électrohydrauliques, Paris: Tec. et doc.-Lavoisier.
- * Guo, X. and Vacca, A., 2021, "Advanced design and optimal sizing of hydrostatic transmission systems", Actuators 10, ID 243.
- * Haimovici, E. M., 1969, L'Hydro Automatique et les Hydrauliques, vol. IV, Montrouge: Imp. de l'Edition et de l'Industrie.
- * Heisler, H., 2002, Advanced Vehicle Technology, Second edition. Oxford: Butterworth-Heinemann.
- * Ho, T. H. and Ahn, K. K., 2010, "Modeling and simulation of hydrostatic transmission system with energy regeneration using hydraulic accumulator", **Journal of Mechanical Science and Technology** 24(5), pp. 1163-1175.
- * Inada, T., Miura, T., and Matsuzaka, K., 2017, "Hydraulic pump and track motor for hydrostatic transmission", **KYB Technical Review** (55), pp. 33–38.
- * Hu, Y., Zeng, Q., Jiang, S., Yu, P., and Yang, Z., 2018, "Dynamic Analysis of Chain Drive System for Scraper Conveyor Based on Amesim", IOP Conf. Series: Materials Science and Engineering 452, ID 042127.
- * Ion Guță, D. D., Popescu, T. C., and Dumitrescu, C., 2010, "Optimization of hydrostatic transmissions by means of virtual instrumentation technique", **Proceedings of SPIE The International Society for Optical Engineering** 7821, ID 782129.
- * INOE 2000 HYDRAULICS AND PNEUMATICS RESEARCH INSTITUTE (IHP BUCHAREST), n.d., 66. Stand for testing hydrostatic transmissions, **EERIS page**, accessed on March 12, 2020, https://eeris.eu/ERIF-2000-000J-0884>.
- * Jelali, M. and Kroll, A., 2003, Hydraulic Servo-Systems: Modelling, Identification and Control, UK: Springer-Verlag.
- * Jia, W., Yin, C., Li, G., and Sun, M., 2017, "Modeling and stability of electro-hydraulic servo of hydraulic excavator", IOP Conf. Series: Earth and Environmental Science (EEMS 2017) 94, ID 012013.
- * Jun, L., Dongyun, W., Xiaobing, X., and Hualin, R., 2017, "Study On Hybrid Modeling Of Hydraulic Excavator", **Topics in Intelligent Computing and Industry Design (ICID)**, 1(2), pp. 30-33.
- * Jung, G., Kim, H., and Kim, J., 2005, "Performance and transmission efficiency analysis of 2-mode hydro mechanical transmission", **Transactions of KSAE** 13(1), pp. 90–98.
- * Kaps Automatic, n.d., *Torque converters*, *digital image*, accessed on April 5, 2022, https://eng.kaps.cz/data/aktuality/main-photo/964.jpg.
- * Kiencke, U. and Nielsen L., 2005, Automotive Control Systems: For Engine, Driveline, and Vehicle, 2nd ed., Germany: Springer-Verlag.
- * Kobold, 2017, Gear Wheel Flow Meter Made of Aluminium for Viscous Fluids Model KZA, electronic data sheet, accessed on April 15, 2021. <www.kobold.com>.
- * Kübler, 2018, Incremental encoders Large hollow shaft optical A020, electronic data sheet, accessed on April 19, 2021, www.kuebler.com.
- * Kugi, A., Schlacher, K., Aitzetmüller, H., and Hirmann, G., 2000, "Modeling and simulation of a hydrostatic transmission with variable-displacement pump", **Mathematics and Computers in Simulation** 53, pp. 409–414.
- * Kumar, A., Das, J., and Mishra, S. K., 2013, "Performance investigation of a proportional valve controlled hydraulic motor used in hydrostatic transmission system", **Proceedings of 7th ICEECSME-2013**, pp. 28–31.
- * Kumar, N., Dasgupta, K., and Ghoshal, S. K., 2015, "Dynamic analysis of a closed-circuit hydrostatic summation drive using bent axis motors", **Proceedings of the Institution of Mechanical Engineers. Part I: Journal of Systems and Control Engineering** 229(8), pp. 761–777
- * Lai, J. C. S. and Grigg, F. W., 1987, "A hydrostatic transmission for a load-haul-dump vehicle", SAE Technical Paper, 871599.
- * Lee, J.-S., Ahn, J.-H., Chae, H.-I., Lee, H.-C., and Rhi, S.-H., 2022, "1-D Modeling of Two Phase Flow Process in Concentric Annular Heat Pipe and Experimental Investigation", **Processes** 10(3), ID 493.
- * Lepădatu, I., Cristescu, C., Chiriță, Al. P., and Mărculescu, C., 2017, "Four-wheel drive high efficiency hybrid transmission for multipurpose motor vehicles", **Proceedings of 2017 International Conference on Hydraulics and Pneumatics HERVEX**, pp. 140-146.
- * Likaj, R. and Shala, A., 2017, "Design of automatic system with hydrostatic transmission", **Annals of Faculty Engineering Hunedoara International Journal of Engineering** 15(2), pp. 159–162.
- * Liu, F., Wu, W., Hu, J., and Yuan, S., 2019, "Design of multi-range hydro-mechanical transmission using modular method", **Mechanical Systems and Signal Processing** 126, pp. 1–20.
- * Magnom, n.d., *Hydrostatic Transmission*, *digital image*, accessed on April 5, 2022, https://magnom.com/wp-content/uploads/2018/06/HydrostaticTransmission-2-online.jpg.
- * Mandal, S. K., Singh, A. K., Verma, Y., and Dasgupta, K., 2012, "Performance investigation of hydrostatic transmission system as a function of pump speed and load torque", **Journal of The Institution of Engineers (India): Series C** 93(2), pp. 187–193.
- * Manring, N. D., 2013, Fluid Power Pumps and Motors: Analysis, Design, and Control, New York: McGraw-Hill.

- * Manring, N. D., 2016, "Mapping the efficiency for a hydrostatic transmission", Journal of Dynamic Systems, Measurement, and Control 138, pp. 031004-1-031004-8.
- * Manring, N. D. and Luecke, G. R., 1998, "Modeling and designing a hydrostatic transmission with a fixed-displacement motor", Journal of Dynamic Systems, Measurement, and Control 120, pp. 45-49.
- * Man, n.d. a, D 0834, D 0836 Euro4 vehicle diesel engines 110-240 kW (150-326 hp), electronic data sheet, accessed on March 14, 2018, <www.man-mn.com>.
- * Man, n.d. b, MANTED® Technical Data and Guide To Fitting Bodies, accessed on February 27, 2018,
- https://www.manted.de/manted/epl/loginmtd.epl?forward=&sprache=us&session=®ISTER_ABRL_BUS=0&from=manted&comman
- * Man, 2017 a, MAN Guidelines to fitting bodies Truck Power take-offs Edition 2017 V1.0, electronic manual, accessed on February 28, 2018, <www.manted.de>
- * Man. 2017 b. MAN Guidelines to fitting bodies Truck Series TGL/TGM Edition 2017 V1.0, electronic manual, accessed on February 28, 2018, <www.manted.de>.
- * MBT, n.d., ROBOSCAN R1MC, accessed on March 18, 2022, http://www.mbtelecom.ro/Produse/ROBOSCAN%20R1MC.
- * Merritt, H. E., 1967, Hydraulic control systems, US: John Wiley & Sons.
- * Meyer, R., 1970, Introduction to Mathematical Fluid Dynamics, New York: Wiley-Interscience.
- * Mercedes-Benz, n.d., DATE TEHNICE Unimog U 219 U 535, accessed on November 16, 2020, https://www.mercedes-benz- trucks.com/ro_RO/models/unimog-implement-carrier/technical-data.html>.
- * Miller, M. K., Khalid, H., Michael, P., W., Guevremont, J. M., Garelick, K. J., Pollard, G. W., Whitworth, A. J., and Devlin, M. T., 2014, "An
- investigation of hydraulic motor efficiency and tribological surface properties", **Tribology Transactions** 57(4), pp. 622-630.

 * Mistry, K. A., Patel, B. A., Patel, D. J., Parsana, P. M., and Patel, J. P., 2018, "Design and analysis of hydrostatic transmission system", IOP Conf. Series: Materials Science and Engineering (IConAMMA-2017) 310, ID 012048.
- * Mohanty, A. and Yao, B., 2011, "Integrated direct/indirect adaptive robust control of hydraulic manipulators with valve deadband", IEEE/ASME Transactions on Mechatronics 16(4), pp. 707-715.
- * Murrenhoff, H., 2008, Servohydraulik Geregelte Hydraulische Antriebe / Servo hydraulics Controlled hydraulic drives, 3., neu überarbeitete Auflage / 3rd, newly revised edition, Aachen: Shaker Verlag.
- * National Instruments, n.d., USB-6211 _ QUARC Data Acquisition Card Support, electronic data sheet, accessed on June 18, 2020,
- * Nervergna, N. and Rundo, M., 2020, Passi Nell'oleodinamica / Steps in hydraulics, Torino: Epics.
- * Neto, M. M. and Góes, L. C. S., 2017, "Use of LMS Amesim® Model to Predict Behavior Impacts of Typical Failures in an Aircraft Hydraulic Brake System", Proceedings of The 15th Scandinavian International Conference on Fluid Power, SICFP'17, pp. 29-43.
- * Nie, D. and Fu, C., 2020, "The application of closed hydraulic system of hoisting mechanism in auto crane", Jordan Journal of Mechanical and Industrial Engineering JJMIE 14(1), pp. 37-41.
- * Paoluzzi, R. and Zarotti, L. G., 2013, "The minimum size of hydrostatic transmissions for locomotion", Journal of Terramechanics 50, pp. 153-164.
- * Pandey, A. K., Dasgupta, K., and Kumar, N., 2019 a, "Steady-state performance investigation of closed-circuit hydrostatic system: A practical approach", Kuwait Journal of Science 46(1), pp. 76-83.
- * Pandey, A. K., Vardhan, A., and Dasgupta, K., 2019 b, "Theoretical and experimental studies of the steady-state performance of a primary and secondary-controlled closed-circuit hydrostatic drive", Proceedings of the Institution of Mechanical Engineers, Part E: Journal of Process Mechanical Engineering 223(5), pp. 1024-1035.
- * Park, S. H., Alam, K., Jeong, Y. M., Lee, C. D., and Yang, S. Y., 2009, "Modeling and simulation of hydraulic system for a wheel loader using AMESim," Proceedings of ICCAS-SICE 2009: ICROS-SICE International Joint Conference 2009, pp. 2991-2996.
- * Parker Hannifin Corporation, 2014, Denison GOLD CUP® Application Handbook Piston Pumps & Motors For Open & Closed Circuits, electronic manual HY28-2668-01/GC/NA,EU, accessed on April 8, 2022, <www.parker.com>.
- * Parker Hannifin Corporation, 2022, Denison GOLD CUP® Product Catalog Piston Pumps & Motors For Open & Closed Circuits, Catalogue HY28-2667-01/GC/NA,EU, accessed on April 11, 2022, <www.parker.com>.
- * Pepperl+Fuchs, 2020, Frequency voltage current converter KFU8-FSSP-1.D, electronic data sheet, accessed on July 20, 2021, <www.pepperl-fuchs.com>.
- * Pettersson, K., Larsson, L. V., Larsson, K. V., and Krus, P., 2014, "Simulation aided design and testing of hydromechanical transmissions", Proceedings of the 9th JFPS International Symposium on Fluid Power, pp. 487-495.
- * Poclain Hydraulics, n.d. a, CreepDrive™, accessed on September 24, 2020, ">https://poclain-h
- * Poclain Hydraulics, n.d. b, CreepDrive Consistent Low Speed Drive, electronic brochure, accessed on September 24, 2020, <www.poclainhvdraulics.com>
- * Poclain Hydraulics, 2017 a, CDM 222-050 CreepDrive Motor, Technical Catalog, accessed on September 22, 2020, <www.poclainhydraulics.com>
- Poclain Hydraulics, 2017 b, P90 Variable Displacement Pump, Technical Catalog, accessed on September 23, 2020, <www.poclain- hydraulics.com>.
- * Poclain Hydraulics, 2020, CDM 20 CreepDrive Motor, Technical Catalog, accessed on August 10, 2021, <www.poclain-hydraulics.com>.
- * Poclain Hydraulics, 2021 a, CDM 10 CreepDrive Motor, Technical Catalog, accessed on August 10, 2021, <www.poclain-hydraulics.com>.
- * Poclain Hydraulics, 2021 b, CreepDrive™ System Low Speed Applications, Technical Catalog, accessed on September 7, 2021, <www.poclain-hydraulics.com>.
- * Poclain Hydraulics, 2021 c, Power Transmission Valves, Technical Catalog, accessed on November 5, 2021, <www.poclainhydraulics.com>.
- * Popescu, T. C., Ion Guta, D. D., and Calinoiu, C., 2010 a, "Modern instruments for analysis of hydrostatic transmissions", UPB Scientific **Bulletin, Series D: Mechanical Engineering** 72(4), pp. 201-210.
- Prabel, R. and Aschemann, H., 2017, "Torque control of a hydrostatic transmission using extended linearisation techniques", Proceedings of The 15th Scandinavian International Conference on Fluid Power, SICFP'17, pp. 352-360.
- * Rahmfeld, R. and Skirde, E., 2010, "Efficiency measurement and modeling essential for optimizing hydrostatic systems", Proceedings of 7th International Fluid Power Conference (7. IFK) 3, pp. 53-66.
- * Roccatello, A., Mancò, S., and Nervegna, N., 2007, "Modelling a variable displacement axial piston pump in a multibody simulation environment", Transactions of the ASME. Journal of dynamic systems, measurement and control 129, pp. 456-468.
- * Rossetti, A. and Macor, A., 2019, "Continuous formulation of the layout of a hydromechanical transmission", Mechanism and Machine Theory 133, pp. 545-558.
- * Rossetti, A. and Macor, A., 2013, "Multi-objective optimization of hydro-mechanical power split transmissions", Mechanism and Machine **Theory** 62, pp. 112-128.

- * Rossetti, A., Macor, A., and Scamperle, M., 2017, "Optimization of components and layouts of hydromechanical transmissions", International Journal of Fluid Power 18(2), pp. 123–134.
- * Ruggeri, M., 2002, "Flexible automotive strategy (FAST) for hydrostatic transmissions", **Proceedings of the 5th JFPS International Symposium on Fluid Power** 3, pp. 787-793.
- * Rydberg, K.-E., 2007, "Design of energy efficient hydraulic systems System concepts and control aspects", **Proceedings of ISFP'2007: 5th International Symposium on Fluid Power Transmission and Control**.
- * Sathiyaseelan, A., and Selvan, A. M., 2020, "Modeling and Simulation of a Fighter Aircraft Cabin Temperature Control System Using AMESim", **SAE Technical Paper**, 2020-28-0497.
- * Schneider Electric, 2022, Energy meters iEM3100 / iEM3200 / iEM3300 series, **User manual DOCA0005EN-13**, accessed on April 8, 2022, <www.se.com>.
- * Shearer, L., Murphy, A., and Richardson, H., 1967, Introduction to System Dynamics, Reading, Pennsylvania: Addison-Wesley.
- * Shi, X., Sun, G., and Liu, H., 2013, "Analysis of torque loading system based on hydraulic energy closed-loop", **TELKOMNIKA** 11(12), pp. 7197-7205.
- * Siemens, 2020, Simcenter Amesim 2020 User guide / Help contents, Plano, Texas, USA.
- * Sill, J., Molla, S., and Ayalew, B., 2011, "Modelling and control of handling dynamics for a hydrostatically driven vehicle", **International Journal of Heavy Vehicle Systems** 18(3), pp. 322-340.
- * Singh, R. B., Kumar, R., and Das, J., 2013, "Hydrostatic transmission systems in heavy machinery: Overview", **International Journal of Mechanical and Production Engineering** 1(4), pp. 47–51.
- * Skorek, G., 2013, "Energy efficiency of a hydrostatic drive with proportional control compared with volumetric control", **Polish Maritime Research** 20(3), pp.14-19.
- * Stringer, J., 1976, Hydraulic system analysis: an introduction, Hoboken, NJ, USA: John Wiley & Sons.
- * Sunny, S., Pawar, S., Ozarkar, S., and Biswas, S., 2014, "Hydrostatic transmission as an alternative to conventional gearbox", IJRET: International Journal of Research in Engineering and Technology 3(5), pp. 136–142.
- * Ting-ting, M. and Guo-ping, Y., 2016, "Study on Hydraulic Vibration System of Roller Based on AMESIM", International Journal of Research in Engineering and Science (IJRES) 4(7), pp. 28-37.
- * Tripathi, J. P., Ghoshal, S. K., Hasan, M. E., Dasgupta, K., and Das J., 2018, "Speed control of a hydrostatic drive using inverse steady state model", IOP Conf. Series: Materials Science and Engineering (International Conference on Mechanical, Materials and Renewable Energy) 377, ID 012115.
- * U.M.P., n.d., Axial piston units / Pompe hidraulice cu pistoane axiale, electronic catalog, accessed on September 23, 2020, <www.ump.ro>.
- * Vacca, A. and Franzoni, G., 2021, **Hydraulic Fluid Power: Fundamentals, Applications, and Circuit Design**, Hoboken, NJ, USA: John Wiley & Sons
- * Vasiliu, G. C., Vasiliu, D., Vasiliu, N., and Ion Guţă, D., 2014, "Numerical simulation of the mechanical feedback servopumps by AMESIM", **U.P.B. Sci. Bull., Series D,** 76(3), pp. 189-198.
- * Vasiliu, N. and Catană, I., 1988, **Transmisii hidraulice și electrohidraulice / Hydraulic and electrohydraulic transmissions**. Vol. I Maşini hidraulice volumice / Vol. I Positive displacement hydraulic machines, Bucharest: Technical Publishing House.
- * Vasiliu, N. and Vasiliu, D., 2004, **Acționări hidraulice și pneumatice / Hydraulic and pneumatic drives**. Vol. I, Bucharest: Technical Publishing House.
- * Vrcan, Ž., Siminiati, D., and Lovrin, N., 2011, "Design proposal for a hydrostatic city bus transmission", **Engineering Review** 31(2), pp. 81-80
- * Wang, J., Xu, H., Xu, X., and Pan, C., 2017, "Design and simulation of liquid cooled system for power battery of PHEV", **IOP Conf. Series:** Materials Science and Engineering, 231, ID 012025.
- * Wei, H. -B. and Su, W. -B., 2022, "Simulation Based on AMESim and Performance Experiment of Ocean Current Hydraulic Power Generation," **Proceedings of 5th International Conference on Energy, Electrical and Power Engineering (CEEPE)**, pp. 1265-1269.
- * Wei, X., Wang, L., Ni, X., Han, S., Zhao, X., and Li, S., 2021, "Speed control strategy for pump-motor hydraulic transmission subsystem in hydro-mechanical continuously variable transmission", **Journal of Mechanical Science and Technology** 35(12), pp. 5665-5679.
- * Wilson, W. E. and Lemme, C. D., 1968, "The Hydromechanical Transmission Ideal and Real", SAE Technical Paper, 680605.
- * Wu, W., Luo, J., Wei, C., Liu, H., and Yuan, S., 2020, "Design and control of a hydro-mechanical transmission for all-terrain vehicle", **Mechanism and Machine Theory** 154, ID 104052.
- * Xiang, Y., Mutschler, S., Brix, N., Brach, C., and Geimer, M., 2020, "Optimization of hydrostatic-mechanical transmission control strategy by means of torque control", **Proceedings of 12th International Fluid Power Conference (12. IFK)**, pp. 421-431.
- * Yilun, W., 2005, Hydraulic transmission, Harbin: Harbin Engineering University Press.
- * Zarotti, L. G., Nervegna, N., and Miotto, G., 1979, "Hydrostatic transmissions controls Is there space for optimization?", **SAE Transactions** 87(3), pp. 2090-2101.
- * Zarotti, L. G. and Paoluzzi, R., 1996, "In quest of the transmission size", **Proceedings of the Third JHPS International Symposium on Fluid Power**, pp. 295-300.
- * Zeman, P., Kemmetmüller, W., and Kugi, A., 2015, "Mathematical modeling and analysis of a hydrostatic drive train", **IFAC-PapersOnLine** 48(1), pp. 508–513.
- * Zhou, W., 2019, "Simulation of Hydraulic System Faults for Marine Machinery Based on AMESim," **Journal of Coastal Research** 94(sp1), pp. 357-361.

Annex 4 - Thesis bibliometric statistics

New references (≥ year 2013)	Old references (< year 2013)	TOTAL of references	*Since the publication date of the information on the websites could not be determined, the related references (marked as "n.d." – "no date") have been all considered older than 2013.	
59	23	82		
5	26	31		related references (marked as "n.d." – "no
64	49	113		
20	0	20		
				2013.
-		-		
	(≥ year 2013) 59 5	(≥ year 2013) (< year 2013) 59 23 5 26 64 49 20 8 0 10*	(≥ year 2013) (< year 2013)	